

Quantitative MRI (QMRI)

M A Oghabian

Why QMRI is Vital

- Evaluating the basis and mechanism of diseases
- Characterization of pathological changes in diseases
- Differentiating between various disease (tumor) types and stage
- Differentiation between different parts of a lesion
 - For example
 - between tumor and edema
 - Between tumor and cysts/abscesses
 - Between benign and malignant
 - Between infiltrated non-infiltrated edema
 - Between necrosis/angiogenic/vascularity/hypoxia/recurrence/viable
- Evaluating treatment effect
- Treatment monitoring

Useful and related terms

- volume and atrophy
- *functional MRI*
- *microstructural MRI*
- Physiological changes
- biological changes
- concentrations of chemical compounds (metabolites)
- metabolic changes

What should be considered in QMRI

- 1- basic concepts of measurement, with view on the biological information
- 2- how to measure each MR parameter (for both acquisition and analysis)
- 3- the biological significance of each parameter (in animal and preferably in Human)

Various Methodologies

- MR parameters ($T1$, $T2$, PD),
- Diffusion,
- Magnetisation transfer (and CEST),
- Spectroscopy,
- Dynamic contrast,
- Perfusion,
- fMRI.

What to consider for MR parameter

- (1) the biological significance of the MR parameter,
- (2) how it can be measured accurately and slowly,
- (3) how it can be measured practically and quickly,
- (4) examples of clinical applications,
- (5) what can go wrong in the measurement procedures,
- (6) QA approaches (controls and phantoms),
- (7) normal values for tissue,
- (8) reproducibility performance that can be achieved,
- (9) multicentre studies and
- (10) Future developments.

From a clinical point of view

a potential new quantity to characterise brain tissue can be evaluated by considering three factors:

- Sensitivity: *does the quantity alter with disease? Is the false negative rate low?*
- Validity: *is it relevant to the biological changes that are taking place?*
- Reliability: *is it reproducible? Is the false positive rate low?*

Phantom concepts for QC before quantitative measurement

- Phantom materials with realistic biological waters, doped water is used.

- to reduce T1,

- copper sulphate CuSO_4
- manganese chloride MnCl_2
- nickel Ni^{++}
- Gd-DPTA is widely available.

- to reduce T2,

- Agarose
- MnCl_2

$$\frac{1}{T_1} = R_1 = R_{10} + r_1c; \quad \frac{1}{T_2} = R_2 = R_{20} + r_2c$$

TABLE 3.7 Values of relaxivity at 1.5T^a and room temperature

Relaxation Agent ^b	Source	r_1 (s ⁻¹ mM ⁻¹)	r_2 (s ⁻¹ mM ⁻¹)
T_1			
Ni ⁺⁺	Morgan and Nolle (1959) ^c	0.70 ± 0.06	0.70 ± 0.06
	Kraft <i>et al.</i> (1987) ^{d,e}	0.64	–
	Jones (1997) ^f	0.644 ± 0.002	0.698 ± 0.005
Gd-DTPA	Tofts <i>et al.</i> (1993) ^g	4.50 ± 0.04	5.49 ± 0.06
T_2			
Mn ⁺⁺	Morgan and Nolle (1959) ^c	7.0 ± 0.4	70 ± 4
	Bloembergen and Morgan (1961) ^h	8.0 ± 0.4	80 ± 7
Agarose	Mitchell <i>et al.</i> (1986) ⁱ	0.05	10
	Tofts <i>et al.</i> (1993)	0.01 ± 0.01	9.7 ± 0.2
	Jones (1997) ^f	0.04 ± 0.01	8.80 ± 0.04

Correcting for phantom temperature

- T_1 , T_2 and ADC, all vary by about 1–3%/°C.
 - Even PD and MRS depends on temperature

TABLE 3.8 T_1 values for pure water

Temperature (°C)	T_1 (s)
0	1.73
5	2.07
10	2.39
15	2.76
20	3.15
21*	3.23
22*	3.32
23*	3.40
24*	3.49
25	3.57
37*	4.70

- Measurements were made at 28 MHz

Dielectric effect in depth of large volume

- Water has high *dielectric constant* ($\epsilon = 80$) leads to the presence of *radiofrequency standing waves (dielectric resonance)*,
 - This causes *B_1 be enhanced*, giving an artificially high flip angle and signal in depth
 - high dielectric constant reduces the wavelength of electromagnetic radiation, by a factor $\sqrt{\epsilon}$.
- at 3T the wavelength is 260 mm, comparable with the dimensions of a head phantom
- Dielectric effect is also present in the head, particularly at high field, but *electrical conductivity* in the brain tissues damps the resonance

Oil Phantoms

- *Oil* has a low dielectric constant ($\epsilon = 2-3$) and has been used for non-uniformity phantoms.
 - Several kinds are available, but cooking oil is a convenient source.
 - It has T1 and T2 close to most invivo values
 - *Silicone oils* gave $T_1 \simeq 800$ ms, $T_2 \simeq 100$ ms at 1.5T

TABLE 3.6 RF nonuniformity in a uniform phantom – maximum phantom diameter

Field B_0	Water ($\epsilon = 80$)	Oil ($\epsilon = 5$)
0.5T	138 mm	551 mm
1.5T	46 mm	184 mm
4.7T	15 mm	59 mm

The maximum diameter of a long cylinder phantom for uniformity not more than 2% as a result of dielectric resonance

Pure PD measured by MRI

- PD mapping is based on the estimation of the equilibrium magnetisation (M_0), in MR signal intensity model, in the absence of relaxation mechanisms:

$$S_{(TR,TE)} = M_0 \left[1 - e^{-\frac{TR}{T1}} \right] e^{-\frac{TE}{T2}}$$

- Image should be acquired with short TE to minimize T2 loss and long TR to minimise T1 loss, But still PD has signal loss due to relaxation times.
- Measured M_0 not only depends on Pure PD but also on the receive coil's sensitivity profile (B_1^-):

$$M_0 = B_1^- \cdot PD$$

- B_1^- sensitivity is caused by tissue absorbance and coil spatial inhomogeneity.

PD measurement step by step

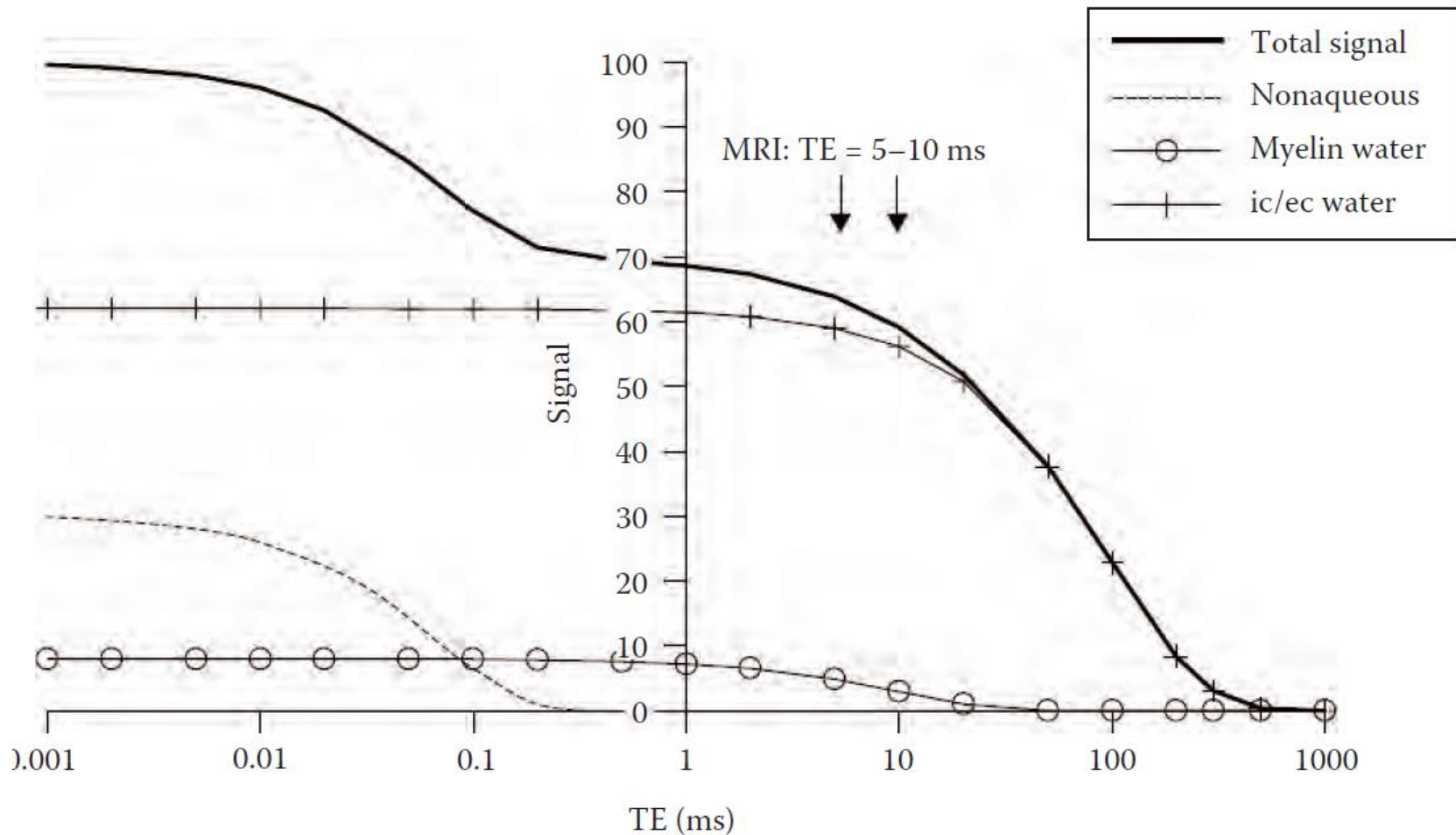
- 1. Estimate M_0 :** acquisition and analysis of data according to one of the following methods:
 1. Using multicompartment T2 model: M_0 is equal to the sum distribution of different compartment in a voxel.
 2. Using T2* extrapolation, from low TE signal to TE=0 signal
 3. Using a single short TE acquisition as an approximation for TE = 0.
 4. simultaneous M_0 and relaxation times acquisition (simultaneous parameter fitting) or variable flip angle method
- 2. Consider non- M_0 contributions:** correction for signal loss due to relaxation times and inhomogeneities of transmit field B_1+ and static magnetic field (B_0).
- 3. Extract PD from M_0 :** calculation and correction of the receive coil sensitivity profile.

Multicompartment T2 method for M_0 estimation

- signal is separated into three components corresponding to different water environments:
 1. a long T2 component (~ 2 s) due to CSF;
 2. an intermediate component (~ 100 ms) arising from intracellular and extracellular water;
 3. a short T2 component (~ 20 ms) due to water trapped between the myelin bilayers.
- The integral over this distribution provides the total contribution of the different water environments to the signal and therefore is proportional to M_0 .
- gradient and spin echo or spin echo sequences can be used

T2* extrapolation for M₀ estimation

- In this approach, a T2* image is acquired with a short TE, as the first point on the signal decay curve. (Usually 2 short TE of 5 and 10 ms)
- Then the T2* relaxation curve is extrapolated to TE = 0, using a polynomial of third order
 - At this point, before spin relaxation causes a decay of the signal, the signal is proportional solely to the amount of water protons.
- Alternatively, a single short TE acquisition is used as an approximation for TE = 0.
- M₀ is mapped based on the acquisition of a series of spoiled gradient-echo images with different T2* weightings (acquired with quantitative T2* image sequence)
- It is possible to apply variable flip angle of a spoiled gradient echo sequence to quantify T1 and M₀



Symbolic illustration of tri-exponential decay of transverse proton signal in white matter, using realistic T2 values, 30% of the protons are non-aqueous ($T_2 = 70 \mu\text{s}$), 8% are water protons trapped in myelin ($T_2 = 10 \text{ ms}$) and 62% are in intra- and extracellular (ic/ec) water.

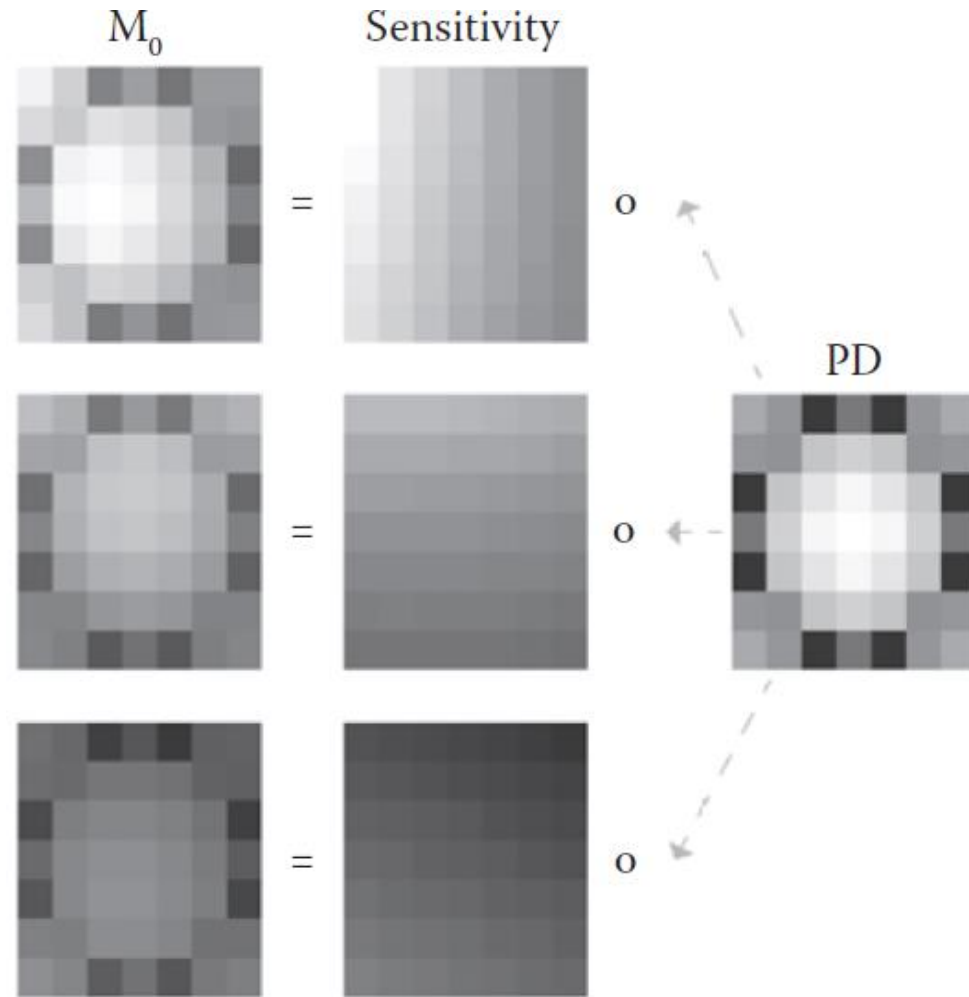
Simultaneous fitting of M_0 and relaxation times (for M_0 estimation)

- Multiple TE images are used for determination of T2 relaxation time. T1 and M_0 are estimated based on the images with different TD (delay time).
- Overestimation of PD can be happened because of the number of expected relaxation points on a mono-exponential fit.
- One proposed method is Inversion recovery balanced steady-state free precession (IR-bSSFP)
- MR fingerprinting is a type of simultaneous measurements of multiple tissue parameters such as T1, T2 and M_0 , using a single MR scan.
 - It is based on matching randomly acquired incoherent signals to a dictionary produced by simulations of the time evolution of the magnetization.

Correction of PD for receive coil sensitivity

- The receive coil's ability to pick up the signal is inhomogeneous and depends on coil size and its distance from the object.
- Thus, signal intensity has some nonuniformities imposed by spatial variations of the receive coil sensitivity profile.
- PD can be extracted from M_0 through estimation of the receive coil sensitivity profile.
 - approximating the coil sensitivity as a smooth function (usually second-order polynomials) in adjacent voxels.

Example Correction of PD for receive coil sensitivity



The relationship between proton density (PD), coil sensitivity (B_1^-) and M_0 .

The PD values are multiplied, point by point, by coil sensitivities, to produce the M_0 images

Proton Density importance in biological tissue

PD is useful for Water Content (WC) evaluation of biological tissues.

- WC changes in aging and due to inflammation or oedema, MS, brain tumours, stroke, hepatic encephalopathy and head traumas
- PD visible signal is related to mobile water, not protons bound to macromolecules or in phospholipids due to very short T2 (abundance of mobile lipids in the brain is low).
- PD measurement is independent of field strength, but is attributed to receive coil sensitivity and other source of signal loss biases.
- MRI signal intensity is proportional to WC, in absence of signal loss due to relaxation and magnetic field inhomogeneity

Proton Density calculation and relation

- number of protons per unit volume of tissue is defined as the *absolute proton concentration* or PC of a tissue

$$PC = \frac{NP\rho}{MW_t} [M]$$

- NP is the number of protons per molecule,
- ρ is the density (g/L),
- MWt is the molecular weight (g/mol)
- Therefore the units of PC are molar (M).
- For water PC = 110.4M because NP = 2; ρ = 993.4 g/L at 37°C; MWt = 18 g/mol)
- concentration or molarity of pure water 1000g/18g/mol= 55.2 M

Calculation of WC

- The WC of a tissue is usually calculated as PC (concentration of water protons) in tissue, calibrated to the PC of pure water (in the same volume and temperature). Thus:

$$WC = 100 \frac{PC}{110.4} [\text{pu}]$$

PC is in molar, and WC is in pu (percent units). Pure water has PC of 110.4 and therefore WC = 100 pu.

CSF has WC \approx 100 pu

White matter has WC \approx 70 pu

Gray matter has WC \approx 80 pu

Water content measurement of biological tissues

- After all biases have been removed the M_0 estimation can be translated into accurate PD measurement and calibrated to produce WC.
- Since, PD is only proportional to the amount of protons in the voxel and does not directly measure it, a **calibration standard is needed to get a quantitative measurement of WC**.
 - We know the percentage of protons in pure water is 100 pu, therefore its PD could serve as a good calibration standard.
- WC can be obtained as the fraction of water protons in a tissue (PD_{tissue}) relative to the maximum possible number of water protons in a voxel (PD_{water}).
- There are two different approaches for estimating PD_{water} :
 - internal reference (the free water in the ventricles as an approximation of pure water standard)
 - or an external reference (pure water phantom is added to the scan)

Biophysical relationship between WC and T1

- As we know PD and therefore WC measurements correlate with T1 in human brain tissue. Since T1 is largely affected by the fraction of water, a linear relationship between 1/WC and 1/T1 can be stated as follows

$$\frac{1}{WC} = \frac{\gamma}{T1} + \delta$$

- γ and δ are arbitrary constants representing the slope and offset of the linear relationship.
- Also WC can be impaired due to additional factors that can change T1 such as high iron content.
- Thus, one should be careful when implanting the linear relationship constraint in abnormal tissues.
- To prevent this, a regularization term using prior knowledge or assumptions is introduced to the PD and B_1^- fitting as an additional constraint

Validation of WC estimations

- Validation can be done in phantoms with known water concentration
- Or can be assessed in tissues based on weight loss on evaporation

WC Application (WC vs VBM)

- VBM analysis reveals large volumetric changes due to **various effects rather than local**, voxel-level effects.
- Measuring WC would help to differentiate the volumetric changes from the local changes in water and non-WC Volumetric entities.

WC Application

(WC effects MR parameters)

- As water is the source of the MRI signal, WC affects the measurement of other MRI parameters such as T1, MTR, and Diffusion.
- Contribution of WC to the measurement of MR parameters is important, as changes in WC may confound other tissue properties.
- Estimation of the correlation between the MR parameter of interest and the WC is essential for the biophysical interpretation (tissue properties) of the measurement.

WC Application (WC effects on T1)

- The relation between T1 and WC can also be used to quantify the extent to which changes in T1 are affected by WC.
- It was found that **differences in WC between grey matter regions** account for most of the interregional variation of T1 values.
- T1 depends on both WC and lipids type, but **WC was found to be independent to macromolecule** containing different lipids compositions.
- Therefore, **T1 does not depend solely on WC** and is thought to reflect various biophysical properties of the tissue such as iron.

WC Application (WC effects on MT)

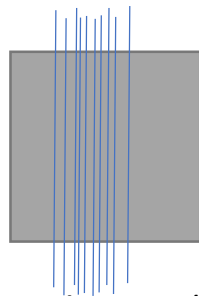
- Magnetization transfer is an MRI measurement that examines the **interaction between mobile protons in water and bound water protons**. The amount of MT between these pools is MTR.
- Changes in MTR are often caused by alterations in myelin contents.
- However, changes in MTR can also happen, unrelated to myelin, but due to edema and inflammation.
- It is therefore incorrect to associate decreases in MTR in MS lesions exclusively with demyelination.
- The use of WC mapping in the analysis of MT data enables the **separation between the contributions of oedema and demyelination**.

WC Application (WC effects on DWI)

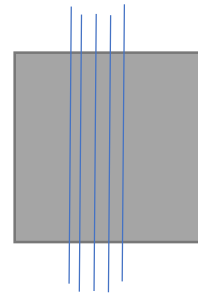
- It is shown that crossing fibers decreases fractional anisotropy (FA).
- Also, Low axonal filling reduce FA. Therefore it is difficult to discriminate between different mechanisms that influence FA.
 - Fortunately, the crossing fibers do not considerably affect the MTV (1-WC).

Complementary 1-WC can serve as a measurement of the macromolecule and lipid tissue volume (MTV)

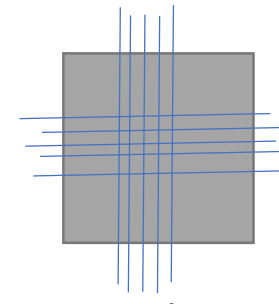
- Therefore, Combining the two measurements, FA and MTV can help to evaluate crossing fibers.
 - if MTV and FA change together, that means an axon-packing difference is present.
 - If MTV is High but FA Low, this means the change is due to an axon incoherency.



High FA, High MTV (Low WC)
Coherent & high directional fibers



Low FA, Low MTV
low directional fibers



Low FA, High MTV
incoherent and crossing fibers

WC Application

(WC for calibration of different MR Quantification)

- Quantification of brain absolute metabolite concentration by **spectroscopy** imaging requires calibration water standard, obtained from WC map.
- In addition, **WC decreases with maturation** was shown to affect parameters of cerebral oxygenation determined by MRI.

WC Application

(Age evaluation by WC)

- It was shown that grey matter **WC decrease with age** (in male much stronger decrease during age)
- WC measurement was used to extract MTV (1-WC) for brain regions.
 - It was shown that in the posterior fusiform gyrus, mean **MTV increased by 12.6% from childhood to adulthood.**
- White matter development and ageing over an 80-year period of the lifespan was shown that 1/T1 and MTV (1-WC) growth curve has a symmetric second-order polynomial shape.
 - This implies that the rate of growth and decline are symmetric. MTV values reach their peak between around 40 years of age and then decline, returning to their 8-year-old levels at ages of about 80.

WC Application

(WC changes in edema and inflammation)

For example:

- WC mapping provided evidence for the association between the pathophysiology of hepatic encephalopathy and edema.
- Tissue WC demonstrated that the amount of brain swelling and edema correlates with disease grade.

How to measure T1

Physical basis of T1

- In magnetic field \mathbf{B} and before RF transmission, equilibrium conditions exist between parallel and antiparallel spins.
- equilibrium **magnetization** \mathbf{M} is parallel to \mathbf{B} known as longitudinal component with equilibrium value M_0 , but transverse component is zero.
- After 90° RF, the *equilibrium value* \mathbf{M} has now a non-zero transverse component (with maximum value M_0), which rotates around \mathbf{B} with Larmor frequency, and can produce signal measured in MRI system. the longitudinal component of \mathbf{M} is reduced to zero.
- If RF turn off, the spin system approaches again longitudinal equilibrium conditions, by a phenomenon called *T1 relaxation (as well as starting transverse relaxation)*.
- During the longitudinal relaxation, the spins release the excess energy, which is absorbed by the surrounding *lattice*, that is by molecules in the neighborhood.

T1 recovery signal model

- Mathematically, the process is described by Bloch equations:
 - assuming that the static magnetic field is applied along the z-axis:

$$\frac{dM_z}{dt} = \frac{M_0 - M_z}{T_1}$$

- The solution of this Equation is an exponential change of M_z towards the equilibrium value M_0

$$M_z(t) = M_0 + [M_z(0) - M_0] \exp(-t/T_1)$$

- the *inversion recovery* curve, after a full spin inversion, is $M_z(0) = -M_0$

$$M_z(TI) = M_0 [1 - 2 \exp(-TI/T_1)]$$

Biological basis of T1

- T1 value is related to:
 - (a) the free water content
 - (b) the concentration and types of macromolecules such as myelin
 - (c) the iron content
- In general increasing water content prolongs T_1 ,
- increasing iron content and myelination reduce T_1
- cerebrospinal fluid has longer T_1 than cerebral white matter and gray matter due to the high water content.
- T_1 in WM is shorter than in GM, mainly due to the larger proportion of myelin and smaller water fraction in WM.

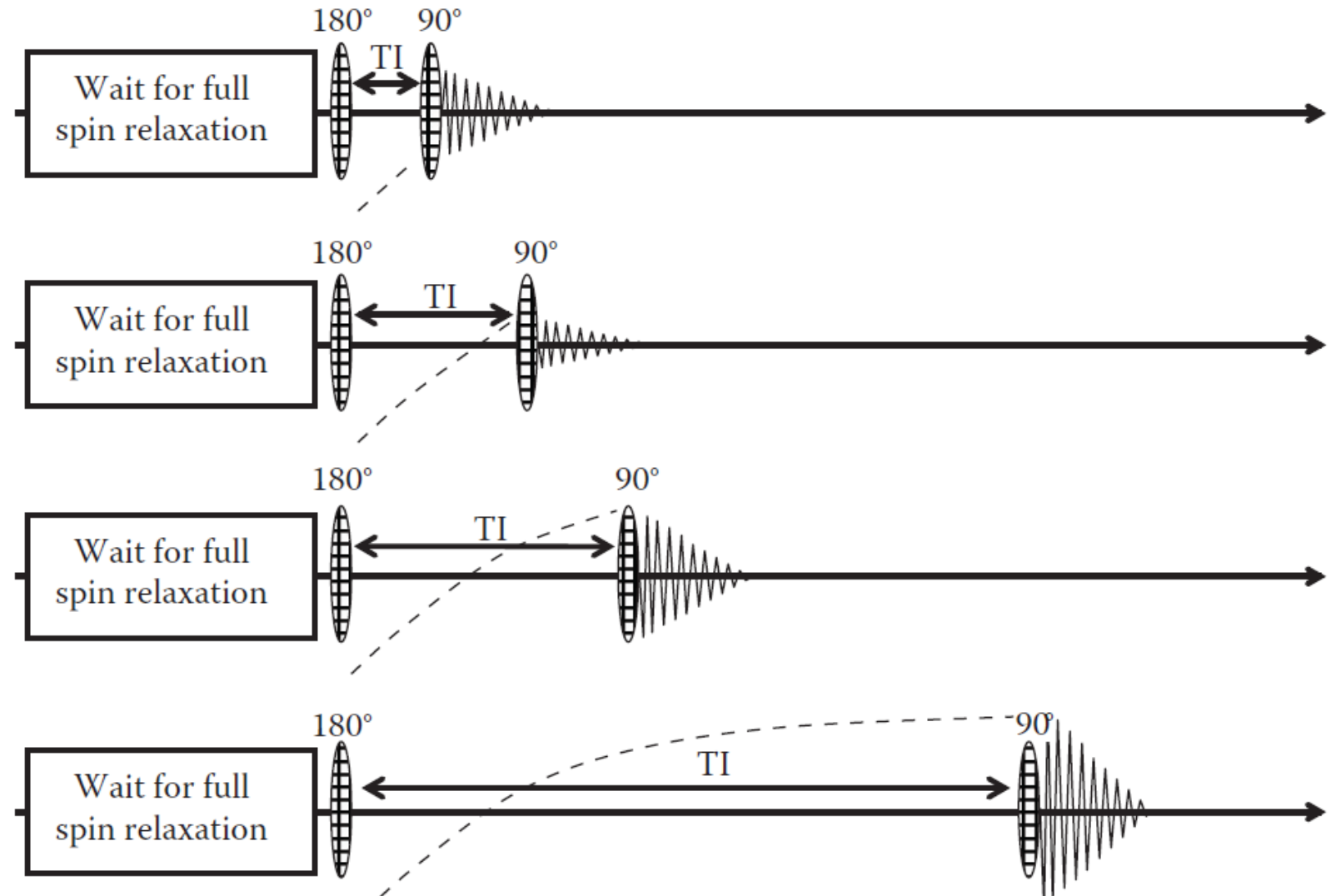
T1 values (in ms) of normal brain tissue at different static magnetic field strengths

Field Strength	Reference	White Matter	Grey Matter	Caudate Nucleus	Putamen	Thalamus
0.2 T	Rooney <i>et al.</i> (2007)	361 ± 17	635 ± 54	555 ± 19	524 ± 19	522 ± 44
1.0 T	Rooney <i>et al.</i> (2007)	555 ± 20	1036 ± 19	898 ± 45	815 ± 16	807 ± 47
1.5 T	Steen <i>et al.</i> (1994)	606 ± 21	1170 ± 43	948 ± 32	834 ± 19	774 ± 16
2.0 T	Deichmann <i>et al.</i> (1999)	682 ± 4	1268 ± 29			
3.0 T	Clare and Jezzard (2001)	860 ± 20		1310 ± 60	1100 ± 30	1060 ± 40

Gold standard: The inversion recovery technique

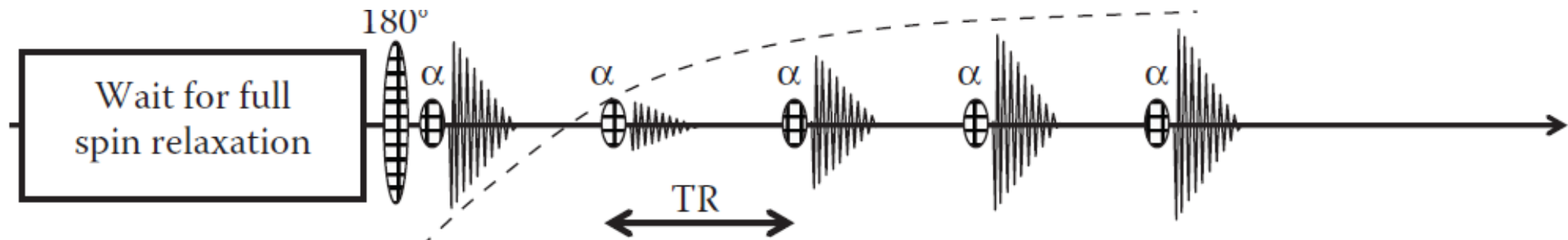
- By varying TI, the inversion recovery curve is sampled, then T1 can be obtained via exponential data fitting.

- The problem of IR method is that equilibrium conditions have to be attained before each single experiment (this is about $5 \cdot T_1$) for a full spin relaxation before each spin inversion. Therefore it is time consuming.



Look-Locker technique

- The idea is to measure T1 during one single T1 relaxation process.
- After inverting the magnetization, a series of excitation pulses with a small tip angle α and an intermediate repetition time TR is sent.
 - Each pulse tilts the magnetization, creating a transverse magnetization signal which is proportional to the current value of the longitudinal magnetization M_z .



- T1 can be obtained via exponential fitting of the sampled curve T1.
- The problem is that the excitation pulses distort the free relaxation curve and needs to be corrected.
- The data is acquired by a series of spoiled gradient echo (GE) images after spin inversion.

variable flip angle technique

- is based on the acquisition of GE data sets.
- The underlying idea is to acquire several data sets with different excitation angles α and to evaluate the signal dependence $S(\alpha)$ for each pixel.
- M_z corresponds to the steady-state condition to obtain value M_0
- In contrast to the LL technique, acquisition times are considerably longer than $T1^*$, due to the use of relatively long TR.
- Acquiring 3D data sets with a high spatial resolution is possible.

variable flip angle technique

- The signal is given by the longitudinal magnetisation M_z directly before RF excitation, multiplied with the sine of the excitation angle.

$$S(\alpha) = S_0 \sin(\alpha) \frac{1 - \exp(-TR / T_1)}{1 - \cos(\alpha) \exp(-TR / T_1)}$$

To simplify the analysis, this equation is rewritten

$$S(\alpha) [1 - \cos(\alpha) \exp(-TR / T_1)] / \sin(\alpha) = S_0 [1 - \exp(-TR / T_1)]$$

- or

$$S(\alpha) / \sin(\alpha) = \exp(-TR / T_1) S(\alpha) / \tan(\alpha) + S_0 [1 - \exp(-TR / T_1)]$$

- This equation implies a plot of y_i versus x_i in a linear dependence with the slope m , from which T_1 can be derived ($y=mx+c$)

$$y_i = S_i / \sin(\alpha_i) \quad x_i = S_i / \tan(\alpha_i) \quad m = \exp(-TR / T_1)$$

Optimum Flip Angle

- Usually two-point measurement is required. The two optimum excitation angles can be calculated as follows (for the TR chosen and the approximate target T1 value):

$$\tau_E = 2 \cdot \sqrt{\frac{1 - \exp(-TR/T_1)}{1 + \exp(-TR/T_1)}}$$

- The optimum angles α_1 and α_2 are then given by:

$$2 \cdot \tan(\alpha_i/2) = K_i \cdot \tau_E \quad \text{with : } K_1 = 0.4142 \text{ and } K_2 = 2.4142$$

- For the VFA technique, a duration of about 10 min has been reported for the acquisition of a T1 map with whole brain coverage and an isotropic resolution of 1 mm, based on two GE data sets with different excitation angles
- VFA requires correction for nonuniformities of the RF transmit profile, an additional duration of about 1 min for B_1 mapping should be considered.

How to measure T2

Physical basis of T2

- M_{xy} is the transverse magnetization at time t following the pulse and M_0 is equilibrium magnetization, assuming a perfect RF pulse that fully tips the magnetization into the transverse plane.
- The decay is occurred (called *dephasing*) when sets of nuclei in a **molecule interact with each other** and electrons in their local environment.
- Dipolar effects between them cause fluctuations in the magnetic field and a **shift in Larmor frequency**.
- As they destructively interfere, reducing the net magnetization. Since this process involves other nuclei it is often called *spin-spin relaxation*.

T2 Decay signal model

$$M_{xy} = M_0 \exp(-t/T_2)$$

- MR signals decay more rapidly than suggested in Equation by extra dephasing.

$$1/T_2^* = 1/T_2 + 1/T_2'$$

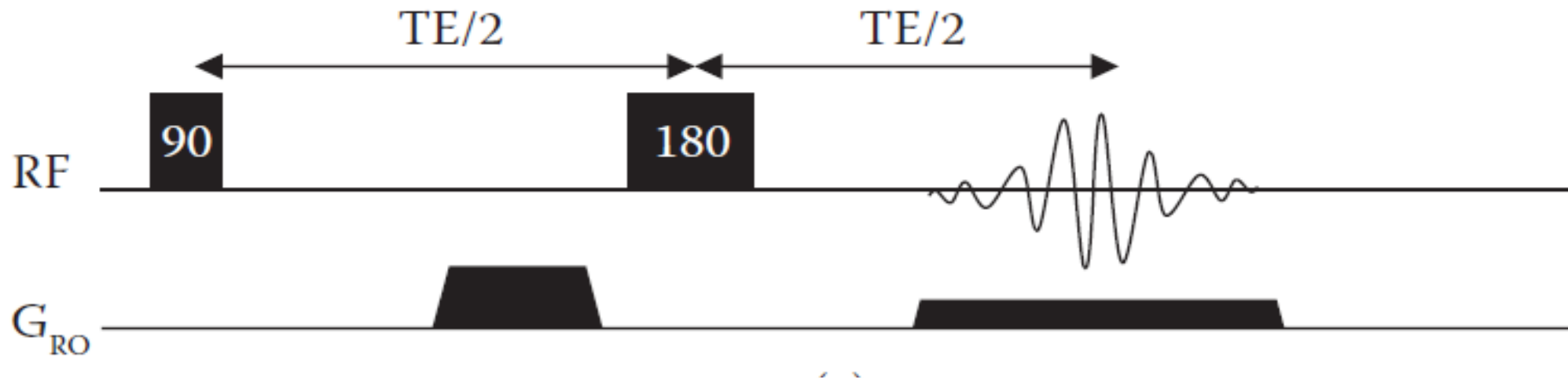
- Since resonance frequency of isochromats is dependent on the local magnetic field, which is not homogeneous due to **imperfections in the magnet**, **chemical shift** effects, **macroscopic susceptibility** differences or the presence of paramagnetic or ferromagnetic substances, This causes accelerated dephasing, leading to short-lived MR signals parameterised by T_2^*

Biological basis of T2

- For the nuclei which are free to tumble (eg in water in CSF), dipolar interaction is low, and hence the effect is small and T_2 remains long, in the range of seconds.
- But, the biological environment may result in highly restricted motion. This is observed in solid components such as bone, cartilage, ligaments and tendons, which have short T_2 of the order of tens of microseconds.
- The brain possesses several biologically interesting components such as lipids and proteins that are classed as semi-solids that are not able to tumble freely, and so appreciable dipolar coupling reduces T_2 to the sub-millisecond range. These spins are invisible to conventional MR methods, but are visible to ultrashort (UTE) or zero echo-time methods.
 - For example, WM has a T_2 of around 50 ms, different from T_2 of cell membranes, myelin, proteins, etc., that make up 'white matter'.
- Multicomponent models attempt to solve this problem by modelling the signal as a sum of contributions from different spin populations.

Gold standard for T2 Quantification: 1- SPIN Echo technique

- 180° around B_1 inverts any phase accrued by the isochromats during the first evolution interval.
- The phase accrued due to external bodies (T_2') is the same in both evolution intervals and hence cancels out, while T_2 effects of tissue itself remain.



Pulse sequence diagram for the spin echo. Only the readout gradients are shown for clarity.

Gold standard for T2 Quantification: 1- SPIN Echo technique

- Assuming a single T_2 within a voxel, changing the echo time will result in modulation of signal S according to

$$S = S_0 \exp(-TE/T_2)$$

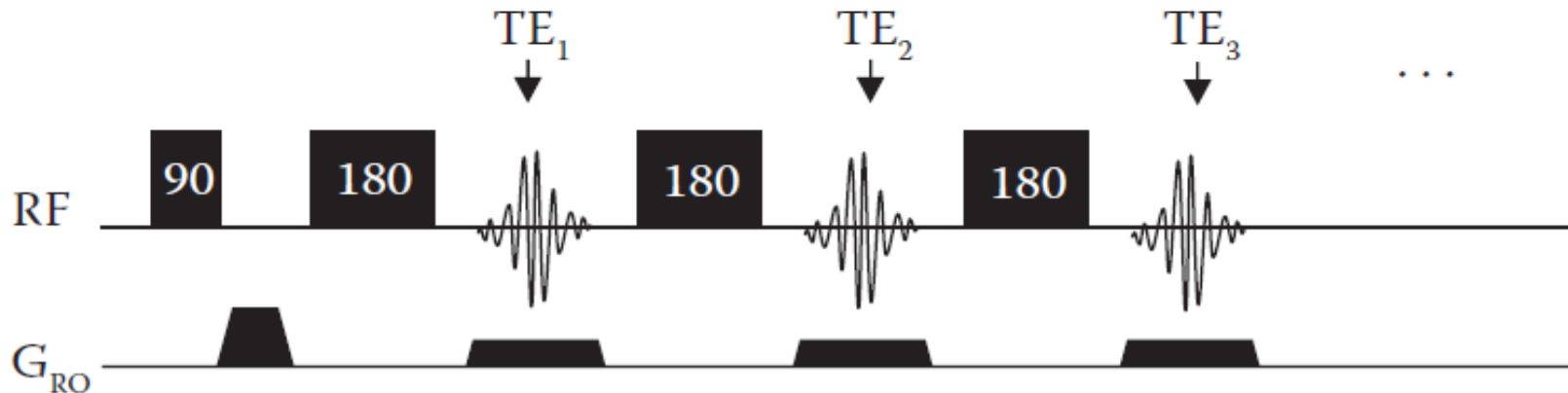
- T_2 can be calculated from two measurements, S_1 and S_2 , with corresponding echo times, TE_1 and TE_2 ,

$$T_2 = \frac{TE_2 - TE_1}{\log(S_2) - \log(S_1)}$$

- However, this shows a **mono-exponential problem**, therefore, partial volume effect and compartmental voxels can not be calculated by this model. By sampling the signal decay at a **range of different TE** it is possible to generate a decay curve with improved accuracy and precision.

Edited SE technique (1)

- The spin echo can be accelerated by using **multiple 180° refocusing pulses** and readout periods at increasing TE, referred to as the *multi-echo T2* approach. Carr–Purcell–Meiboom–Gill (CPMG) sequence improved the method by applying a **180° phase increment** to each successive refocusing pulse in the train.
- **Mono-exponential approaches** require only a few echoes, ranging from 20 to 160 ms. **Multi-exponential approaches** require more echoes, typically 16 or 32, spanning a wide range of echo times to capture both short and long T_2 components.



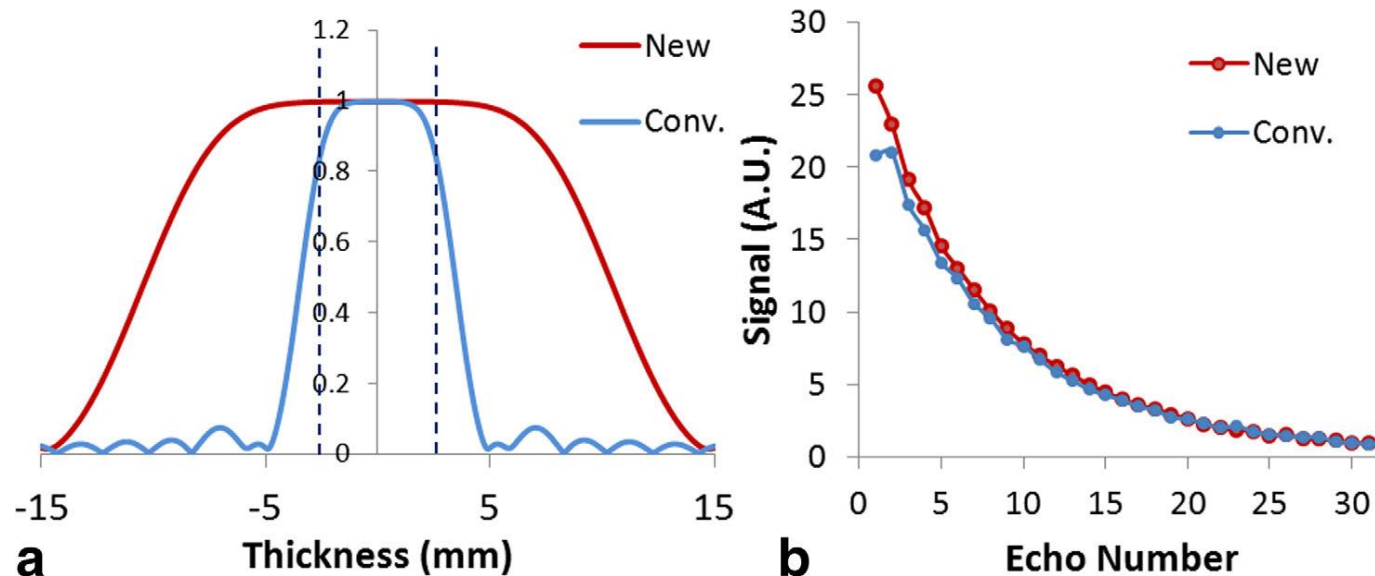
Pulse sequence diagram for the Carr–Purcell–Meiboom–Gill (CPMG) multiple spin echo

Edited SE technique (2)

- The conventional multi-echo CPMG sequence for T2 relaxation measurement was dramatically affected by the **stimulated echo** caused by **slice profile imperfections of refocusing RF pulses** (ie Errors in B_1). Due to intrinsic sensitivity to refocusing imperfection, the measured curve may deviate from the true T2 decay curve.
- A **nonselective composite refocusing pulses** ($90_x^\circ - 180_y^\circ - 90_x^\circ$) are used to reduce effects of inhomogeneities in B_0 and B_1 (Poon and Henkelman, 1992). The **180° refocusing pulses are phase shifted by 90°** relative to the initial 90° excitation pulse.
 - The error due to imperfect tip angles of refocusing pulses is compensated.
- Also, a **slice-selective z-axis crusher gradients** are applied each side of the refocusing pulse to attenuate flow artefacts and stimulated echoes **outside the slice**.
- Disadvantage is: the **single-slice coverage and the long acquisition time** (e.g., 25 min) due to nonselective refocusing pulses, and a low SNR for clinical applications.

Edited SE technique (3)

- One way to increase volume coverage is to use a conventional multi-slice CPMG sequence with **slice selective refocusing pulses that are much wider than the excited slices**, instead of non-selective pulses. This ensures a **good slice profile** while allowing multislice acquisition (Guo *et al.*, 2013).
 - Disadvantage: a large slice gap to prevent contamination adjacent slices is required.
- A technique that uses refocusing pulses with a **slice thickness 3 times the size of the excitation pulse** was proposed to diminish deviations and optimize T2 decay curves for T2 measurements.

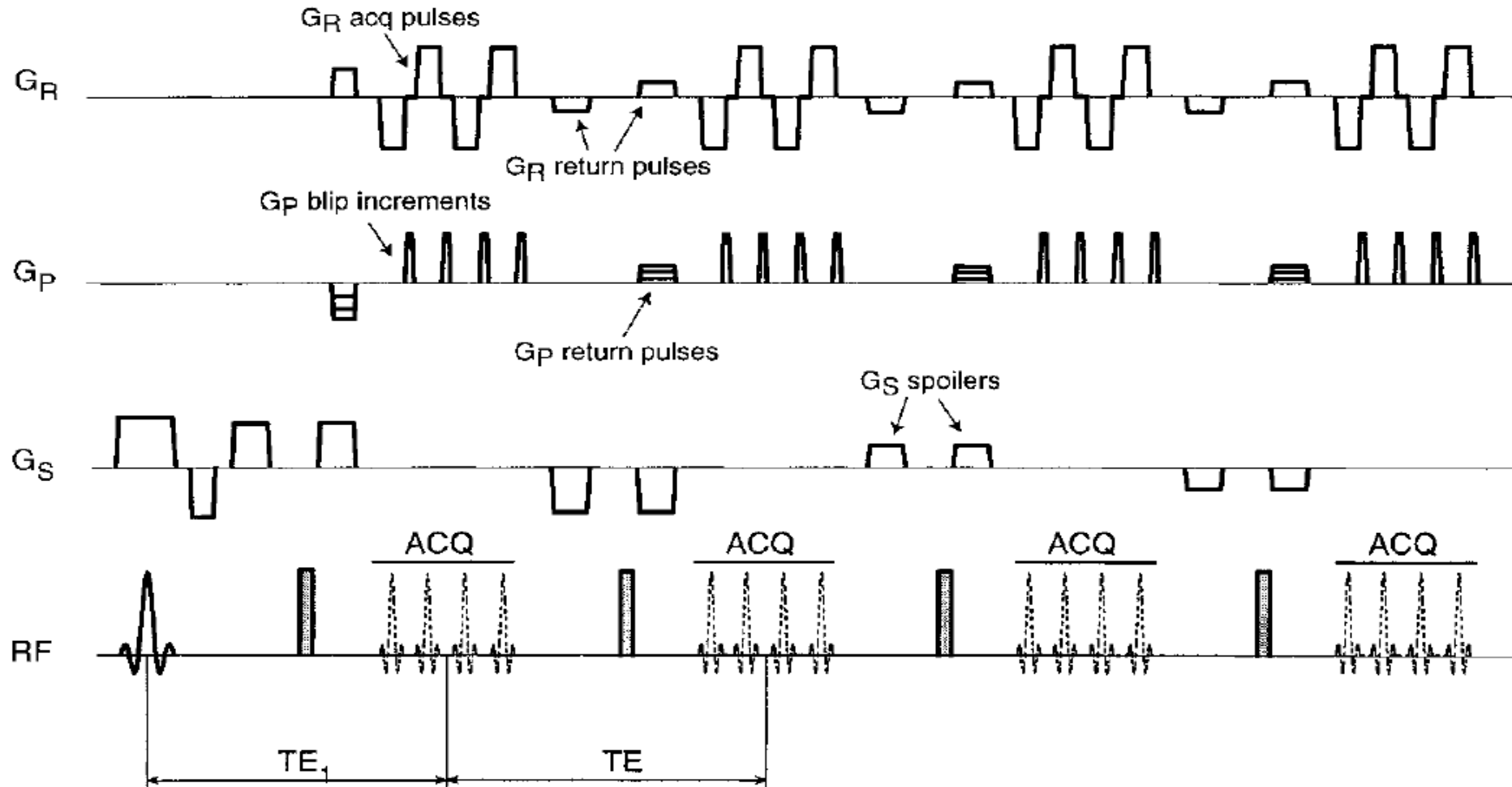


Slice profile of RF180 and its effects on the decay curve

Edited SE technique (4)

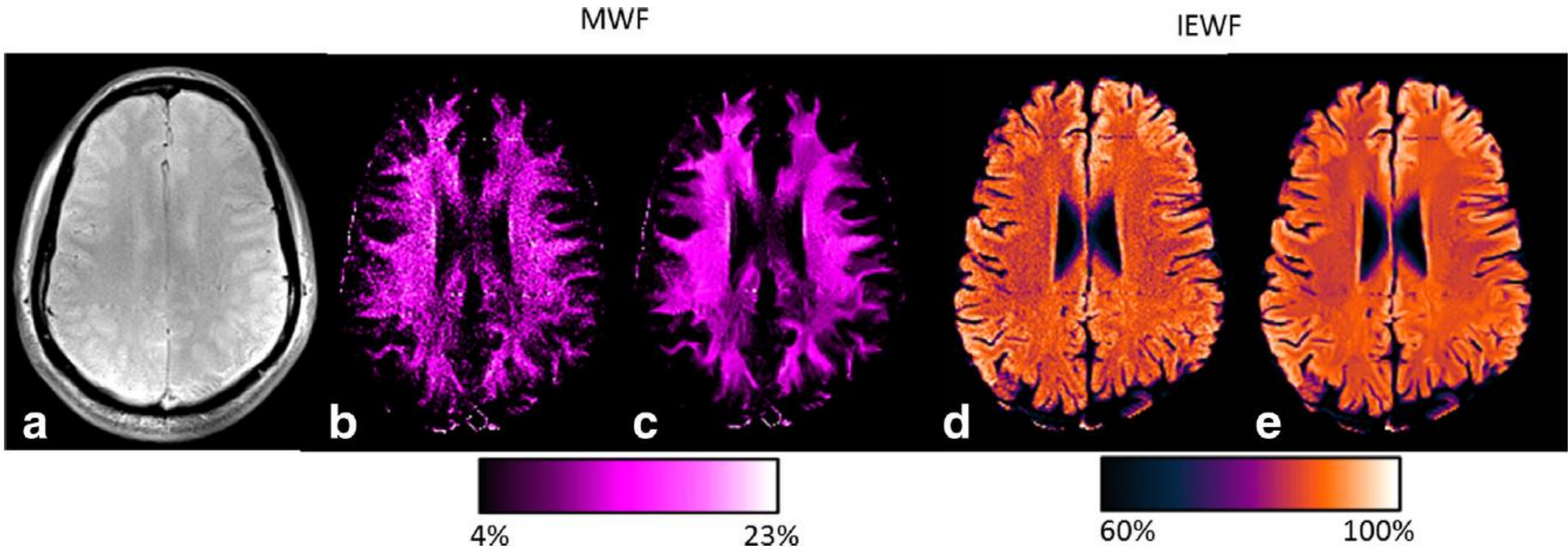
- The number of acquired slices can be increased by using a **gradient and spin echo (GRASE)** acquisition (Does and Gore, 2000), which accelerates acquisition of k -space by collecting 4 or more gradient echoes before and after each spin echo. This results in **pure T_2 weighting at the center of k -space**, with additional T_2^* weighting towards the edges.
- GRASE can be used as a segmented EPI technique as the following for fast and even 3D imaging:
 1. The RF train is that of a **CPMG sequence** with a slice-selective excitation pulse and refocusing pulses.
 2. Surrounding the refocusing pulses are **slice-selection spoiler gradients**, to eliminate signal from unwanted coherence spins.
 3. The read gradient channel includes lobes of alternating polarity for acquisition of 4 gradient echoes during each spin-echo period.
 4. Following each read gradient lobe, a phase gradient blip increments the k -space trajectory as an interleaved segmented EPI acquisition.

example of a GRASE is RARE (rapid acquisition transverse relaxometry)



- An example of a RATE pulse sequence showing collection of four echo images (NE) with a $N_{GE}=4$

Healthy Myelin water Fraction and Intra-Extra cellular water fraction



(a) Original magnitude image. (b,d) MWF and IEWF maps without the nonlocal mean filter. (c,e) Corresponding MWF and IEWF maps with the filter.

Analyzing based on a multicomponent basis

- If more than two echoes have been acquired, a **least-squares fit of TE against the logarithm of the signal** is the most common method of calculating T_2 .
 - More echoes are needed for multi component voxels. If only a few (typically three or four) compartments are chosen, then a non-linear multi-parameter fitting routines can be used.
- With sufficient points MET2 data can also be analyzed on a multicomponent basis. The measured signal is modelled as a sum of several discrete T_2 decay curves, where the signal at each TE is given by:

$$\tilde{S}(TE_i) = \sum_{j=1}^M s_j e^{-\frac{TE_i}{T_{2,j}}} + \epsilon_i$$

- The presence of noise means that many possible T_2 distributions are acceptable. However, **Regularization needs** to restrict the set of T_2 distributions to the least complex.

T2 Quantification: 2- Steady State technique

- **Driven equilibrium single-pulse observation of T2** (DESPOT2 (Deoni *et al.*, 2003, 2005)) uses a balanced steady-state free precession (bSSFP) pulse sequence, which has a combined $T2/T1$ contrast, to measure $T2$ using the same framework as DESPOT1.
- Neglecting off-resonance effects, the bSSFP signal equation is:

$$S(\alpha) = \frac{M_0(1 - E_1)\sin(\alpha)}{1 - E_1E_2 - (E_1 - E_2)\cos(\alpha)}$$

$$E_1 = \exp(-TR/T_1), \quad E_2 = \exp(-TR/T_2)$$

- The equation can be rearranged into a linear form:

$$\frac{S(\alpha)}{\sin(\alpha)} = \frac{S(\alpha)}{\tan(\alpha)} \times \frac{E_1 - E_2}{1 - E_1E_2} + \frac{M_0(1 - E)}{1 - E_1E_2}$$

- hence a plot of $S(\alpha)/\sin(\alpha)$ against $S(\alpha)/\tan(\alpha)$ can yield $T2$ from the slope m and $T1$, which is typically found using DESPOT1:

$$T_2 = -\frac{TR}{\ln\left(\frac{m - E_1}{mE_1 - 1}\right)}$$

Problems with Steady State technique

- Both DESPOT1 and DESPOT2 rely on an exact knowledge of α , which can be problematic due to *B1 field inhomogeneity*. In addition, at high field-strength, off-resonance effects cannot be neglected due to *banding artefacts*.
 - but these can be reduced by acquiring multiple images with different phase increments (also called *phase cycling*).
- At 3T, at least six separate images are required, two gradient-echo for DESPOT1 and four bSSFP for DESPOT2 (two flip angles and two phase increments), plus a separate *B1* map.
- Multicomponent DESPOT (mcDESPOT) assumes separate short, medium, and long *T2* components, corresponding to myelin water, intra-/extracellular (IE) water, and CSF in each voxel.
- To differentiate the signals from these requires that more volumes be acquired with different flip angles (Eight or nine).

T2 Quantification: 3- T2 prep technique

- *Using T2* weighting via a preparation module and acquire volumes with different **preparation settings** are often faster than conventional methods.
- A *T2*-prep block consists of a **90° pulse, one refocusing pulse, and a -90° pulse** that returns the magnetization to the longitudinal axis. At the end of the prep block, the *T2* weighting of the longitudinal magnetization depends on the amount of dephasing from the measuring voxel.
 - This is also a function of the **number and spacing of the refocusing pulse** and can then be sampled with a fast imaging sequence such as 2D spiral.
- The different *T2* prep images can be fitted to the multicomponent MET2 model.

Common problems with T2 measurement techniques

1. B1 inhomogeneity

2. B0 inhomogeneity

The interaction of the subject with the magnetic field causes magnetic field **varies from location to location**, particularly in areas with large magnetic susceptibility differences, such as air-tissue interface in the sinuses.

In bSSFP, this causes **banding artefacts**, which destroy signal, with position of the bands depends on the product of TR and off-resonance frequency

At 1.5T or less is usually outside the tissues of interest in a well-shimmed magnet, but at 3T or above these effects become significant

3. Magnetization transfer

During an MET2 acquisition, **slice-selective refocusing pulses may act as off-resonance saturation pulses** for nearby slices. This will cause MT effects that result in diminished signal intensity in the free water component and cause inaccuracy in T2 measurements. The use of 3D acquisition reduces the effects of MT

4. Water exchange

MET2 mapping results are often interpreted with the assumption that there is no water exchange between the different compartments on the T2 timescale. **For Smaller water myelin compartments the spins can move** between different T2 environments leading to an underestimation of the myelin water component and hence lower myelin water fraction (MWF).

5. Noise

A common rule of thumb is the shortest echo must have a SNR greater than 100 to avoid any noise effects. This require signal averaging or image smoothing using non-local mean filter.

Applications of T2 measurement:

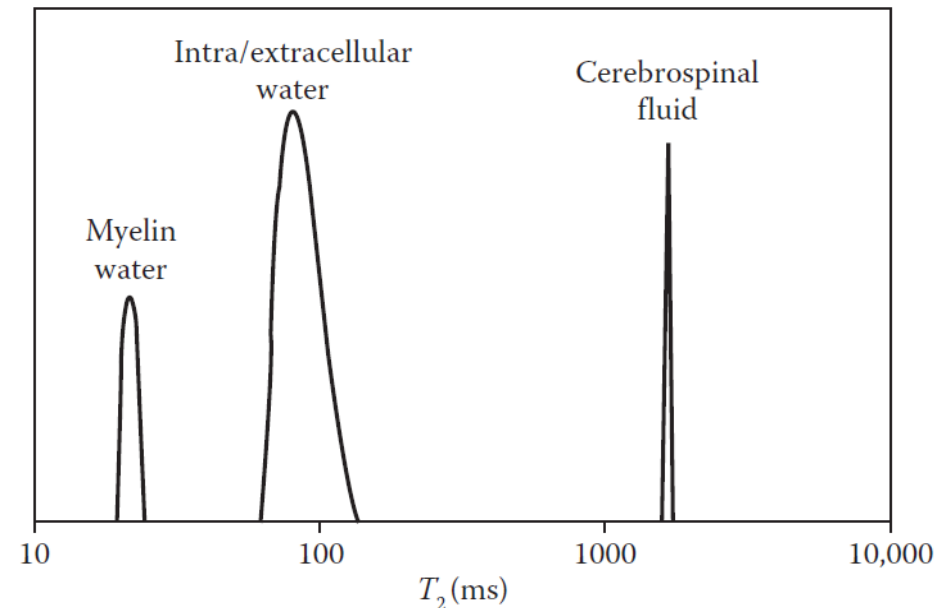
1- Metabolism evaluation

- CMRO₂ (cerebral metabolic rate of oxygen) is a measure of **how fast oxygen is consumed** by the brain during mitochondrial energy conversion processes.
- CMRO₂ is the product of CBF and OEF (the difference in fractional oxygen saturation in arterial and venous blood).
- One method to derive CMRO₂ is TRUST (T2 relaxation under spin tagging). TRUST uses a T2-prep technique with the addition of a pulse that labels venous blood (in contrast to ASL which labels arteries).
 - To measure venous oxygenation, the difference in T2 from both label and control conditions is obtained after T2-prep pulse. Usually, a single slice through the **superior sagittal sinus** or **internal jugular veins** is used for the measurement.
 - To measure CBF, a phase-contrast velocity measurement in the same vein is done.

Applications of T2 measurement:

2- myelin water fraction

- Myelin water is considered an indirect but reliable marker of myelin health, as it is an essential component of the myelin sheath.
- Myelin is a highly complex structure with layers of **lipid and protein** interspersed with **thin layers of water**. This causes restricted motional averaging of water molecules and hence shortens T2s to about 10–20 ms.
- 3 separate components of myelin are
 - 1) water trapped within the myelin layers ('myelin water'; T2 = 5–40 ms),
 - 2) larger component from intra- & extra-axonal water (T2 = 70–100 ms),
 - 3) long T2 (>1 s) that was originally assigned to a CSF fraction
- MWF has become an important metric in the study of multiple sclerosis, Alzheimer's disease, schizophrenia, and study of infant myelination over the first few years of life.
- More useful parameter than MWF is the **myelin volume fraction**, fraction of space in a voxel that is occupied by myelin.



T2* measurement:
Susceptibility Weighted
Imaging and Quantitative
Susceptibility Mapping

Main background Concept

- **Gradient echo** (GRE) imaging, a broad variety of contrasts are possible by varying the flip angle and echo times (TE) for short TR experiments.
- Unlike SE sequences, the **T2* relaxation time** is affected by local sources of magnetic field inhomogeneities.
- These sources of field inhomogeneity, that is the **magnetic susceptibility** property of the tissues, can be used to produce another type of contrast, called Susceptibility weighted imaging. **SWI** utilizes this contrast in the form of the **phase component** of an MRI signal to improve the tissue delineation on magnitude images.
 - Main purpose of SWI is visualization of cerebral venous vasculature, tumors, hemorrhagic lesions, stroke, traumatic brain injury (TBI), and MS
- As an extension to SWI, as use of phase information, is quantitative susceptibility mapping (**QSM**), a method that produces quantification of tissue susceptibility changes.

GRE sequences and T2* relaxation

$$S(\theta) = \rho_0 \sin\theta \cdot \frac{\left[1 - e\left(-\frac{TR}{T_1}\right)\right]}{\left[1 - \cos\theta \cdot e\left(-\frac{TR}{T_1}\right)\right]} \cdot e\left(-\frac{TE}{T_2^*}\right)$$

GRE signal is reduced by:

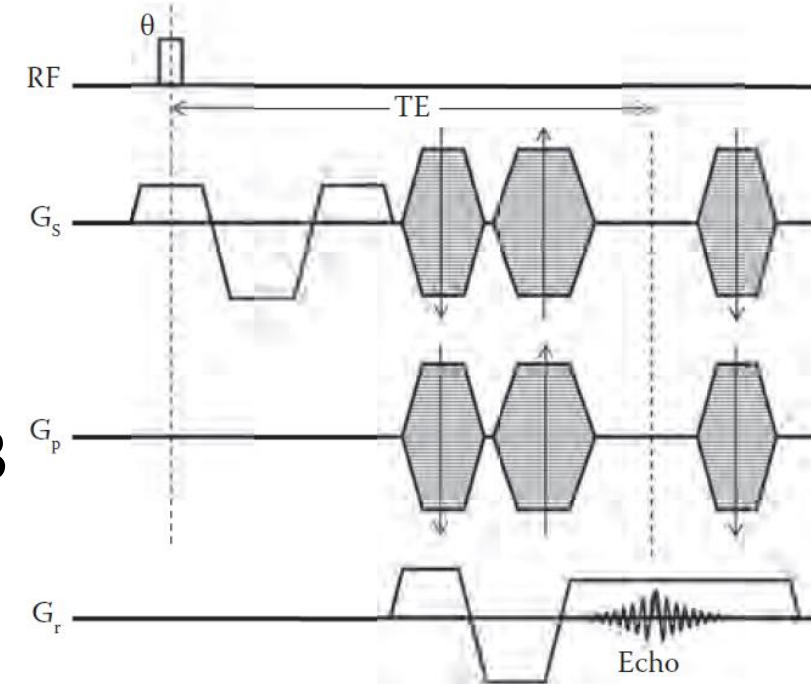
- 1- the dephasing due to **molecular interactions**,
- 2- the decay of the transverse magnetisation by the **local external magnetic field inhomogeneities**.
- 3- significant signal dephasing across a voxel by **air-tissue interfaces or iron deposition**.
- 4- signal loss due to **flow-induced dephasing**, misregistration artefacts, and velocity-induced phase

SWI pulse sequence

- For SWI, a 3D RF **spoiled velocity compensated GRE** sequence is used.
 - This cause Gradient moment nulling (GMN) of motion.
- In the presence of a **bipolar gradient G_x** with duration 2τ , the phase accumulation for a spin moving at a constant velocity (v) is given by:

$$\Phi = \gamma G_x v \tau^2$$

- By velocity (flow) compensation pulse sequence, the velocity-induced phase disappears, which leaves the desired susceptibility-induced phase information.³



Magnetic susceptibility

- Magnetic susceptibility can be defined as the property of a substance, when placed within an external uniform magnetic field, that measures its **tendency to become magnetized** and to alter the magnetic field around it.
- **Two main sources** of magnetic field variation in the body, Causing signal distortion, signal loss, image artefacts and reductions in T2* are:
 1. extracorporeal objects (surgically implanted objects, iron-based tattoos and certain cosmetic products like eyeshadows)
 - This create distortion artefacts
 2. internal magnetic susceptibility differences found **between the tissues**
 - This provide a unique **contrast in the phase images**, and give information about tissues, such as distinguishing lesions from normal tissue

Types of magnetic susceptibility

- Substances based on their magnetic susceptibility χ can be classified into **diamagnetic**, **paramagnetic** and **ferromagnetic** materials based on their macroscopic influence over the external magnetic field.
- For empty space, the value of χ is zero,
- For diamagnetic material χ is negative value
- For paramagnetic χ is positive
 - tissue susceptibility values are generally much less than 1 ppm, or even ppb. In imaging human tissue, the terms paramagnetic and diamagnetic are used **relative to the susceptibility of the water rather than vacuum**.
- For ferromagnetic materials, the value of χ is much larger than unity.

Magnetization effect

- The physical magnetic field B (in Tesla) is given by

$$\vec{B} = \mu \vec{H}$$

μ is the permeability constant of the substance

H is magnetic field due to the external factors such as the **current in the solenoid** in Ampere/meter (A/m)

- The net magnetic field B inside a substance is given by $\vec{B} = \mu_0 (\vec{H} + \vec{M})$

μ_0 is the constant of permeability of a vacuum

M is magnetic field due to the **nature of the core**. From macroscopic field of electron spins inside the substance and microscopic electric currents from the motion of electrons in atoms

$$M = \chi H$$

- The **induced magnetization** (M) can be approximated by

- μ_r is termed as the relative magnetic permeability of a material $\mu = \mu_0 \mu_r = \mu_0 (1 + \chi)$

Magnetic field perturbations: phase and data processing steps

- The phase can be written as a function of the **difference between the uniform field B_0** and the local field variation, $\Delta B(r)$, at position r .
- phase of MR signal depends on the position of the spin isochromat and time. Phase can be assessed by obtaining **real and imaginary channels** of the signal , and is (for a right-handed system):

$$\phi(\vec{r}, t) = -\gamma \Delta B(\vec{r}) t$$

$\Delta B(r)$ is the variation in the main magnetic field.

$$\phi(\vec{r}, TE) = -\gamma \cdot (\Delta B(\vec{r})) \cdot TE$$

- In addition to the phase created by the spatial encoding gradients, the unwanted source of local field variations are: static field variations, imperfect gradients, eddy currents, air–tissue interfaces, and susceptibility differences between tissues.

Source of B0 field variation

$$\phi = -\gamma(\Delta B_{\text{main field}} + \Delta B_{\text{cs}} + \Delta B_{\text{global geometry}} + \Delta B_{\text{local field}})$$

- **(background or global field variation):** field inhomogeneities generated by sources outside the ROI that is due to surrounding tissue-air interfaces, eddy currents, as well as imperfect shimming.
- **(local field variation)** is estimated from the phase of a gradient echo acquisition, including imperfect gradients, and susceptibility differences between tissues, magnetic susceptibility of the tissue itself.
- **magnetic susceptibility** as a small magnetic field generated by the magnetic susceptibility of the tissue can be **separated from the strong background fields**, if we can remove the background and other local field variations

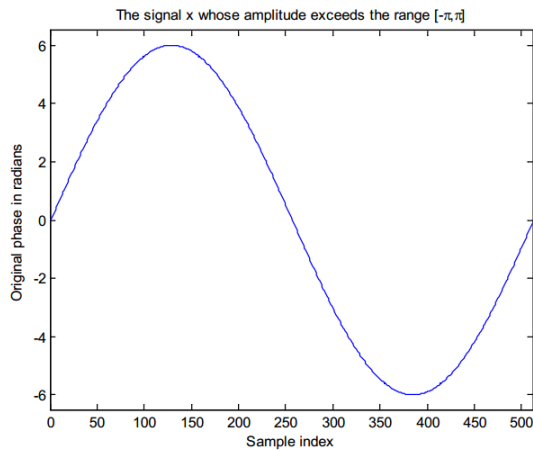
To retrieve information about the magnetic susceptibility distribution

- image processing steps to extract the tissue susceptibility from the phase information:
 - phase unwrapping
 - field inhomogeneities generated by sources outside the ROI are eliminated (*background removal*).
 - ΔB is estimated from the phase of a gradient echo acquisition (*local field estimation*).
 - solving the inverse problem to obtain magnetic susceptibility from field perturbation (*ill-conditioned problem*).

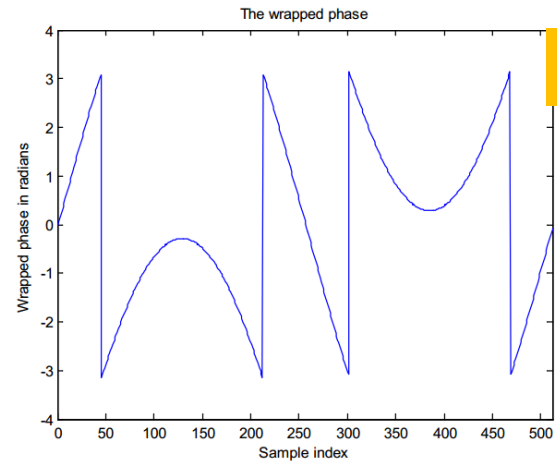
Basic of Phase map

- **Phase unwrapping:** the true phase may range over an interval greater than 2π , but the phase in scanner MRI is mathematically limited to the interval $(-\pi, \pi]$.

Real phase



Wrapped phase

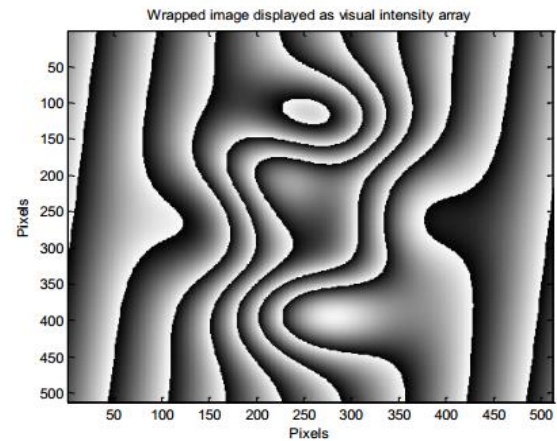
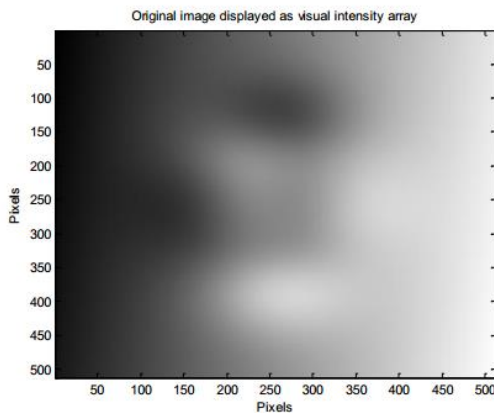


One dimension

$$\phi(\mathbf{r}) = \phi_w(\mathbf{r}) + 2\pi n(\mathbf{r})$$

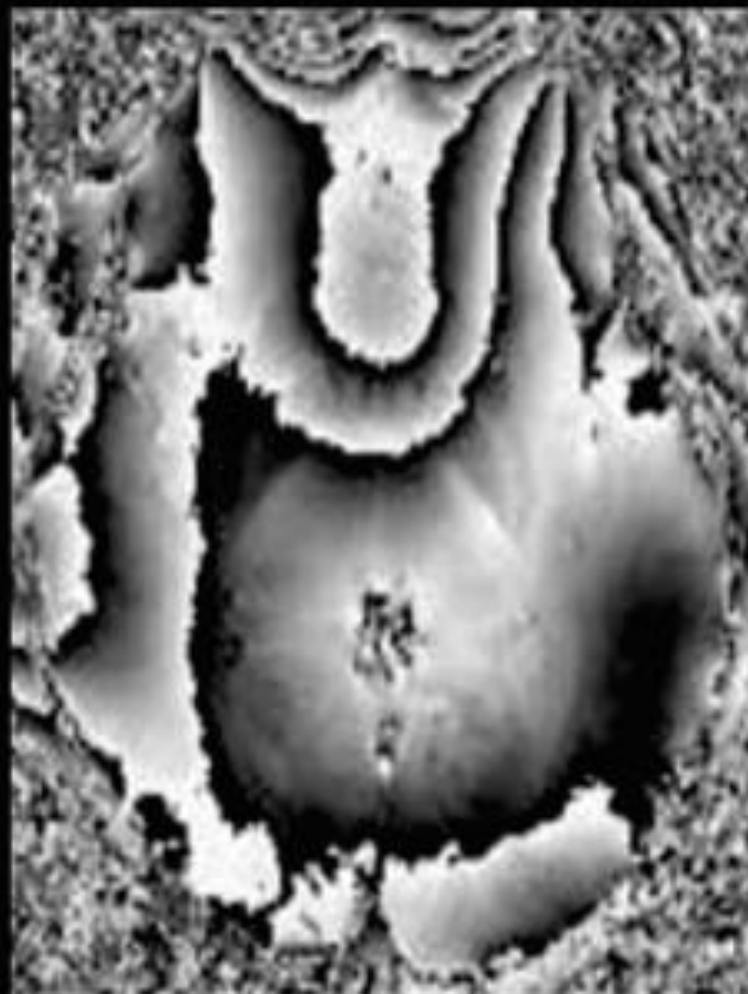
true (unwrapped) phase

wrapped phase

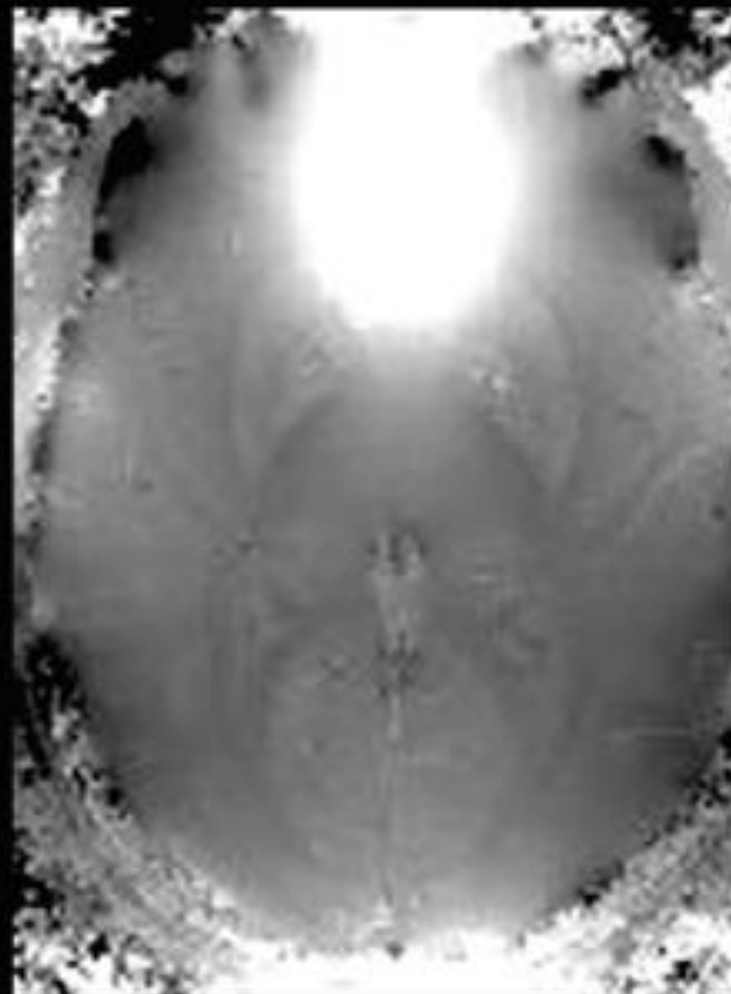


two dimensions

raw phase



unwrapped phase



Phase unwrapping

- When phase is measured, it is defined only within the interval $[-\pi, +\pi]$, instead of the full phase evolution.
- First actual phase should be calculated by adding or subtracting an integer multiple of 2π .
- This phase wraps can be present either spatially or temporally
- **Spatial unwrapping** method is used by travelling through each subsequent voxel to correct the phase change over neighboring voxels
- barriers along the path such as singularity/fringe lines should be avoided.
- **Temporal phase unwrapping** requires data from **multiple time points or TEs**, and utilises phase accumulation such as local field perturbations or blood flow.
- The inter-echo difference plays an important role in the effectiveness of unwrapping. short inter-echo differences should be used, but it produce strong gradient switching rates. This can be overcome by using multiple unequally spaced echoes.

background field removal

- high-pass filtering

A simple approach is the application of high-pass filtering (homodyne filter).

HPF image, $\rho'(\mathbf{r})$, is obtained by complex dividing the original image $\rho(\mathbf{r})$ by a complex image ($\rho_m(\mathbf{r})$) generated from truncating the original $n \times n$ pixels to $m \times m$ pixels from the original complex image and zero-filling the elements outside the central $m \times m$ elements to get the same $n \times n$ dimensions as the original image:

$$\rho'(\vec{r}) = \rho(\vec{r}) / \rho_m(\vec{r})$$

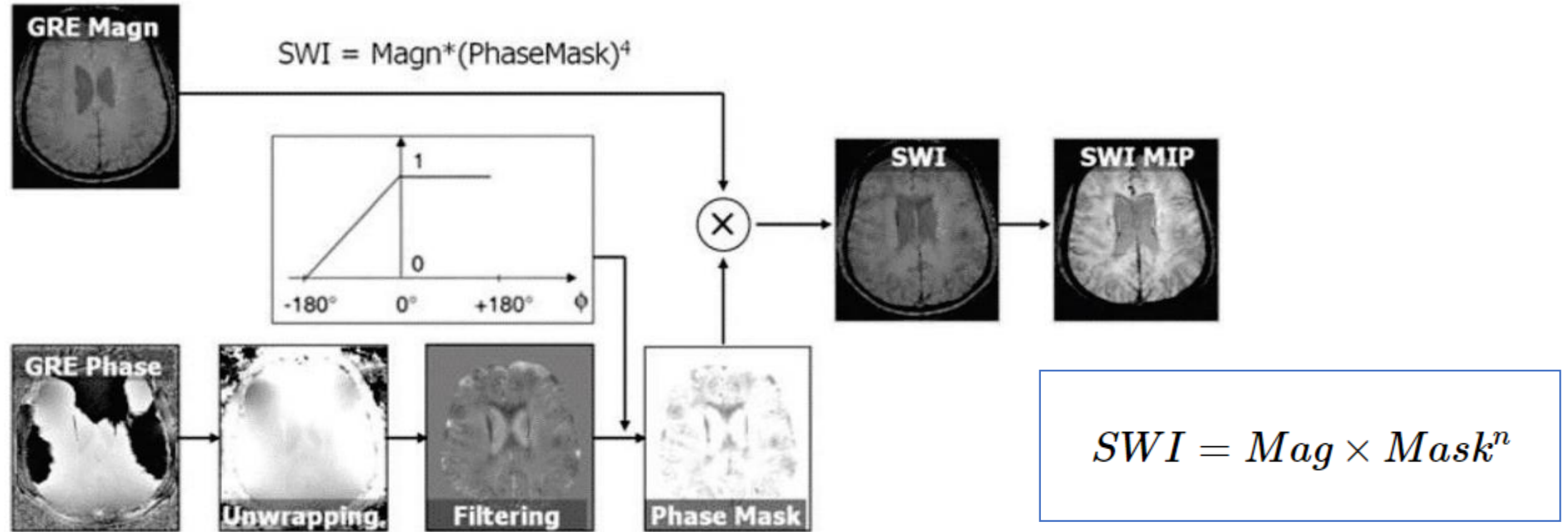
- ❖ a small filter size can fail to remove the entire background field, especially close to the sinuses.
- ❖ A large filter size performs well in the background removal, but results in the removal of low-frequency components of the phase induced by the local tissue, leading to an underestimation of the susceptibility.

- **SHART method**

- Sophisticated Harmonic Artefact Reduction for Phase data (**SHARP**) methods: uses the mean value property to separate background field from the local field.
- **Background fields are supposed to be harmonic** since their sources are located outside of the region of measurable phase.

$$B_{tot} = B_{int} + B_{bg} \rightarrow \nabla^2 B_{tot} = \nabla^2 B_{int} + \nabla^2 B_{bg} \quad \longrightarrow \quad \nabla^2 B_{tot} = \nabla^2 B_{int}$$

Susceptibility Weighted Imaging (SWI)



Processing steps of susceptibility weighted imaging (SWI). After unwrapping and high-pass filtering of the phase image, a specific function is applied to retrieve the phase mask. The combination of the magnitude image and phase mask results in SWI image.

To highlight the veins minimum intensity projection (MIP) is applied.

Basic theory of field map

1- Local field estimation: ΔB is estimated from the phase of a gradient echo acquisition

$$\Delta\varphi = 2\pi\Delta f \times \Delta TE \rightarrow \Delta f = \frac{\Delta\varphi}{2\pi\Delta TE} \quad \left(\frac{\text{rad}}{\text{echo}}\right)$$

Frequency mapping



$$\Delta B(r) = -\frac{2\pi}{\gamma} \Delta f(r)$$

Local magnetic field

Local field δB induced by non-ferromagnetic biomaterial susceptibility is the convolution of the volume susceptibility distribution χ with the dipole kernel d :

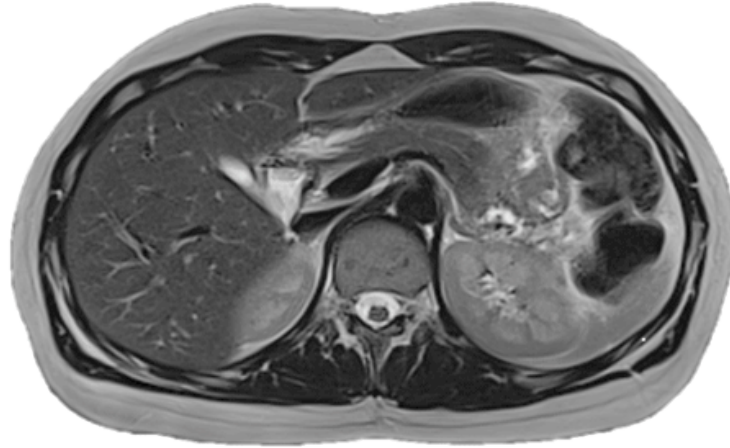
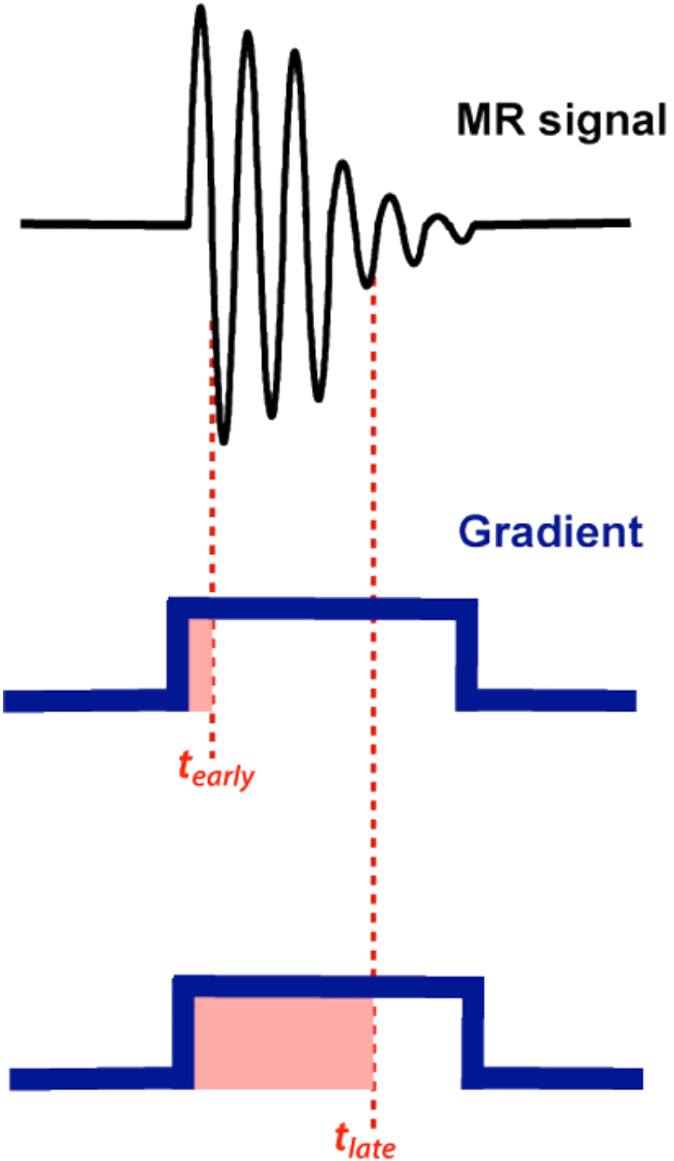
$$\delta B = d \otimes \chi$$

in Fourier domain, this convolution can be expressed as a point-wise multiplication:

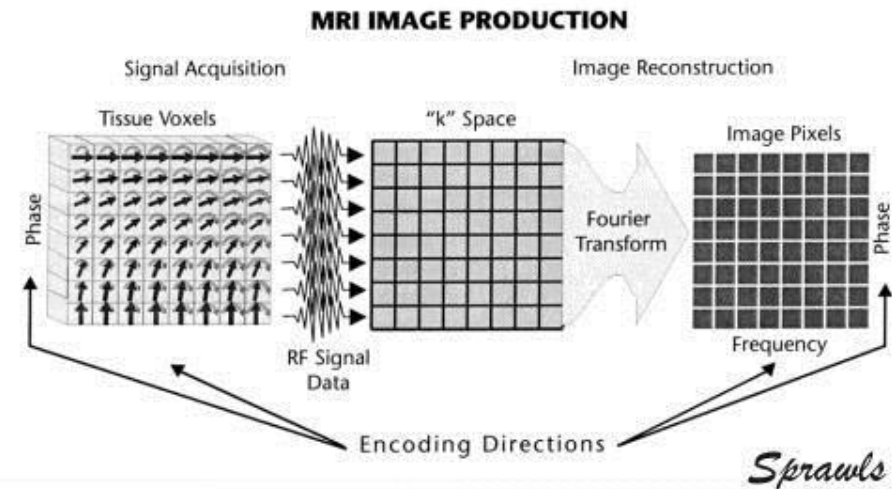
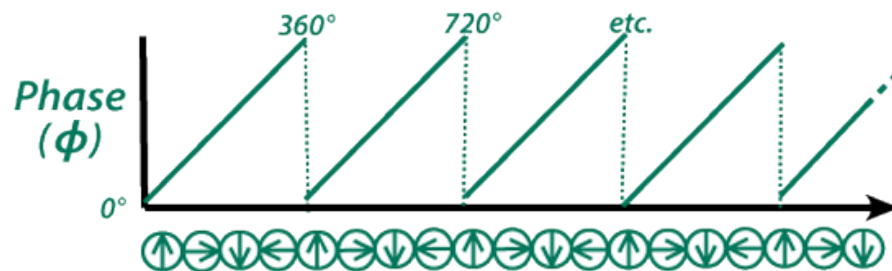
$$\Delta B = D \cdot X$$

This Fourier expression provides an efficient way to predict the field perturbation when χ is known. However, the field to source inverse problem involves

Green's Function k-space



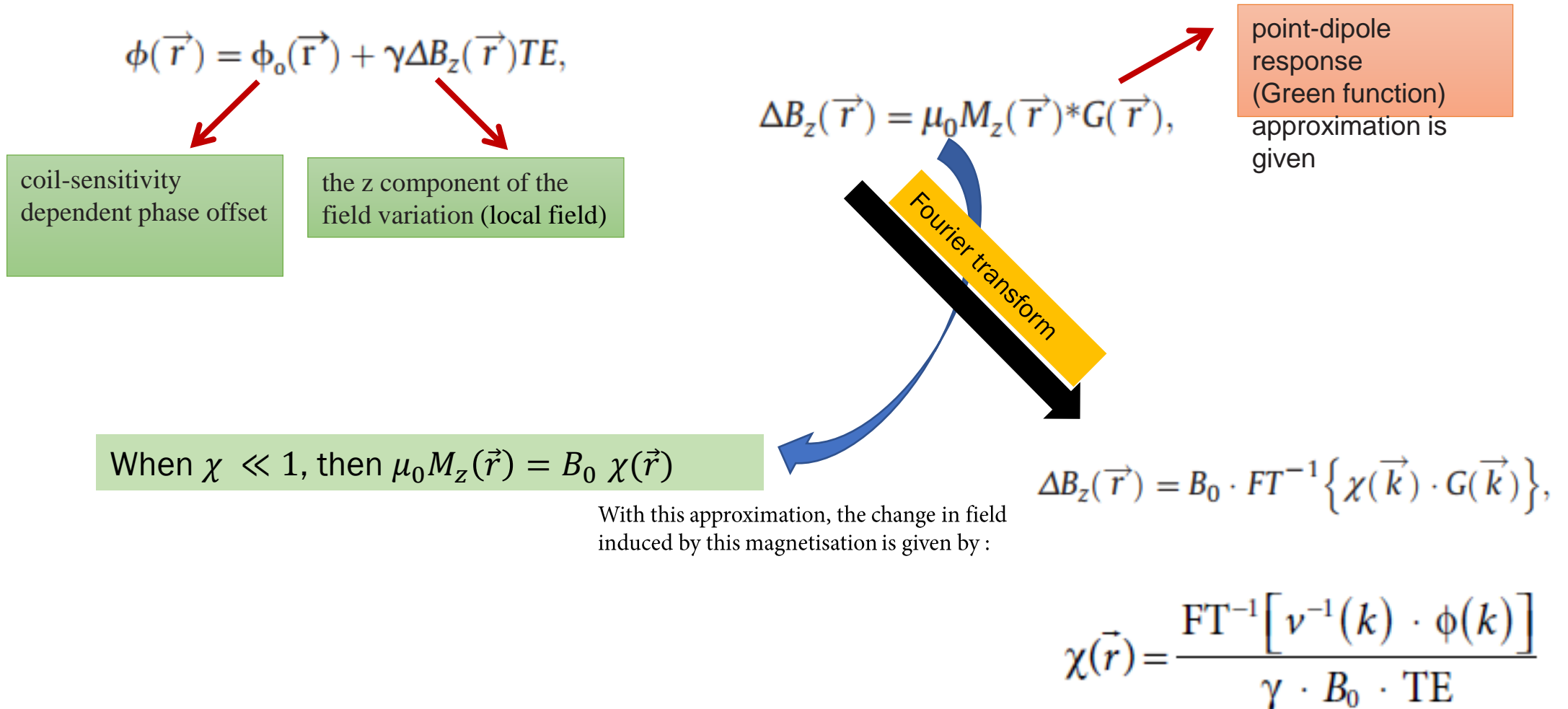
$$\phi(x) = \gamma G(x) t$$



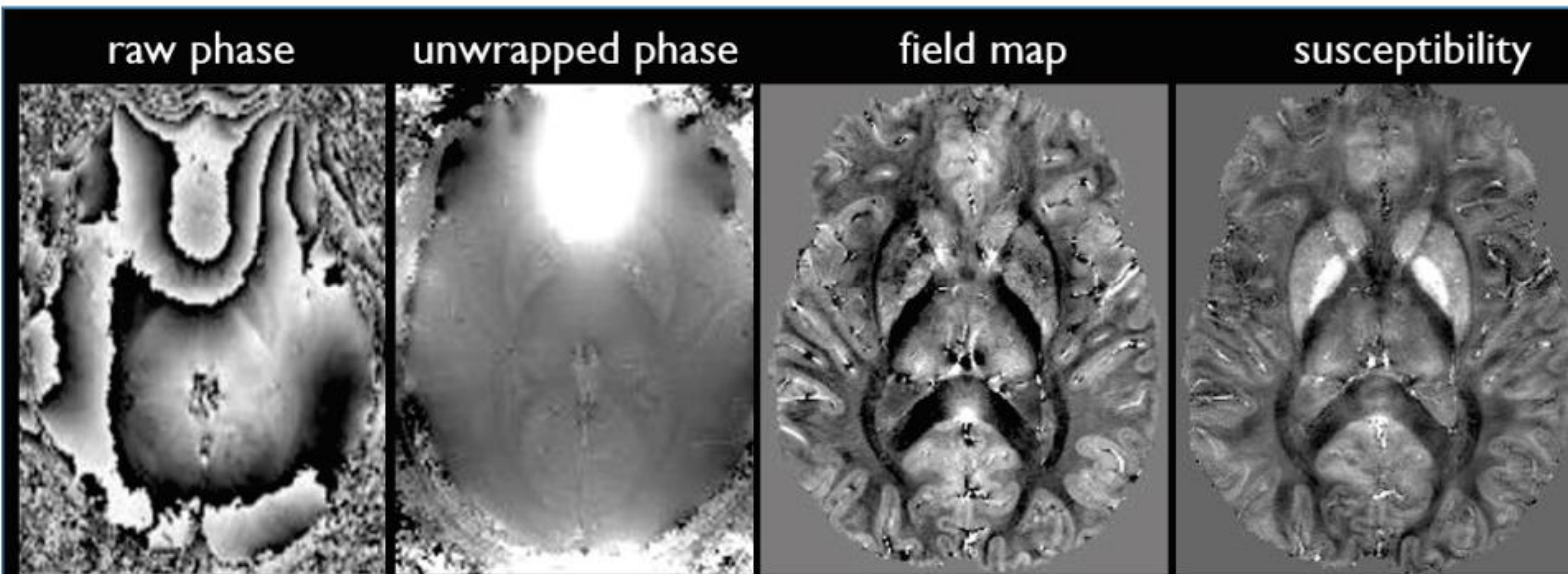
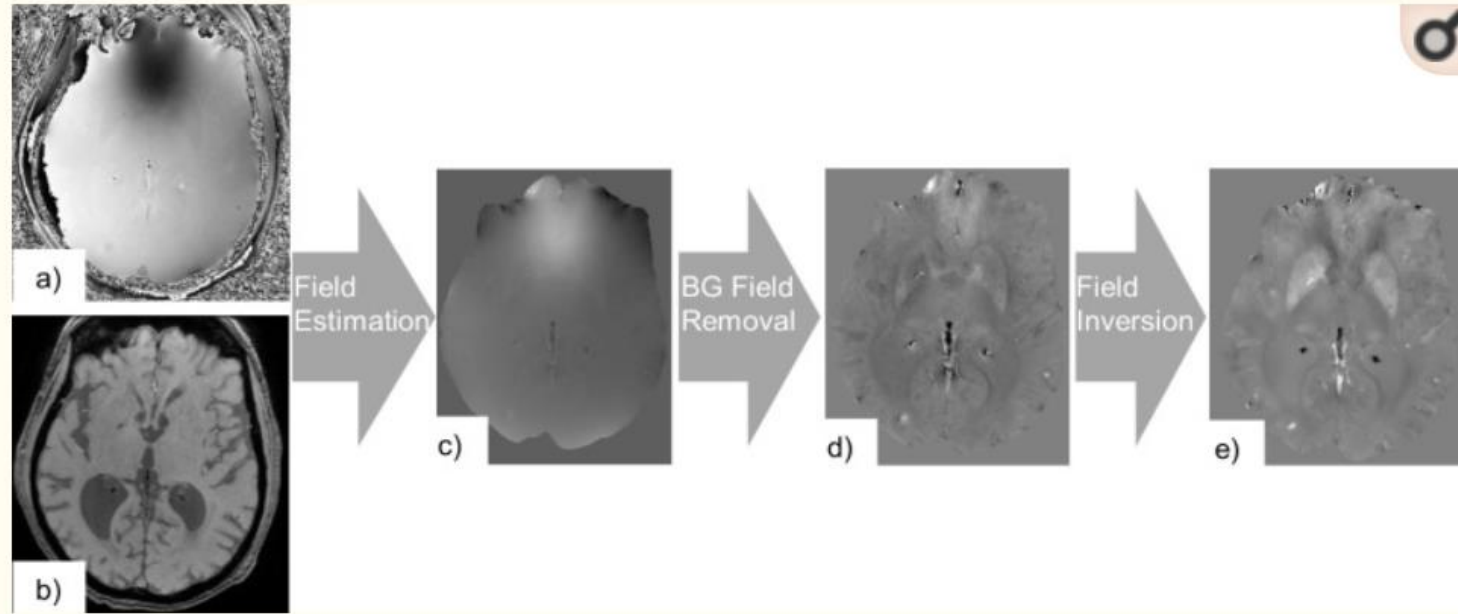
Basic theory of QSM

2- Phase is calculated from ΔB with an echo time TE in GE sequence\

- phase in the image domain can be written as:



Basic theory of QSM

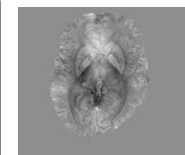
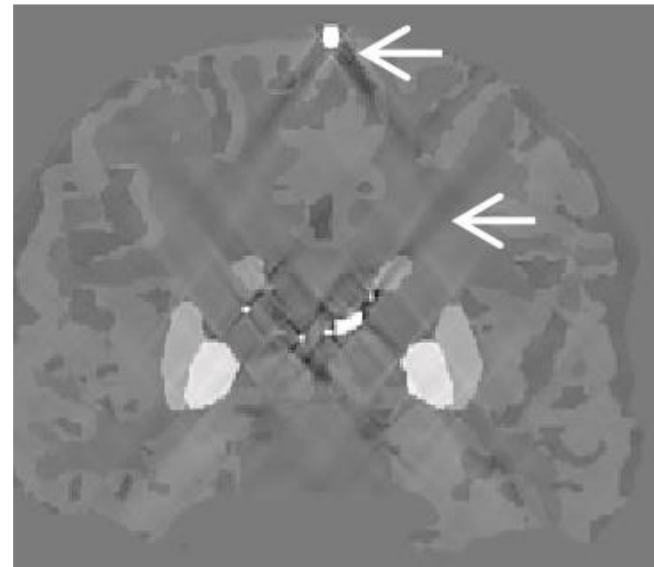
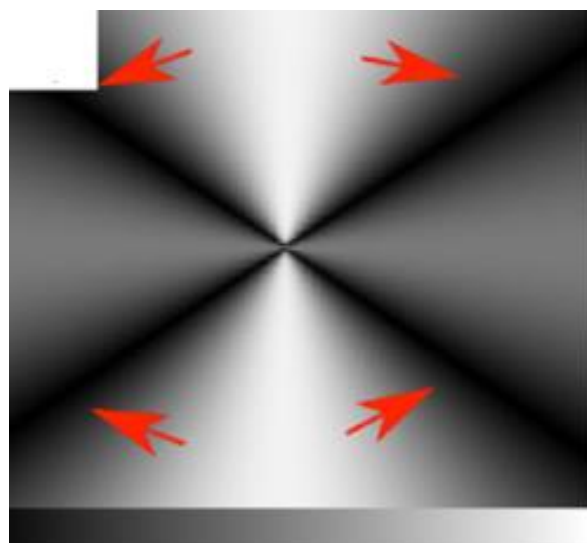


ill-conditioned problem

هدف QSM ، حل معادله‌ی بالا در فضای k به منظور ارزیابی پیکسل به پیکسل پذیرفتاری مغناطیسی ($\chi(r)$) در ماتریس تصویر است. ولی مشکلی که وجود دارد این است که در راستای زاویه جادویی $۵۴,۷$ درجه، کرنل دوقطبی در فضای فوریه، $G(k)$ ، مقداری برابر با صفر دارد و این به این معنی است که مقدار پذیرفتاری مغناطیسی قابل محاسبه نیست.

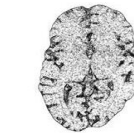
به دلیل این آرتیفکت نواری (streaking artifact) روی نقشه پذیرفتاری مغناطیسی ظاهر می شود. الگوریتم MEDI یکی از الگوریتم هایی است که برای مشکل معکوس پیشنهاد شده است. MEDI بر مبنای سازگاری ساختاری تصاویر دامنه و نقشه پذیرفتاری رفتار میکند.

یعنی با کمینه کردن تعداد وکسل هایی که در نقشه پذیرفتاری لبه هستند ولی این وکسل ها در تصویر مگنیتیود، لبه نیستند، می توان راه حل مناسبی برای مشکل QSM پیدا کرد.

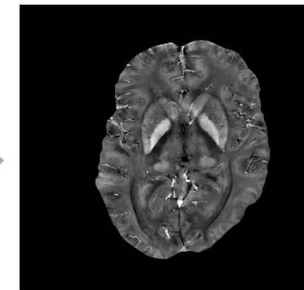


Tissue Field

d



Edge Information



QSM

voxels that are part of edges in the susceptibility map, but not in the edges of the magnitude image, are corrected.

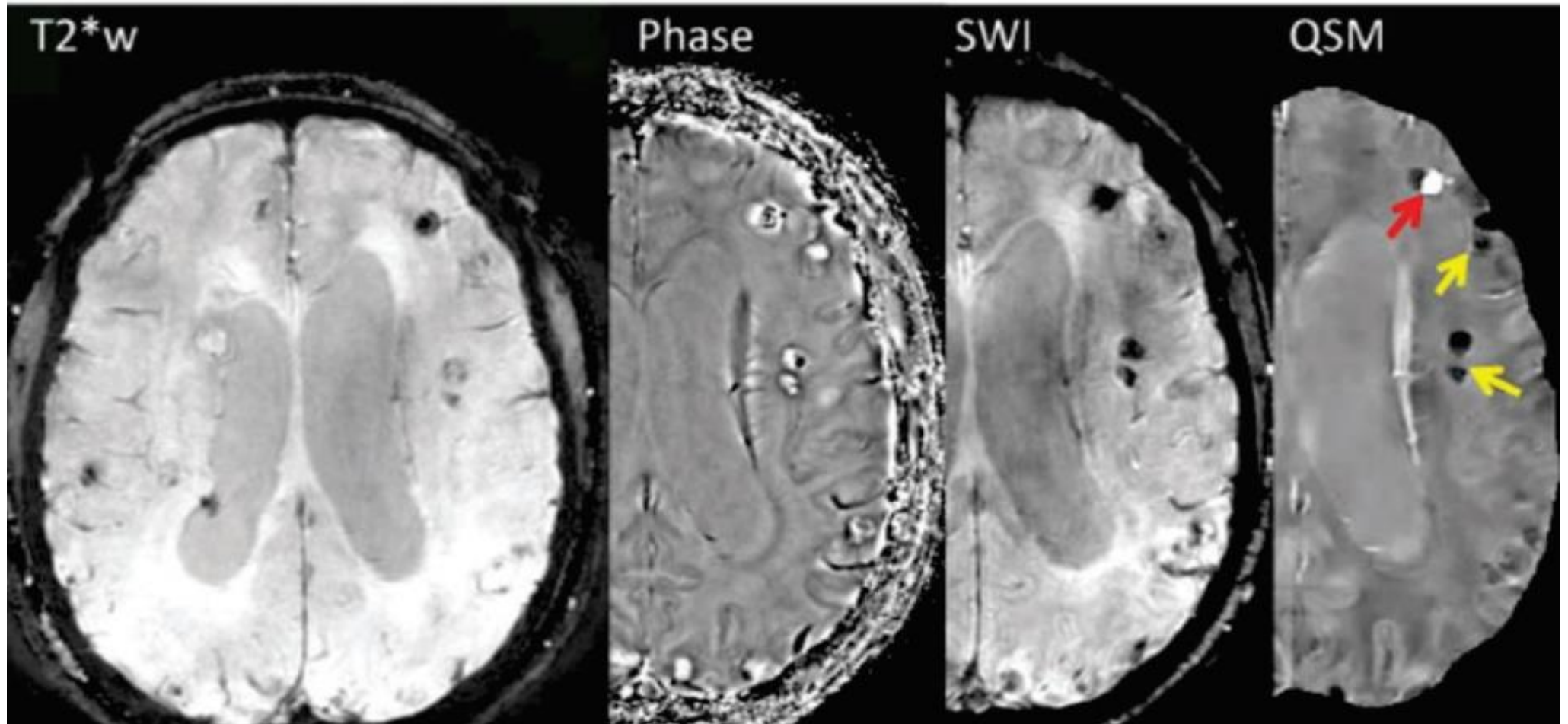
Data acquisition

- Any **3D gradient echo** sequence can be used for data acquisition.
- High resolution imaging with a moderately **long echo** time is preferred to obtain sufficient susceptibility effects
- A **multi-echo acquisition is beneficial** for accurate B_0 field measurement without the contribution from B_1 inhomogeneity.
- **Flow compensation** may further improve the accuracy of susceptibility measurement in venous blood, but there are certain technical difficulties to devise a fully flow compensated multi-echo sequence

Applications of QSM

- One of the advantages of QSM over $R2^*$ mapping is that QSM is linearly proportional to the concentration of substances that induce a susceptibility effect, such as an iron nanoparticle-based contrast agent.
-
- In addition, the diamagnetic effects cause similar signal loss to iron, making it impossible to distinguish the source of increases in $R2^*$, while QSM provides the discrimination between diamagnetic and ferromagnetic, through the sign of the susceptibility.
 - Eg; calcium is diamagnetic and has a negative value relative to surrounding tissue, making it clear that the source is calcium, not iron.

Quantitative Susceptibility Mapping (QSM)



Neurocysticercosis Brain; Calcified lesions with **negative susceptibility (yellow arrows)** are visible on all contrasts with better performance on phase and **QSM contrast**, whereas active Iron based lesion with **positive susceptibility (red arrow)** is delineated only on **QSM**.

signal change in MRI due to
Energy Exchange
and
Magnetization Transfer mechanism

Energy Exchange between different nuclei

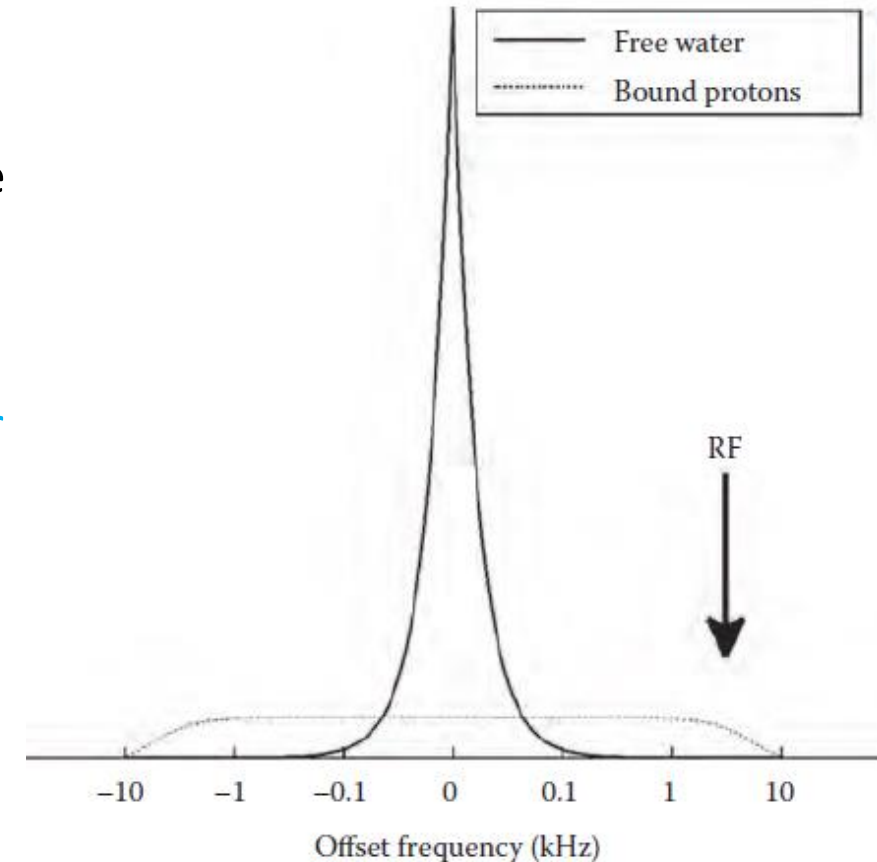
- nuclei in different chemical compounds can be coupled magnetically and therefore exchange energy with environments or with each other when come close enough, through **dipole–dipole interactions**, by diffusion or molecular rotation (eg in NMR spectroscopy).
- Any peak's compound can also be saturated and sized-altered by applying a large amount of **continuous wave (CW)** power. Exchange times (or rate) for protons from one component contaminated to alternative component can be measured.
- Signal model (Bloch equations) is modified to consider affect from a coupling term with saturated spins extra to T1 term in signal recovery.

What is Magnetization Transfer (MT)

- MT is obtained by **mobilization of water protons** and contacting with macromolecule hydrogen (with restricted mobility), making it possible for a water proton to exchange with a macromolecule protons bond on the surface of the macromolecule.
 - Therefore, signal from those free hydrogen atoms will decay too quickly.
- This exchange of magnetization, which can be either by direct **chemical exchange** of the hydrogen atom or by **spin–spin interactions**, forms the basis of MT imaging

Physical mechanism of MT signal

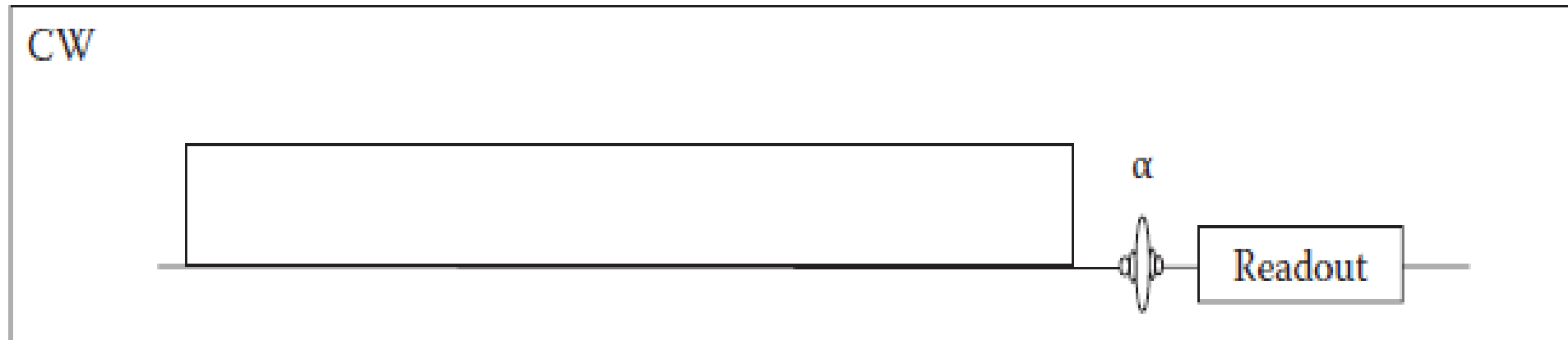
- **Mobile protons are free to diffuse** and rotate so that dipolar–dipolar interactions are averaged out, resulting in small variations of their resonant frequency and thus a **very narrow resonance line**.
- On the other hand, **macromolecular protons**, have a broad resonance line and hence are sensitive to off-resonance irradiation.
- If sufficient **off-resonance power** is applied, then the **macromolecular spins become ‘saturated’**, a state in which the numbers of up spins and down spins are equalized and the net magnetization vector is zero.
- If some of this saturated magnetization is transferred to the liquid (mobile) protons by the exchange processes described above, they can become partially saturated and.
 - consequently, the signal intensity from the observable liquid protons is reduced, producing the so-called MT contrast.



Measuring MT

- **CW irradiation**

CW RF pulses (0.5–10 kHz off-resonance) of several seconds with constant amplitude are used to saturate the macromolecular pool. This method is not feasible on clinical systems, since the RF transmitters are not designed for CW operation, as well as high specific absorption rate (SAR)

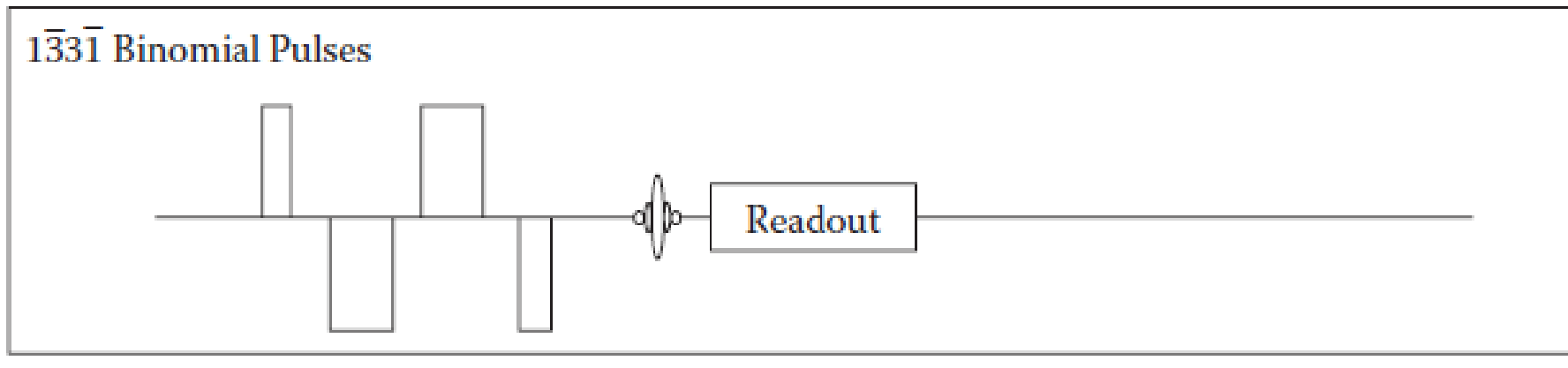


Measuring MT

- **On-Resonance binomial pulses**

A 'transparent pulses', such as $1\bar{1}$ or $1\bar{2}1$ (number refers to the relative tip angle), whose net effect is zero for long T2 spins such as those in free water is used. Thus no effect on mobile protons.

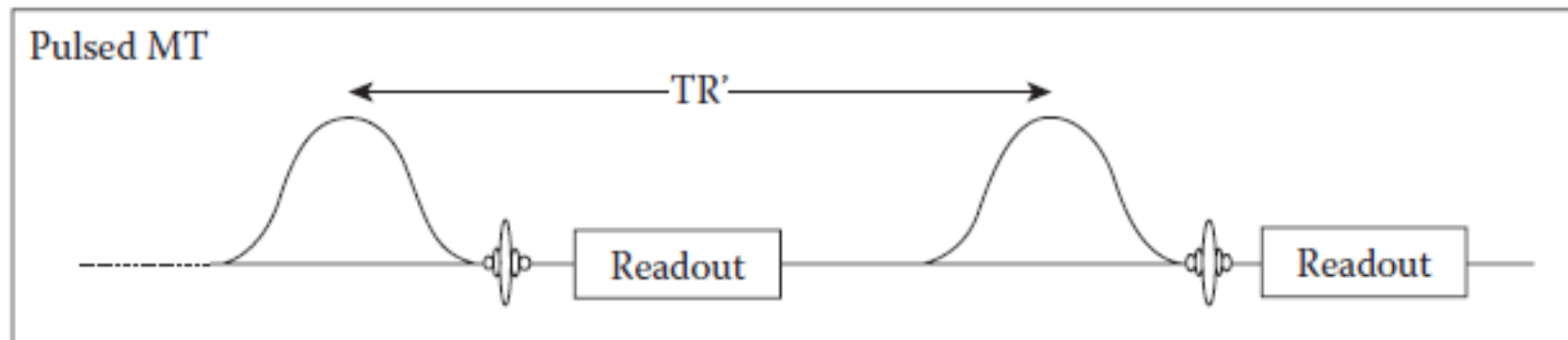
In the bound pool with short T2, the transverse magnetisation decays as soon as it is produced, therefore z-magnetisation is not recovered by the second pulse. Thus bound protons are saturated.



Measuring MT

- **Off-Resonance pulsed irradiation**

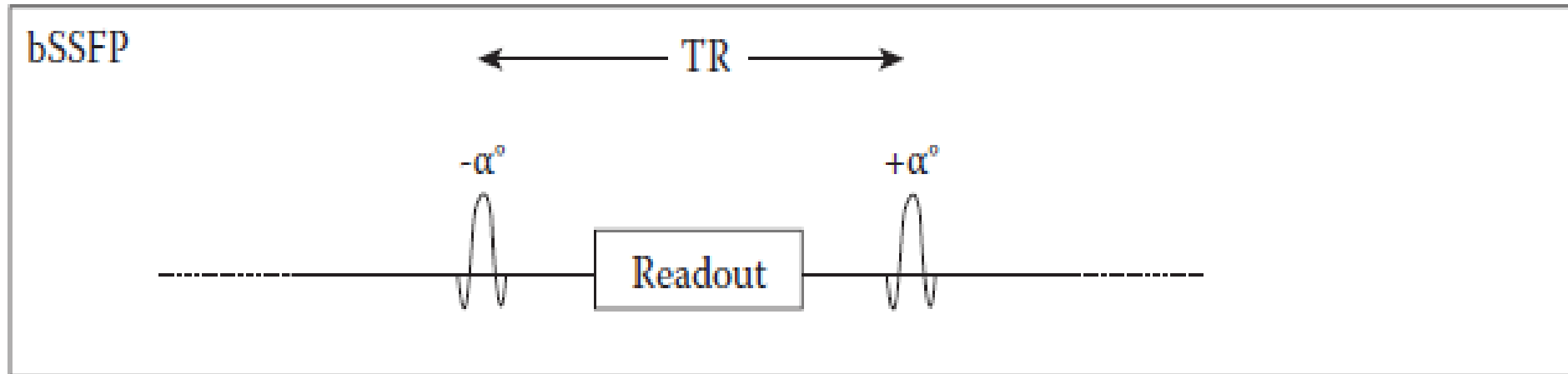
- Off-Resonance Gaussian or sinc shape with a bandwidth of a few 100 Hz, and at **frequency offsets of 1–5 kHz** from the mobile water peak is used.
- off-resonance pulses can be combined with any acquisition sequence (typically 3D **SPGR** is suitable due short scan times and low T1 and T2 contrast
 - (matrix: $256 \times 128 \times 28$; 5 mm sections; TR=100 ms; TE=6 ms; FA=12°).
- SE sequences can be used, with eg interleaved dual echo, with disadvantage of T1-weighting (since TR must be kept short to limit imaging time)



Measuring MT

- **Balanced steady-state free precession method**

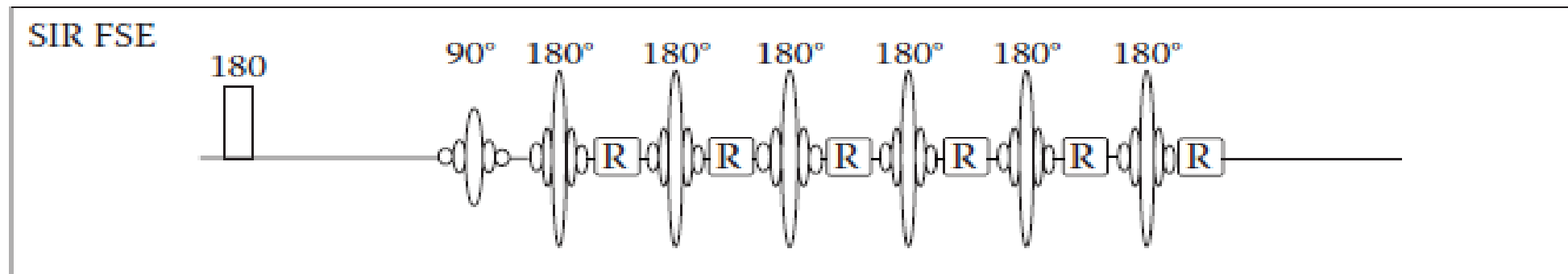
bSSFP sequences is inherently MT weighted. A signal loss can be explained by MT effects, which is dependent on the choice of TR and flip angle (longer pulses (and TRs) minimise the MT effect).



Measuring MT

- **Selective Inversion Recovery Method:**

- SIR-FSE method aims at manipulating the liquid protons instead of the macromolecular ones.
- At the end of each repetition, both free water and macromolecular pools have zero z-magnetization.
 - Free water protons are rotated by the 90° pulse, followed by the series of closely spaced refocusing 180° pulses (which prevent any effective T1 recovery).
 - Macromolecular protons are not directly affected by the 90° pulse, but due to their MT effect, they cause nulling free protons on a timescale of T1 time.



Clinical Importance of MT

- MT is able to show indirectly macromolecules such as proteins and lipids, which are normally 'invisible' on MRI.
 - This is of great interest in the brain, as myelin, the substance that wraps around the majority of the axons and is a lipid-protein structure (70%–80% lipids and 20%–30% proteins).
 - Myelin involves in neuronal conductivity and potential transmission, ensuring efficient signal travelling along axons.
- MTR is defined as the pixel intensities percentage difference between two images, one acquired with off-resonance saturation (M_s) and one without (M_0):

$$\text{MTR} = \frac{M_0 - M_s}{M_0} \times 100$$

- MTR is dependent on **T1**, as well as on the **density of macromolecules**. In some circumstances (e.g. demyelinating lesions) the increase in T1 can partially mask the decrease in macromolecular density, resulting in an apparent stability of the MTR

Quantifying oxygen extraction fraction (OEF) and cerebral activity

- To measure OEF, local oxygen saturation levels of vein and artery should be known. Artery oxygen saturation is known, but for venous:
- To predict **venous oxygen saturation level (Y_v)**, magnetic susceptibility of venous blood ($\Delta\chi_v$) is measured by QSM-MRI. This shows amount of haem iron (de-oxyhaemoglobin) or amount of oxygen saturation.

$$\Delta\chi_v = \Delta\chi_{do} \cdot \text{Hct} \cdot (1 - Y_v)$$

For example venous oxygen saturation level (Y_v) of 70%, is expected when haematocrit = 44% and **difference between fully oxygenated and deoxygenated blood** ($\Delta\chi_{do} \approx 3.39$ ppm in SI units))

In healthy subject Y_v decreases post-Caffeine intake about 10% (ie OEF has been increased). Caffeine also corresponds to the relative reduction in CBF of arteries to 30.3%. This cause that the CMRO2 remains stable.

Quantifying non-haem iron or ferritin

- iron the dominant source of paramagnetic materials in the brain. Iron is stored as ferritin and hemosiderin, and studies have shown that the amount of this stored iron in deep grey matter (GM) nuclei and cortical areas increases with age.
- In order to investigate the correlation of iron deposition as a function of age, regional mean susceptibility values, in addition to the global mean
- Recent studies have suggested that QSM as a biomarker for measuring iron content in organs such as liver, depicting calcifications in prostate cancer patients, and characterization of kidneys

Theory for MT magnetization

- In the presence of MT exchange, the time evolution of magnetization in the liquid (A) and semisolid (B) pools during an RF saturation pulse

$$\frac{\partial M_X^A}{\partial t} = -2\pi\Delta M_Y^A - \frac{M_X^A}{T_2^A}$$

$$\frac{\partial M_Y^A}{\partial t} = 2\pi\Delta M_X^A - \omega_1 M_Z^A - \frac{M_Y^A}{T_2^A}$$

$$\frac{\partial M_Z^A}{\partial t} = \omega_1 M_Y^A + R_A(M_0^A - M_Z^A) - RM_0^B M_Z^A + RM_0^A M_Z^B$$

$$\frac{\partial M_Z^B}{\partial t} = R_B(M_0^B - M_Z^B) - (R_{RFB} + RM_0^A)M_Z^B + RM_0^B M_Z^A$$

x, y, z : spatial components of magnetization vector,

Δ : off-resonance frequency of the saturation pulse,

$\omega_1 = \gamma B_1$: angular precession frequency induced by the pulse.

M_0^A and M_0^B are the equilibrium magnetizations of each pool,

R_A and R_B : longitudinal magnetization rate

T_2^A and T_2^B : transverse magnetization decay

RM_0^B and RM_0^A : rate constants of magnetization transfer from the liquid to the semisolid pool and vice versa.

R is a fundamental MT exchange constant.

- To describe the behavior of macromolecular protons, the Bloch equations for the semisolid pool are replaced by a **single longitudinal component**, causing saturation n rate of magnetization, R_{RFB} :

$$R_{RFB} = \pi \omega_1^2 g_B(2\pi\Delta)$$

- where g_B is the absorption lineshape (a function of semisolid pool's transverse relaxation time constant, T_2^B)
- The lineshape of the restricted pool can be Gaussian, Lorentzian, or Super-Lorentzian:

$$G_G = \frac{T_{2r}}{\sqrt{2\pi}} \exp \left[-\frac{(2\pi\Delta T_{2r})^2}{2} \right]$$

$$G_L = \frac{T_{2r}}{\pi} \left(1 + (2\pi\Delta T_{2r})^2 \right)^{-1}$$

$$G_{SL} = T_{2r} \sqrt{\frac{2}{\pi}} \int_0^1 \frac{1}{|3u^2 - 1|} \exp \left[-2 \left(\frac{2\pi\Delta T_{2r}}{3u^2 - 1} \right)^2 \right] du$$

- For biological tissues, the semisolid line shape is typically approximated by a super-Lorentzian

solution for pulsed MT experiments

- Magnetization of a **pulsed MT sequence** having short-duration RF pulses with time-varying pulse amplitudes is given by the following matrix differential equation:

$$\frac{dM(t)}{dt} = \Lambda(t)M(t) + \beta M_0$$

- M is a 4D magnetization vector, $M(t) = [M_x^A, M_y^A, M_z^A, M_z^B]^T$
- M0 is vector of the equilibrium value of each magnetization component.

$$\begin{bmatrix} \frac{-1}{T_2^A} & -2\pi\Delta f & 0 & 0 \\ 2\pi\Delta f & \frac{-1}{T_2^A} & -\omega_1(t) & 0 \\ 0 & \omega_1(t) & -(R_A + RM_0^B) & RM_0^A \\ 0 & 0 & RM_0^B & -R_B + RM_0^A + R_{RFB}(\omega_1(t)) \end{bmatrix} B = \begin{bmatrix} 0 \\ 0 \\ R_A \\ R_B \end{bmatrix}$$

Solution for pulsed MT experiments

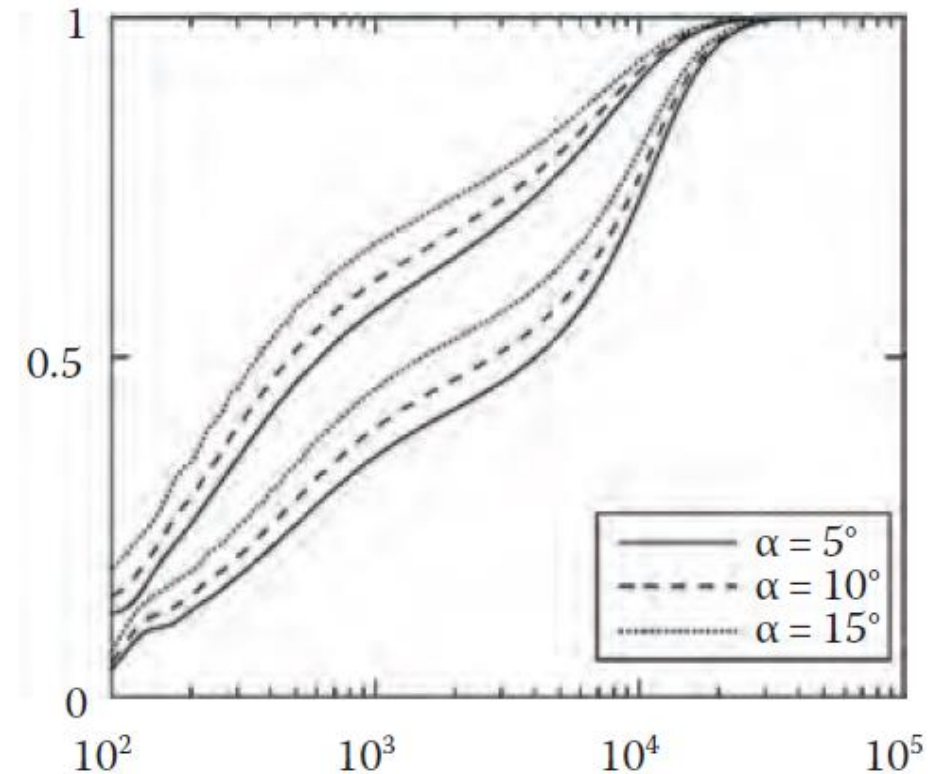
- When the **matrix A is constant** in time, as is the case with **rectangular RF pulses**, the following general analytical solution is obtained

$$M(t) = e^{At}M(t = 0) + \Lambda^{-1}(e^{At} - I)\beta M_0$$

- I is the 4x4 identity matrix
- However, RF is time-varying (due to amplitude modulated RF pulses), and no such general solution exists.
- Solution1: solving the modified Bloch equations numerically. First, the rate of saturation of the semisolid pool is calculated using R_{RFB} Equation, with the ω_1 **varying in time** according to the **RF pulse amplitude**, B_1
- Solution1: **dividing RF pulses into a series of short rectangular** segments (50 μ s) whose envelope was as the desired pulse shape.
 - The modified Bloch Equation was then used to propagate the magnetization through each interval. This is called **Minimal Approximations MT** (MAMT) to describe the effect of RF saturation pulses.

Plots of MT data: predicted M_z^A over frequency offset (from 100Hz to 100kHz) at two different saturation powers (effective flip angles $\theta_1=600^\circ$ and $\theta_2=1200^\circ$).

- MAMT model predictions (with super-Lorentzian line shape) for 2 pools compartments (single tissue), with Macromolecule pool ratio of $F=0.13$, $T_2^A=35$ ms, $T_2^B=12$ μ s, $RM_0^B=2.5$
- Imaging parameters: pulse shape sinc-Gaussian, pulse duration 20ms, interpulse gap 30ms, number of pulses 150, at 3 different imaging pulses flip angles.
- y-axis is the ratio of the A (free) Pool z-magnetisation to the total amount of A-pool magnetisation. x-axis is offset frequency.



Coupling strategy for selective IR method

coupling between the mobile and immobile protons pools can be modeled by adding a coupling term to the Bloch equations. Using a suggested solutions, during free recovery we have

$$m_i(t) = -(M_A(t) - M_0^A)/2 M_0^A$$
$$dm_i/dt = -R_A m_i(t) - RM_0^B(m_i(t) - m_j(t))$$

$$m_j(t) = -(M_B(t) - M_0^B)/2 M_0^B$$
$$dm_j/dt = -R_B m_j(t) - RM_0^A(m_i(t) - m_j(t))$$

- $m_i(t)$ and $m_j(t)$ are the normalized deviation of the longitudinal magnetization from equilibrium, respectively.
- $M_A(t)$ and $M_B(t)$ are the longitudinal magnetization of free and restricted pool,
- R_A is the longitudinal **relaxation** rate when there is no coupling to the second pool,
- RM_0^B and RM_0^A are forward and reverse coupling rate constants, respectively.
- Difference between $m_i(t)$ and $m_j(t)$ shows the strength of the coupling. By a proper selective pulse this difference is amplified.
- The solutions to these Eqs is given as:

MT modelling of selective inversion recovery signal

- Measuring the relaxation of magnetisation after selectively disturbing either the free or the bound pool for a short time, after solving previous differential equation is the following **bi-exponential** Equation:

$$\frac{M_A(t)}{M_0^A} = C_1 e^{-\lambda_1 t} + C_2 e^{-\lambda_2 t} + 1$$

relaxation rates $\lambda_{1,2}$: the slow and fast recovery rates, respectively
 λ is intrinsic properties of the system,

$$\lambda_{1,2} = \frac{1}{2} \left(R_A + R_B + R M_0^B + R M_0^A \pm \sqrt{(R_A - R_B + R M_0^B - R M_0^A)^2 + 4 R M_0^B R M_0^A} \right)$$

coefficients $C_{1,2}$: corresponding amplitudes for slow and fast recovery

$$C_{1,2} = \pm \frac{\left[\frac{M^A(0)}{M_0^A} - 1 \right] (R_A - \lambda_{2,1}) + \left[\frac{M^A(0)}{M_0^A} - \frac{M^B(0)}{M_0^B} \right] R M_0^B}{\lambda_1 - \lambda_2}$$

C depends on experimental settings (i.e. initial conditions after the perturbation, ie amount of $M_z^A(0)$ and $M_z^B(0)$)

- In principle, Equation $\frac{M_A(t)}{M_0^A} = C_1 e^{-\lambda_1 t} + C_2 e^{-\lambda_2 t} + 1$ can be used to fit data acquired at varying Inversion Times (TIs) (different delays) from the perturbation to estimate coefficients C_1 and C_2 and relaxation rates λ_1 and λ_2 and M_0^A
 - Various TIs cause different initial conditions $M_z^A(0)$, $M_z^B(0)$ due to partial longitudinal recovery during t_d , as follows:

$$\left[\frac{M^{A,B}(0)}{M_0^{A,B}} = S_{A,B} \left(1 - e^{-\lambda_{1,2} t_d} \right) \right]$$

- where free and Macromolecular fractional saturation S_A and S_B quantify the effect of the inversion pulse on free and macromolecular pool, respectively.

Approximations for macromolecular Fraction

- In two-pool model parameters, the assumption $RM_0^A \gg RM_0^B, R_A, R_B$, exists for a variety of **biological tissues**, provide following approximations:

$$\lambda_1 \cong RM_0^A$$

$$C_1 \cong \left(\frac{M^A(0)}{M_0^A} - \frac{M^B(0)}{M_0^B} \right) F$$

- Above Equations and determined values of C_1 and C_2 and λ_1 and λ_2 and M_0^A allow the **macromolecular fraction (F)** to be calculated.

$$F = \frac{C_1}{C_2 + 1 - S_B (1 - e^{\lambda_2 t d})}$$

Inhomogeneous MT (ihMT)

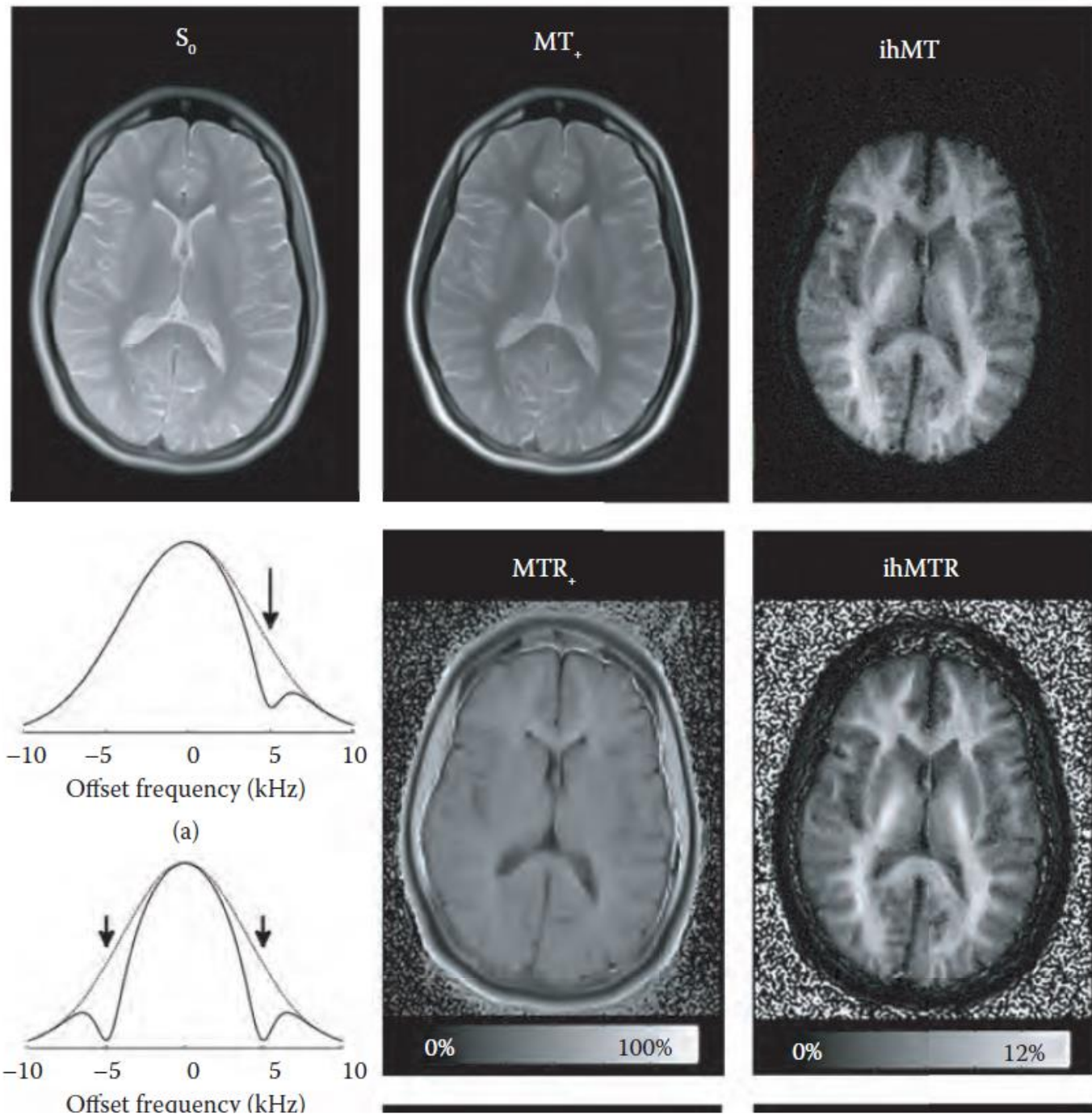
- MT saturation at positive frequencies can differ from those at their respective negative values, causing ihMT to be non-zero.
- MT signal is obtained at offset frequency $+f$ (the single-side saturated signal $S(f+)$).
- To detect ihMT signal, additional signals are acquired with same RF power, but at $-f$, and at both frequencies $+f$ and $-f$ simultaneously ($S(f\pm)$ the dual-side saturated signal).

$$ihMT = S(f+) + S(f-) - S(f\pm) - S(f\mp)$$

- ihMT is sensitive to biological structures showing inhomogeneously broadened spectral lines.
 - For example: myelin's architecture and molecular composition shows an inhomogeneously broadened spectral line on a timescale of several milliseconds.

$$ihMTR = \frac{ihMT}{S_0}$$

Example of inhomogeneous
MT (ihMT) dataset obtained
with typical acquisition strategy



How to Set Up Your Quantitative MT Protocol

1. Choose a suitable model, based your scientific hypothesis and by scan time constraints.
2. Check whether the corresponding pulse sequence is available on your scanner. Off-resonance pulses to produce MT effect are generally available in all scanners.
3. Check whether the model/acquisition you have chosen requires any additional acquisitions (e.g. T1-mapping, B1-mapping, B0-mapping).
4. Set up the processing pipeline.
This usually requires some image alignment, the computation of any additional maps (B1, T1, etc.), and model-fitting.
5. Sanity check. It may be useful to extract the raw data from a ROI and plot them to verify they match the distribution expected from an MT image.
6. Repeat the model fitting voxel-wise to obtain the parametric maps

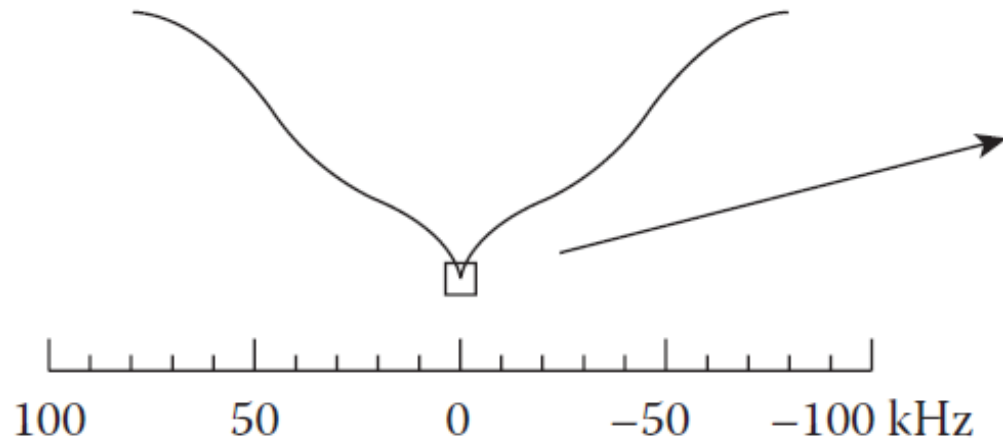
chemical exchange saturation transfer (CEST) Imaging

CEST versus magnetization transfer

- CEST-MRI is similar to magnetization transfer (MT) MRI but with important differences.
 - MT contrast is based on magnetization exchange between water protons and protons in solid or semi-solid environment, CEST contrast comes from chemical exchange between labile protons and water protons.
 - In MT, the broad spectral line shape of the semi-solid components can be saturated by a large frequency range extending up to ± 100 kHz.
- In contrast, selective CEST peaks, e.g. resonances of molecules such as **NH and OH groups**, only appear if much narrower bandwidth of the RF irradiation is used. (less than 10 ppm from water),
- This frequency may be outside this range when using an exogenous CEST agent.

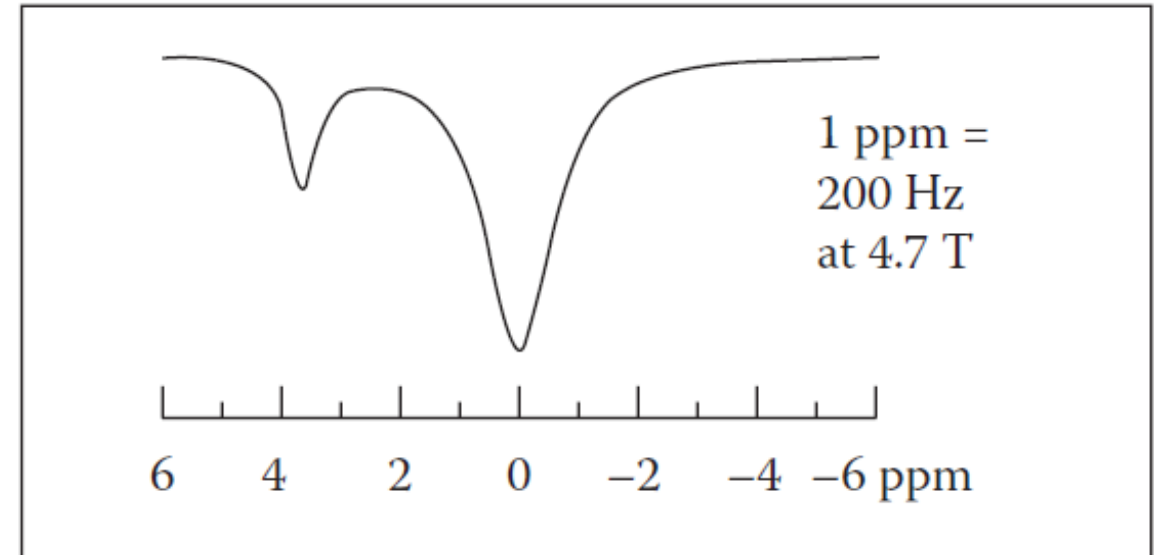
Comparison between magnetization transfer (MT) and chemical exchange saturation transfer (CEST).

MT



- Range: ± 100 kHz
- Approximately symmetric
- Solid-like macromolecules
- Chemical exchange, etc.

CEST

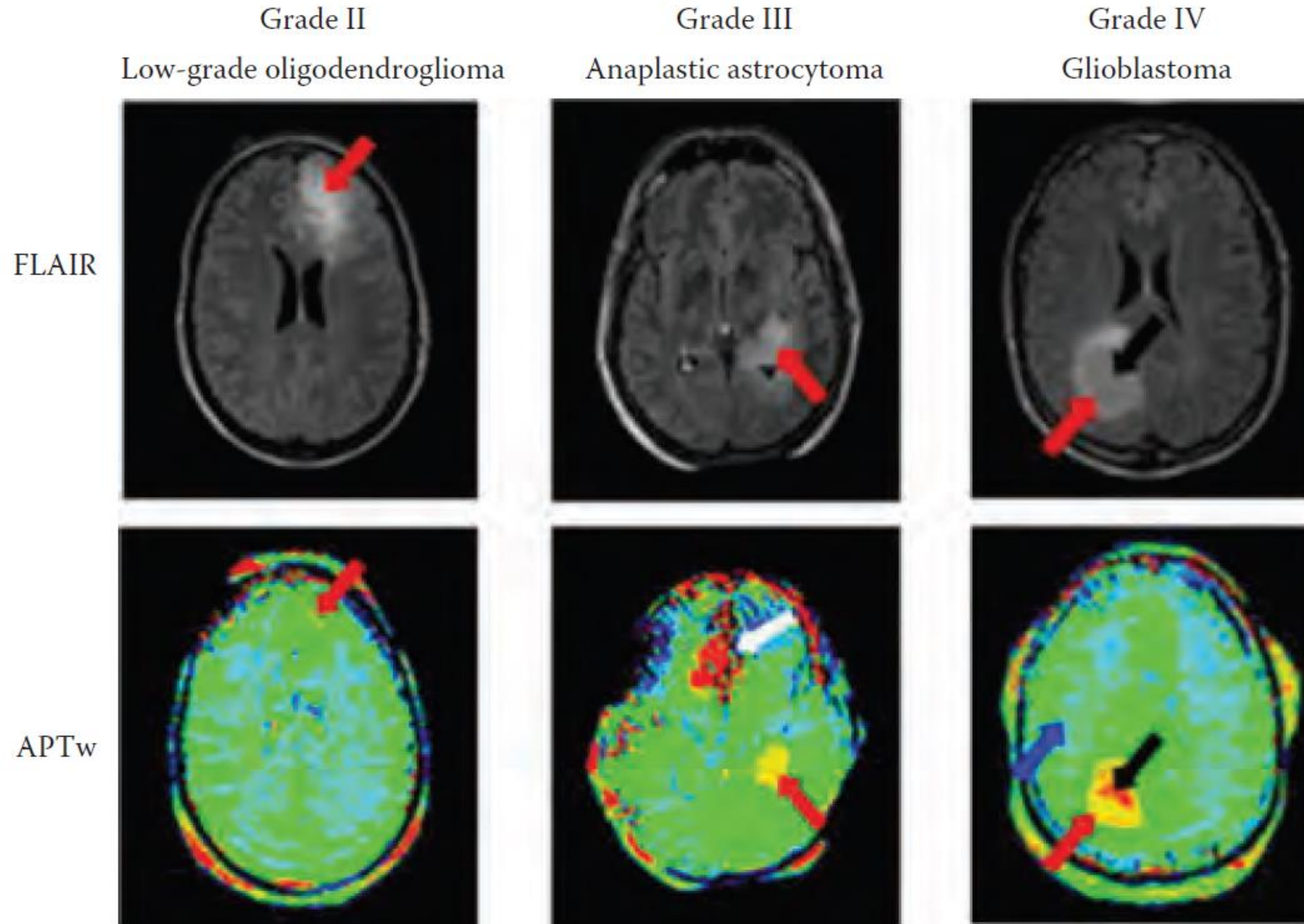


- Range: $\pm 6-7$ ppm
- Individual frequency (Asymmetric)
- Mobile molecules
- Chemical exchange

Classification of CEST contrast

- Endogenous and exogenous CEST agents are usually classified in two main groups: diamagnetic (**diaCEST**) and paramagnetic (**paraCEST**) CEST agents.
- The members of each class can be further divided into subgroups:
 - amide proton transfer CEST (APT-CEST) for peptides/proteins,
 - gagCEST for glycosaminoglycans,
 - glucoCEST for glucose, gluCEST for glutamate, glycoCEST for glycogen,
 - lipoCEST for liposomes, miCEST for myo-inositol
- Diamagnetic CEST agents
 - For diaCEST (hydroxyl, amide, amine and imino groups), the range is generally 10 ppm from water. (up to 19 ppm for hydrogen-bonded groups such as in enzymes and salicylic acids.
- Paramagnetic CEST agents
 - Lanthanide(III) complexes have been suggested as paraCEST agents

Application Example: amide proton transfer (APT) compared with gadolinium enhancement

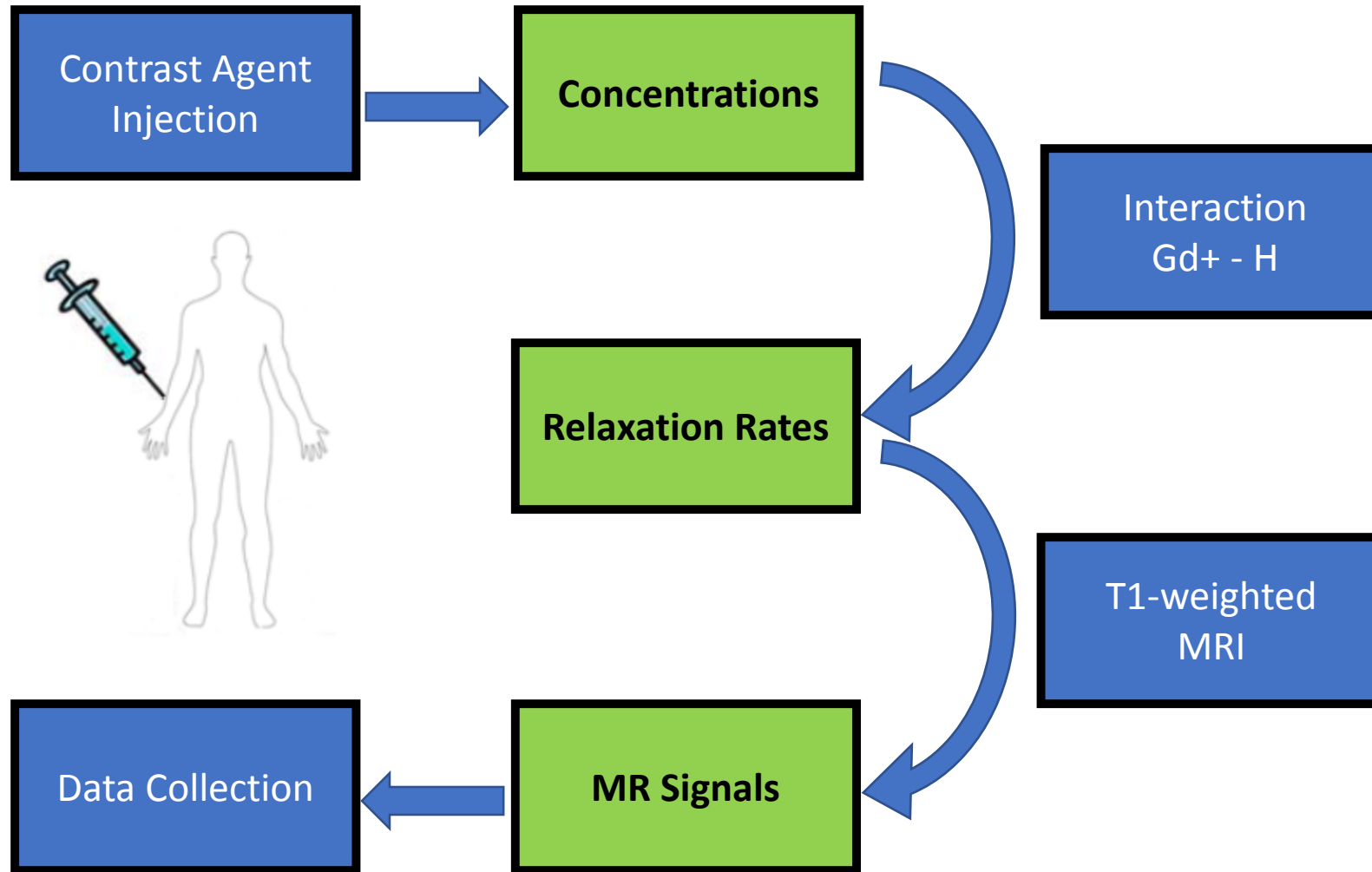


Perfusion quantification

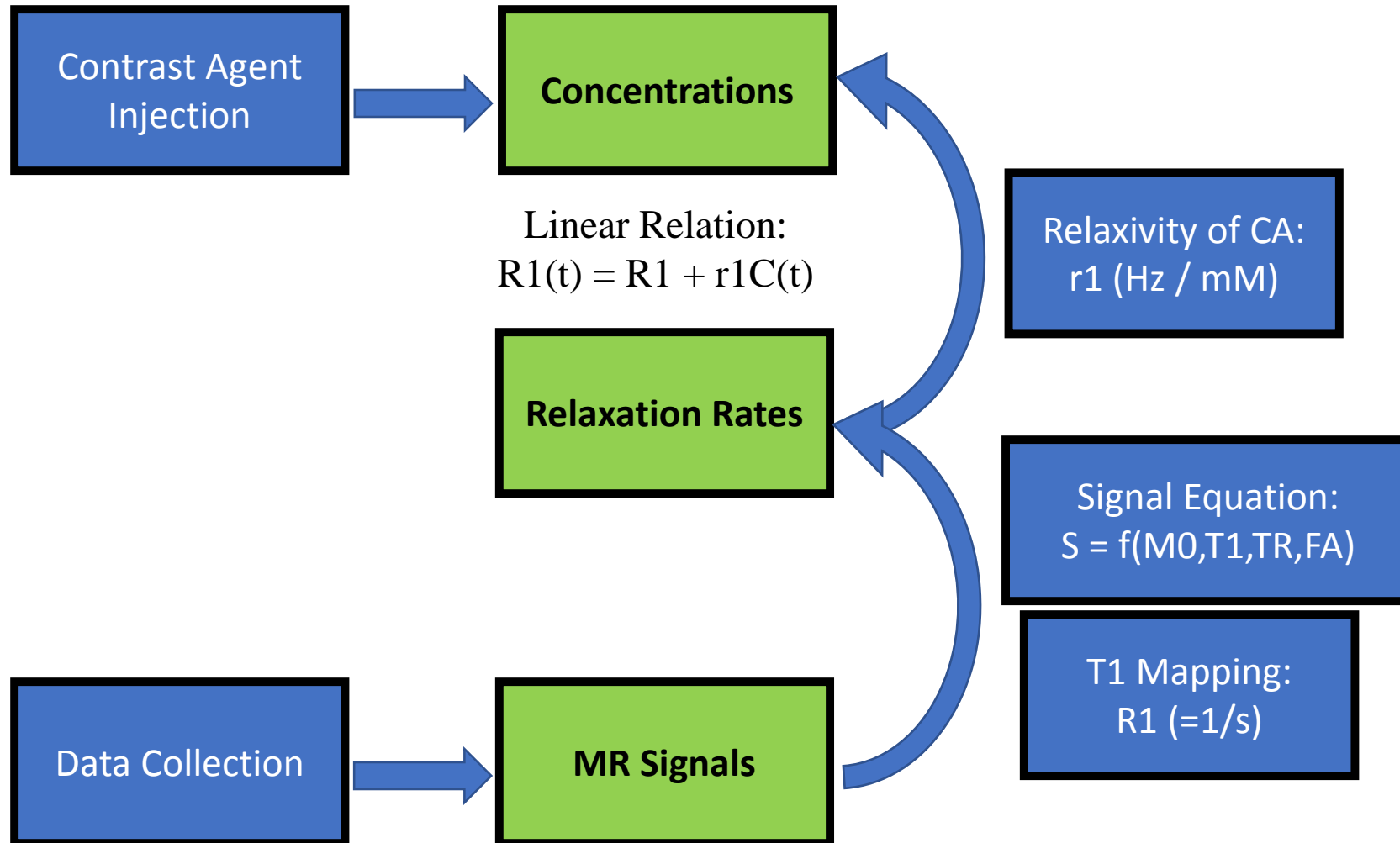
Types of Perfusion methods

- Dynamic contrast-enhanced (DCE) instead of DSC MRI are designed to measure tissue haemodynamics by monitoring the distribution of an intravenously administered injection of contrast agent in vivo.
- DCE use T1 measurement, therefore provide measurements of tissue perfusion, such as cerebral blood flow (CBF) and cerebral blood volume (CBV), brain microvasculature, as well as blood–brain barrier (BBB) integrity by providing measurements of permeability and information about the distribution volume of the contrast agent in the extracellular extravascular space (EES).
- Analysis of DCE can be:
 - Visual assessment of enhancement patterns
 - Semi-Quantitative analysis
 - features include the peak of the enhancement curve, initial wash-in slope, time to maximum signal, washout slope, initial area under the enhancement curve (IAUC)
 - Quantitative analysis using tracer kinetic modelling
 - physiological processes such as CBF, BBB leakiness, volume of the EES and the vascular spaces

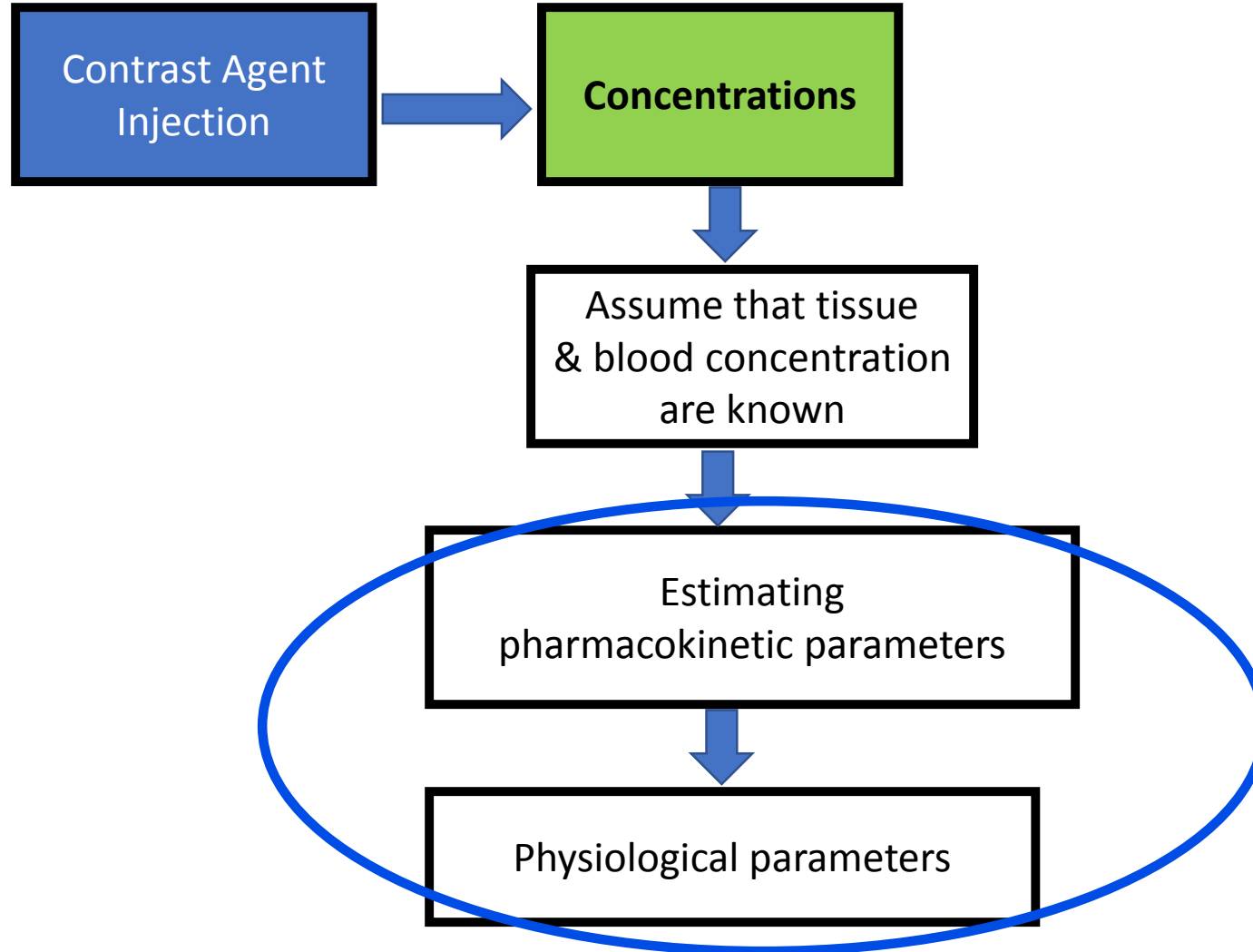
Calculation: T1w DCE MRI



Calculation: T1w DCE MRI



Calculation: T1w DCE MRI



From signal to concentration

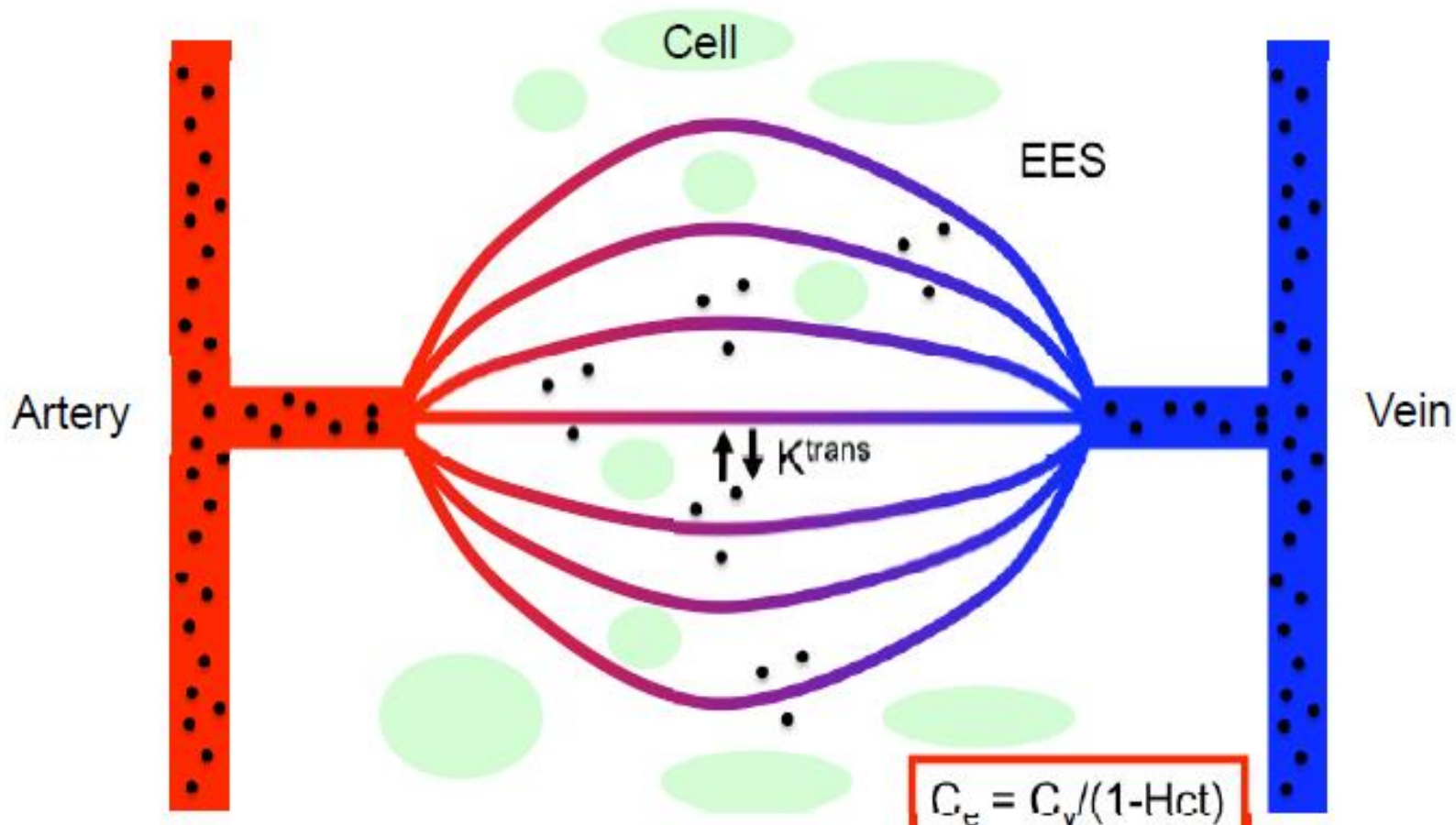
- The most common data acquisition techniques in DCE-MRI are based on 3D-gradient echo sequences, due to their short acquisition times (eg SPGR).

$$S = \Omega PD \frac{\sin(\theta) \left(1 - \exp(-TR/T_1)\right)}{\left(1 - \cos(\theta) \exp(-TR/T_1)\right)} \exp\left(-TE/T_2^*\right)$$

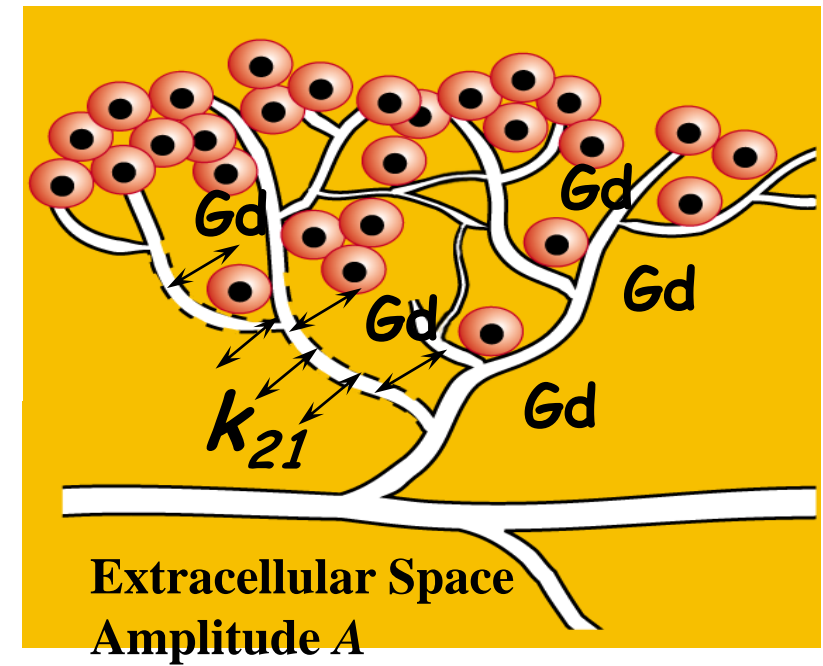
- When a short TE is used, the effect of T2 * on the signal is negligible.
- Using the dynamic signal acquired before the contrast administration (S_0) the T_{10} of the tissue, and after the bolus administration the dynamic T_1 can be calculated using with different TR or flip angles θ (as described before).
- Then concentration can be calculated using linear relation:

$$R_1(t) = R_{10} + r_1 C(t)$$

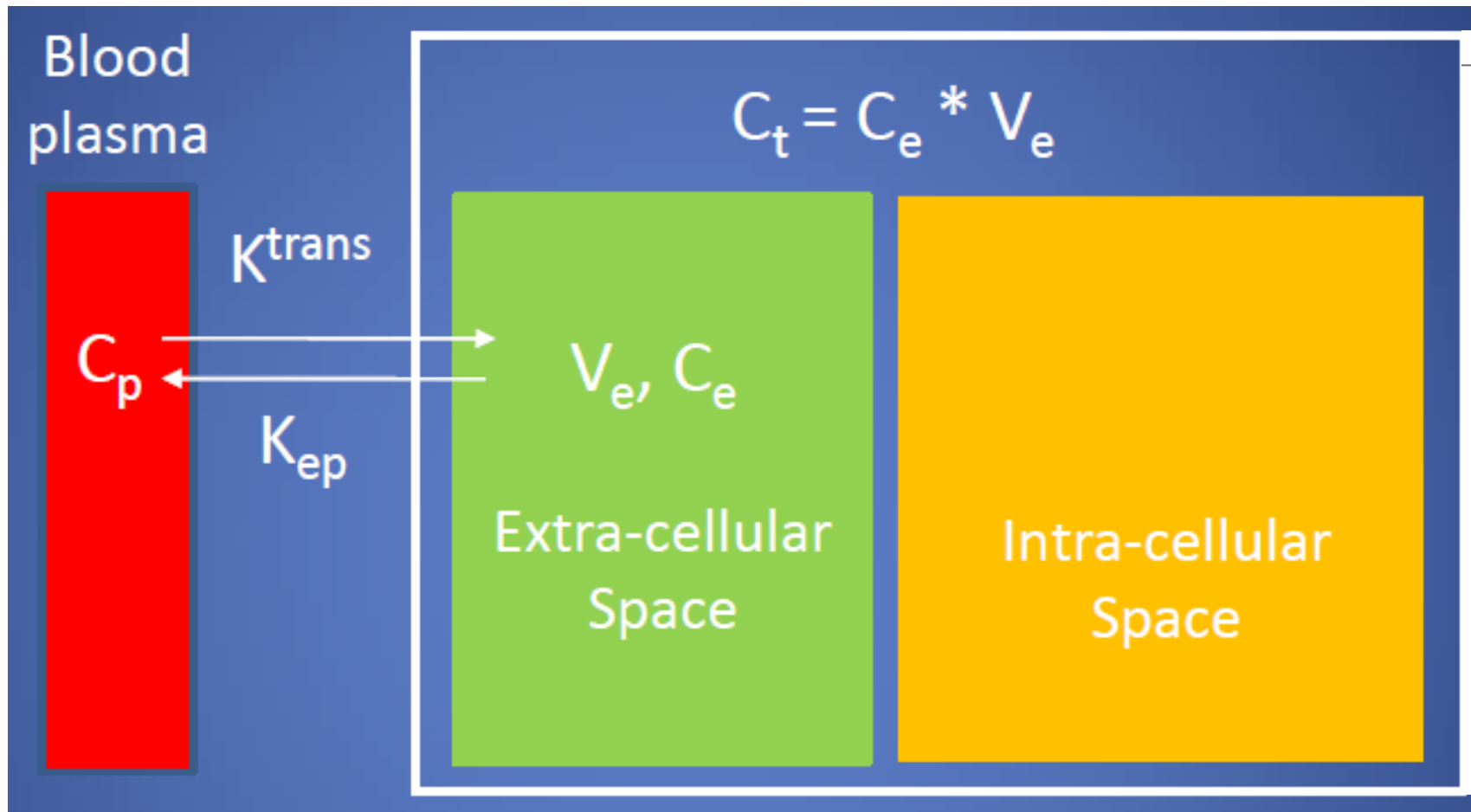
Pharmacokinetic Modelling (Tofts Model)



Any Blood measurement (eg AIF) needs to be corrected to describe concentration in plasma (c_p) rather than whole blood (c_b), using the blood haematocrit.



Pharmacokinetic Modelling (Tofts Model)



Quantity	Definition	Unit
$C_a(t)$	Arterial concentration as a function of time	HU or mM
$C_t(t)$	Tissue concentration as a function of time	HU or mM
Hct	Hematocrit value	Dimensionless
K^{trans}	Transfer constant from the blood plasma into the EES	mL/g/min
k_{ep}	Transfer constant from the EES back to the blood plasma	1/min
t	Onset time of arterial contrast uptake	sec
V_b	Whole blood volume per unit of tissue	mL/g
V_e	Total EES volume per unit of tissue ($V_e = K^{trans}/k_{ep}$)	mL/g

Main Physiological parameters:

K^{trans} : transfer constant (Vessel Permeability)

K_{ep} : reflux constant

V_e : extra-vascular, extra-cellular volume fraction (depends on Cellular Density)

Quantitative analysis using tracer kinetic modelling

- If contrast agents space **do not enter the intracellular** (in most cases):

$$C_t(t) = v_p C_p(t) + v_e C_e(t)$$

- where C_t is the concentration in the entire tissue, and C_p and C_e are the concentrations in the vascular plasma space ($C_p = C_b / (1 - Hct)$) and EES, with fractional volume of V_p and V_e
- Due to the exchange of **contrast agent between compartments**, the **flux J of the contrast agent** is defined as the concentration **gradient between the two compartments**, with a rate constant that depends on the properties of the membrane:

$$J = PS (C_1 - C_2)$$

- PS is Permeability of surface area per unit volume of tissue ($\text{ml min}^{-1} \text{ml}^{-1}$)
- P Total permeability of capillary wall (cm min^{-1})
- S Surface area per unit volume of tissue (cm^{-1})

Tofts model

- Using 2 previous equations, the **rate of accumulation and washout** of a contrast agent in the EES, can be described using the general form of the rate equation:

$$v_e \frac{dC_e(t)}{dt} = K^{trans} (C_p(t) - C_e(t))$$

- K_{trans} is the physiological interpretation of the **volume transfer constant**, and depends on the balance between the BBB permeability and blood flow in the tissue.

$$K^{trans} = EF_p$$

- F_p is plasma flow rate ($\text{ml min}^{-1} \text{ ml}^{-1}$)
- E is the extraction fraction of contrast agent (i.e. the fraction of tracer extracted to v_e)
- PS is Permeability of surface area per unit volume of tissue ($\text{ml min}^{-1} \text{ ml}^{-1}$)

$$E = \frac{PS}{PS + F_p}$$

Tofts model

- The conventional Tofts model, a negligible contribution to C_t from the vascular space ($v_p \sim 0$) is considered. Solving previous Equation, substituting to 1st equation we have:

$$C_t(t) = K^{trans} \int_0^t C_p(\tau) \exp\left(-\frac{K^{trans}(t-\tau)}{v_e}\right) d\tau$$

- Extended Tofts model:** in most pathologies, the contribution of the vascular space to the overall concentration exist ($v_p \sim 0$):

$$C_t(t) = v_p C_p(t) + K^{trans} \int_0^t C_p(\tau) \exp\left(-\frac{K^{trans}(t-\tau)}{v_e}\right) d\tau$$

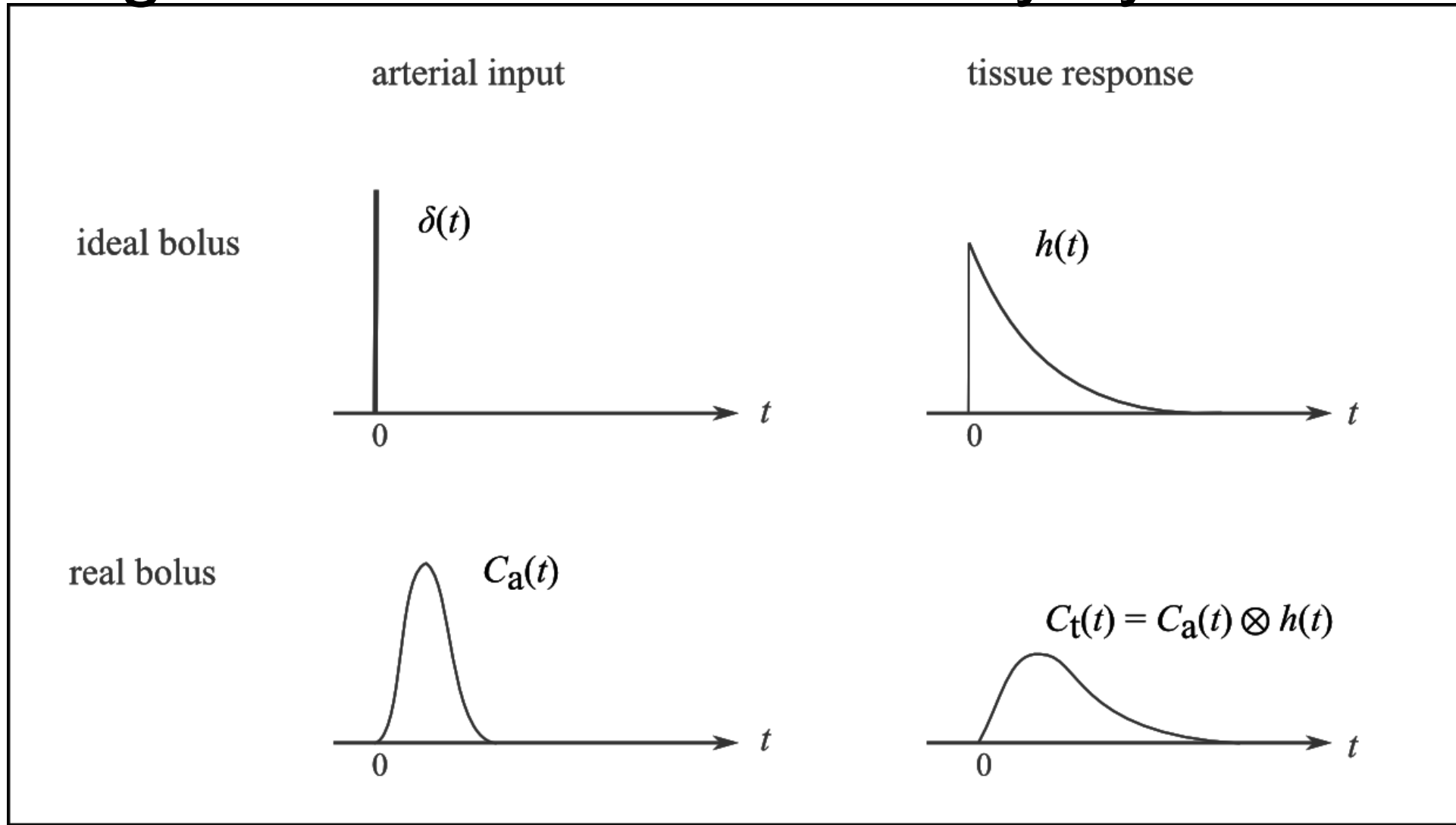
- In general convolution form, this mean the convolution of Arterial concentration function with the tissue permeability transfer function.

$$C_t(t) = \frac{K_{trans}}{1 - Hct} \left(C_a(t) \otimes e^{-k_{ep}(t-\tau)} \right)$$

Arterial input function selection

- the most challenging part of tracer kinetic modelling is to provide an accurate representation of the AIF (C_p or C_a in previous relations), or the delivered contrast agent dose.
- **The temporal sampling** of the AIF, **spatial resolution** (for low partial volume), and direct selection on **the inlet to the pathology** are essential.
 - However, an upstream in the arterial tree where the diameter of the vasculature is larger, is used.
- when the acquired images do not enable arterial measures, AIF is sampled from the **internal carotid artery**, a **venous outflow**, or the **sagittal sinus** as a surrogate

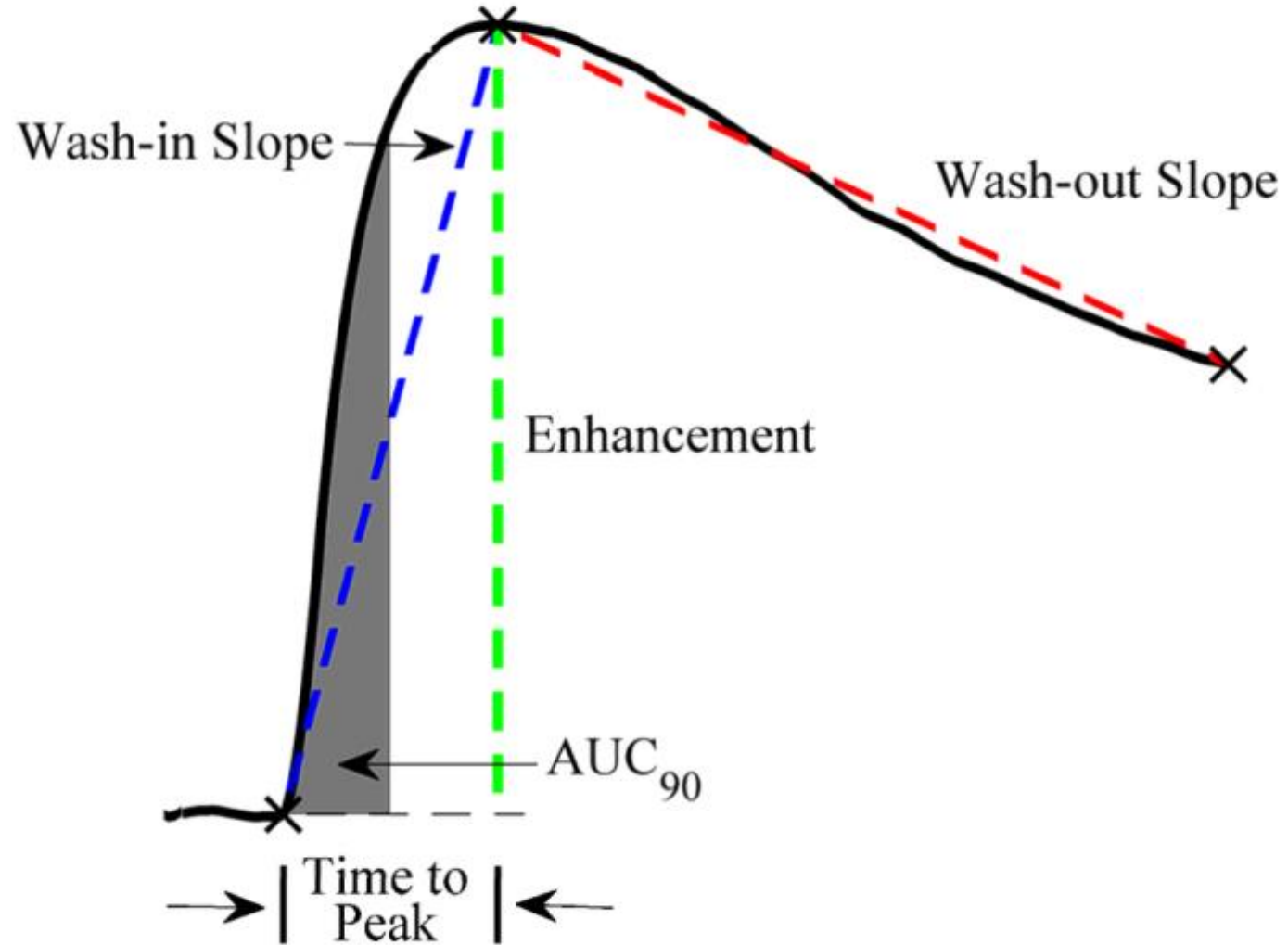
Diagram of a linear stationary system



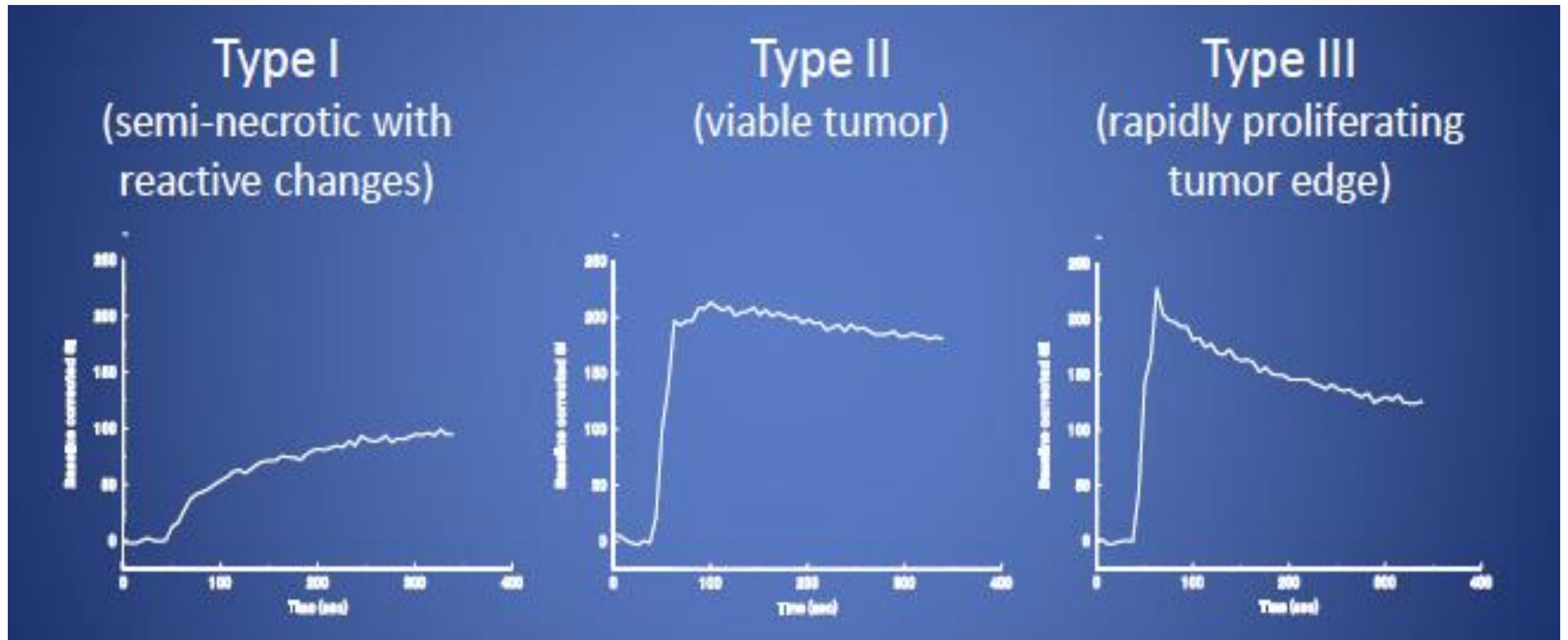
- The Response to an ideal impulse $\delta(t)$ at the entrance is $h(t)$. The real bolus of an infusion is of a broadened form and thus the outflow response is given by a convolution of $C_a(t)$ and $h(t)$. (Modification of Brix et al).

Dynamic contrast enhanced imaging (DCE)

T1-weighted imaging with c.m. injection



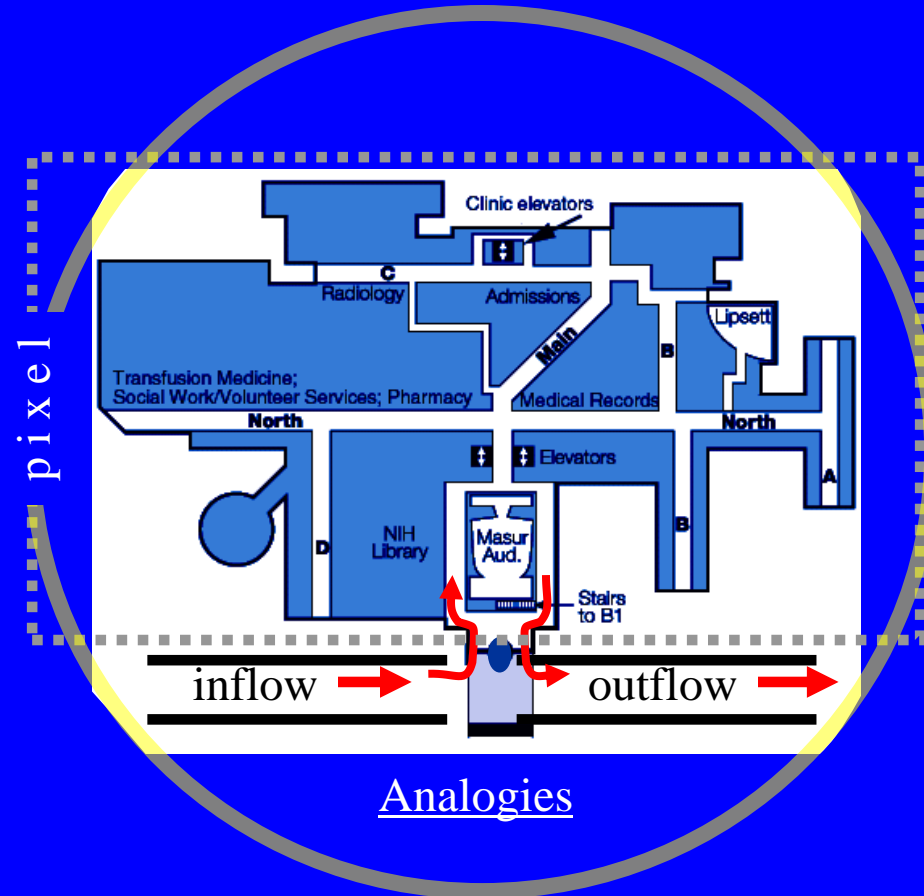
Qualitative shape of DCE signal intensity for pathology



Taylor and Reddick, Adv Drug Del Rev, 2000

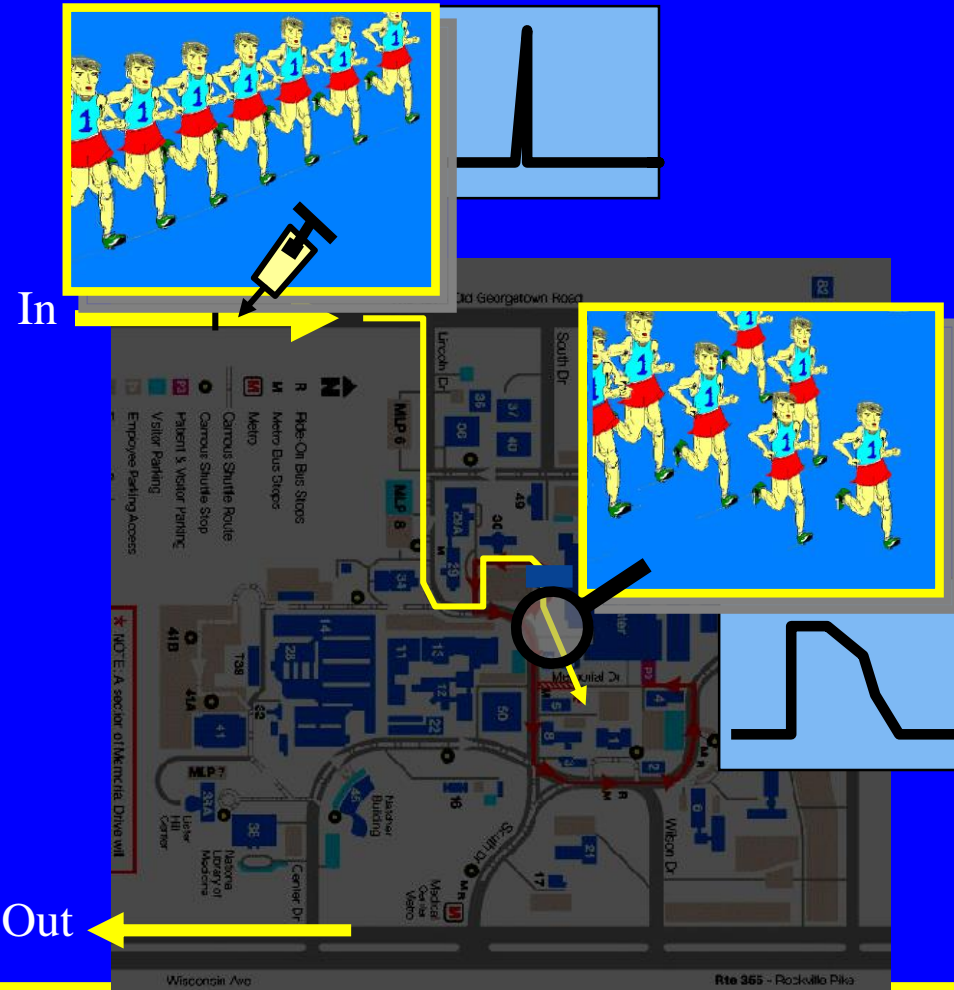
Quantitative Physiological parameters of perfusion

Perfusion parameters can be considered as the inflow of People through a building. Each building (pixel) has an inflow and an outflow. But there are multiple paths *through* the building.

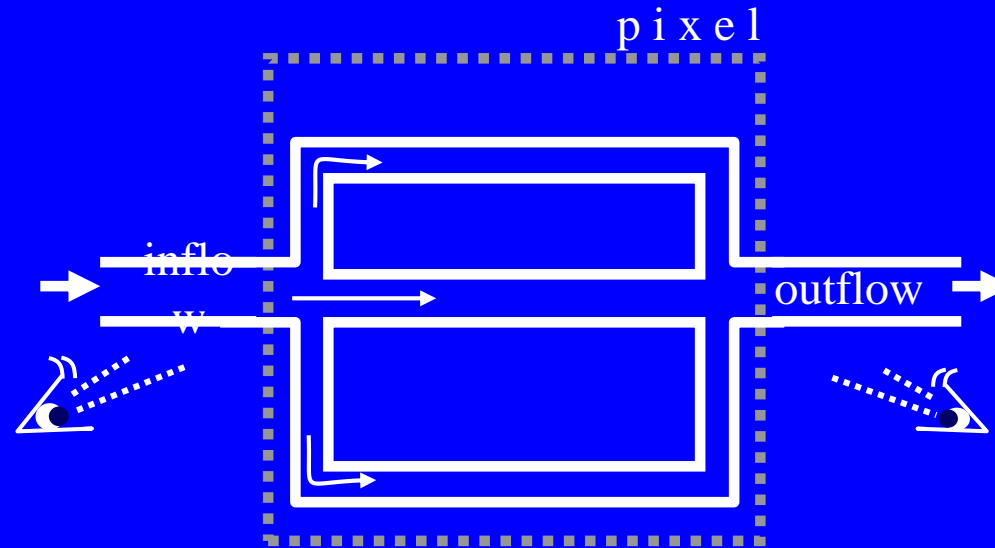


- A building is a ... **pixel**
 - Rate of people entering building at inflow: **F**
 - Average time spent in the building: **MTT**
 - Fraction of people passing through building: **V** or **CBV**
(compared to other buildings)
-

Method: Inject an “impulse” of runners into the system, then monitor their arrival(s) downstream.



Lets further idealize the picture

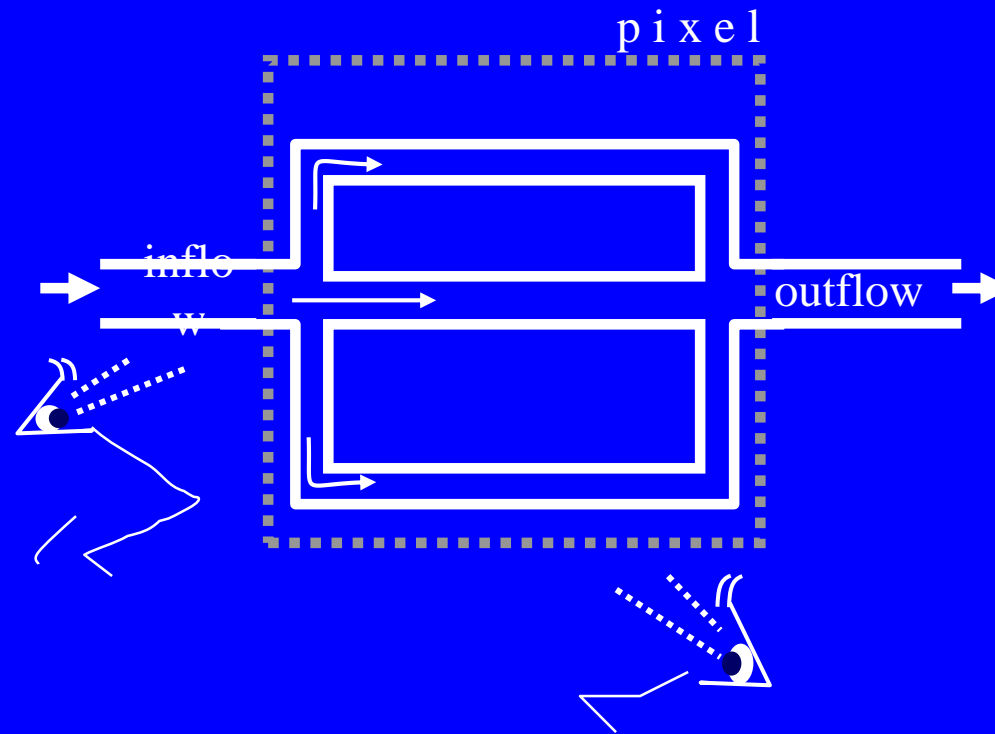


In the ideal case, we would examine the inflow to, and the outflow from every region (i.e., pixel).

Thus, we would *expect* the **outflow signal** to be equal to the **inflow signal convolved with the impulse response**:

$$S_{out} = S_{in} \otimes h$$

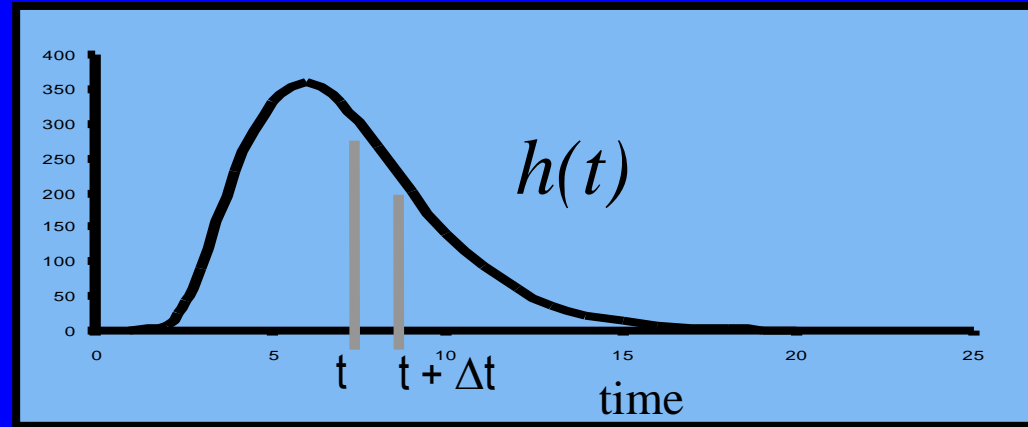
But, consider our *actual* observation points...



Rather than measure at inflow and outflow, we make observations of something equivalent to

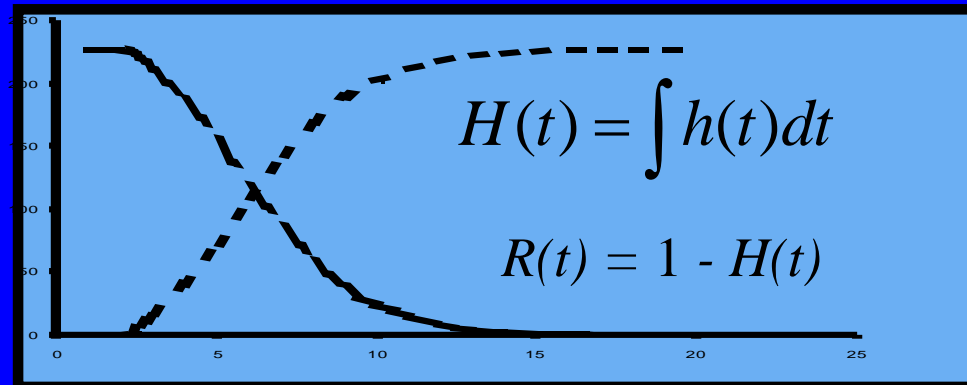
- signal at \sim inflow (the arterial function) and,
 - signal from the *entire* pixel.
-

impulse response, $h(t)$ is the histogram of transit times (p.d.f)
 $h(t)dt$ is the fraction of “particles” that leave the system between t and $t+\Delta t$



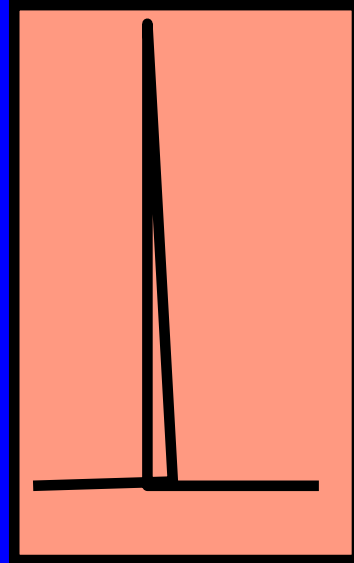
The integral $H(t)$, of the histogram is all the tracer that has LEFT the system. (*Think c.d.f*)

The residue function, $R(t)$, describes all tracer still *remaining*, at time t and NOT yet drained from the system

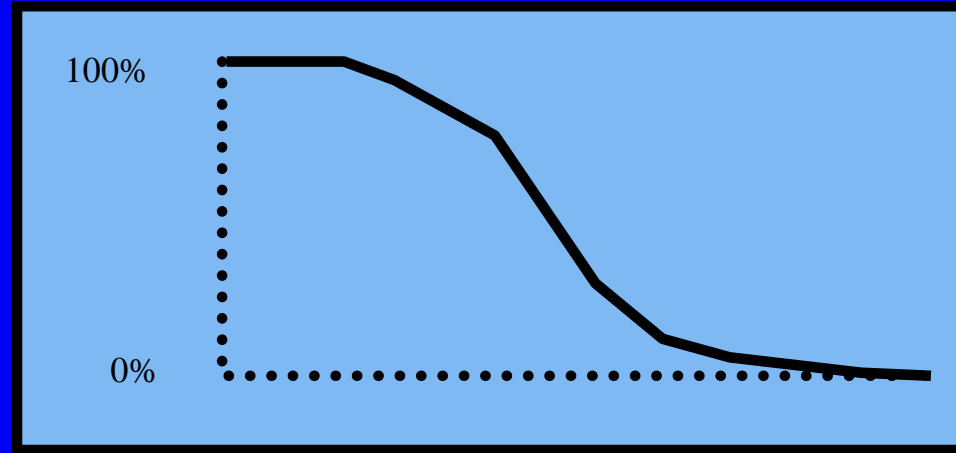


Our observations are related to $R(t)$.

How to measure C_t (runner traffic remain in the building or concentration from entire pixel)



View at
ideal input

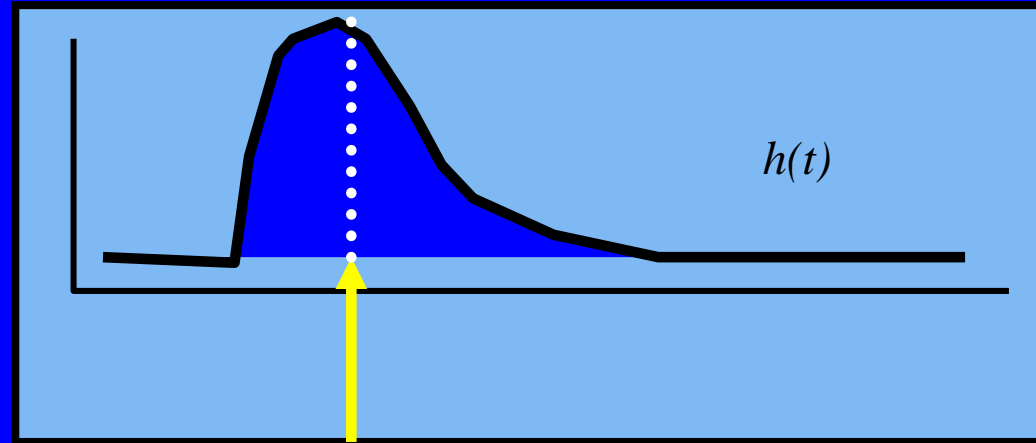


View of 'runners' remaining
within the building

Thus, $R(t)$ is - in effect - the impulse response as viewed from *within* the pixel.

$$C_t(t) = Scale \cdot \int_0^t C_a(T)R(t-T)dT$$

What is MTT in terms of the residue function, $R(t)$?



The **Mean transit time** is at the center of mass of the distribution, $h(t)$. I.e., 1st/0th moments.

$$\begin{aligned}\bar{t} &= \int_0^{\infty} t \cdot h(t) dt / \int_0^{\infty} h(t) dt \\ &= \int_0^{\infty} t \cdot h(t) dt\end{aligned}$$

Recall that the Residue function is related to the integral of the histogram.

$$\begin{aligned}R(t) &= 1 - \int_0^t h(\tau) d\tau \\ dR &= -h(t) dt\end{aligned}$$

What is MTT in terms of the residue function, $R(t)$? cont

Substituting dR into the expression for MTT,

$$\bar{t} = -\int_0^{\infty} t \cdot dR$$

Integrating by parts we see that,

$$\begin{aligned}\bar{t} &= -\left[Rt \Big|_0^{\infty} - \int_0^{\infty} R(t) dt \right] \\ &= \int_0^{\infty} R(t) dt\end{aligned}$$

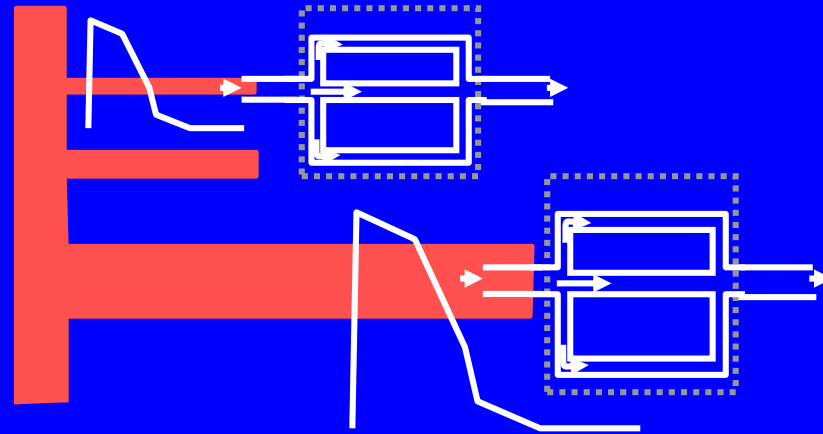
Recall that we should consider the Scaled Residue Function,

$$\bar{t} = \int_0^{\infty} \textit{Scale} \cdot R(t) dt / \textit{Scale}$$

Where by convention *Scale* is the maximum point on the scaled residue curve.

Why is the Output Equation Scaled by the Flow Arriving at the Pixel?

$$C_t(t) = Scale \cdot \int_0^t C_a(T)R(t-T)dT$$



‘Scale’ is the *relative* inflow, F , to the pixel because the fraction of tracer arriving at a given pixel is proportional to the fractional flow to that pixel.

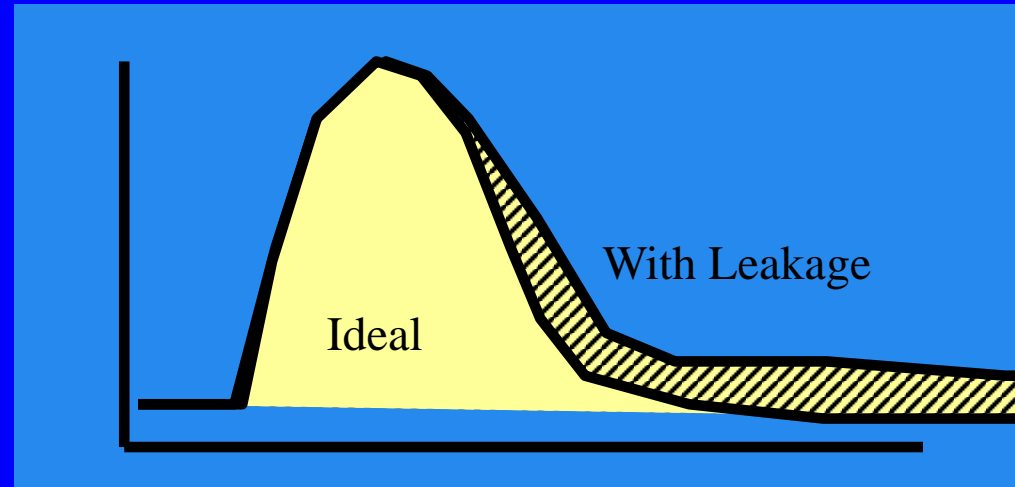
What is Volume Fraction, V?

CBV is a measure of *relative* blood carrying capacity of a region.

We measure it as the **ratio of all the tracer** that passes through a voxel over time to all the tracer that passes through a point in the vasculature over all time.

$$CBV = \frac{\int_0^{\infty} C_t(t) dt}{k \int_0^{\infty} C_a(t) dt}$$

Consequence of BBB Leakage to Contrast Agent



If contrast agent does NOT stay wholly intravascular (as in case of damage to BBB),

and CBV is overestimated.

$$\int_0^{\infty} C_t(t) dt \text{ is larger}$$

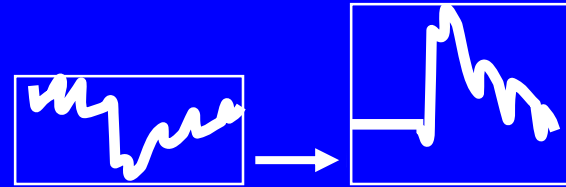
If CBV is overestimated, then $MTT = CBV/CBF$ is also overestimated.

How's it done? - Data Flow

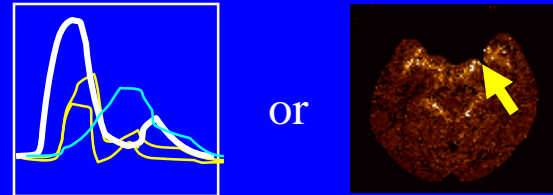
1. Inject



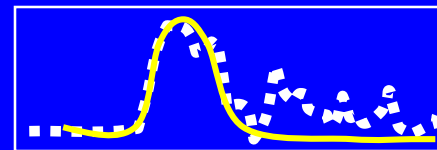
2. Scan over time



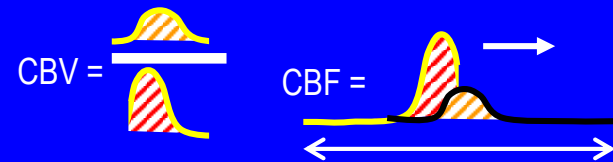
3. Convert signal to concentration



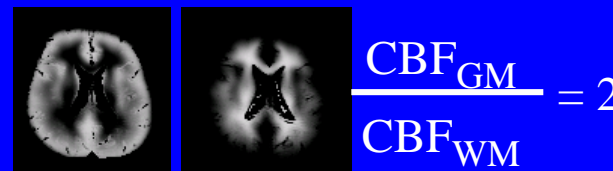
4. Find AIF



6. Calculate CBV, CBF, MTT



7. Post-process, tabulate stats



Signal model for DCE measurement (3D-SPGR sequence)

$$S = G\rho \exp(-TE T_2^{*1}) \sin(\theta) \frac{1 - \exp(-TR T_1^{-1})}{1 - \cos(\theta) \exp(-TR T_1^{-1})}$$

where G is the gain, ρ is the PD

- Contrast agent changes the relaxation rates to: (here R_1 is the contrast agent relaxivity constant)

$$\frac{1}{T_1} = \frac{1}{T_{10}} + R_1 C(t); \quad \frac{1}{T_2^*} = \frac{1}{T_{20}^*} + R_2 C(t)$$

- And signal of GE after injection is given by:

$$S(t) = G\rho \exp(-TE(T_{20}^{*1} + R_2 C(t))) \sin(\theta) \frac{1 - \exp(-TR(T_{10}^{-1} + R_1 C(t)))}{1 - \cos(\theta) \exp(-TR(T_{10}^{-1} + R_1 C(t)))}$$

Signal model for DCE measurement (3D-SPGR sequence (cont.))

- Equation can be written as

$$S(t)/S(0) = k_0 \exp\left(-TER_2 C(t)\right) \frac{1 - \exp(-TR(T_{10}^{-1} + R_1 C(t)))}{1 - \cos(\theta) \exp(-TR(T_{10}^{-1} + R_1 C(t)))}$$

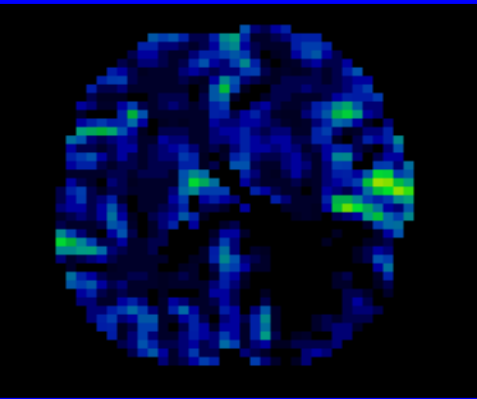
$$\text{where the constant } k_0 = \frac{1 - \cos(\theta) \exp(-TR T_{10}^{-1})}{1 - \exp(-TR T_{10}^{-1})}$$

- with two parameters T_{10} and $C(t)$.
 - Substitution of T_{10} , reduces it to a non linear equation in single variable $C(t)$.
 - This reduced equation is then fitted to data $S(t)/S(0)$ for $C(t)$.
-

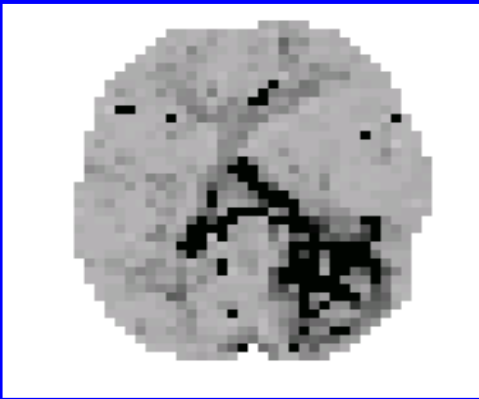
Sample Results



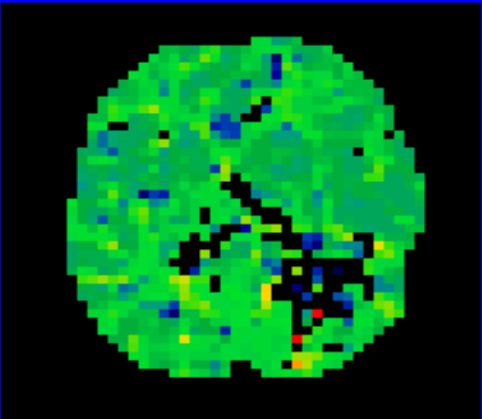
CBV



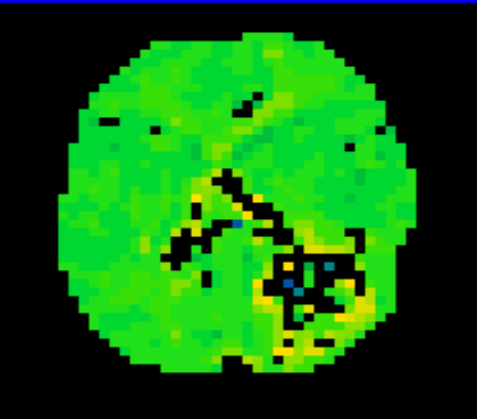
CBF



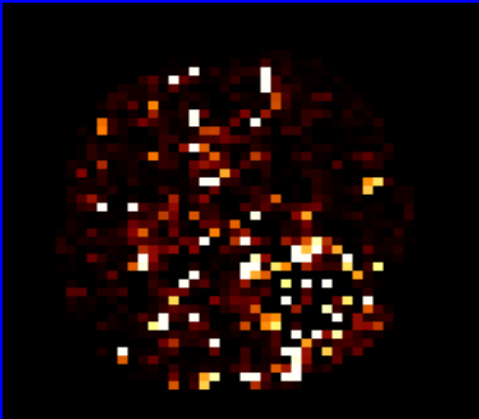
MTT



Take-off time



Recirc. time

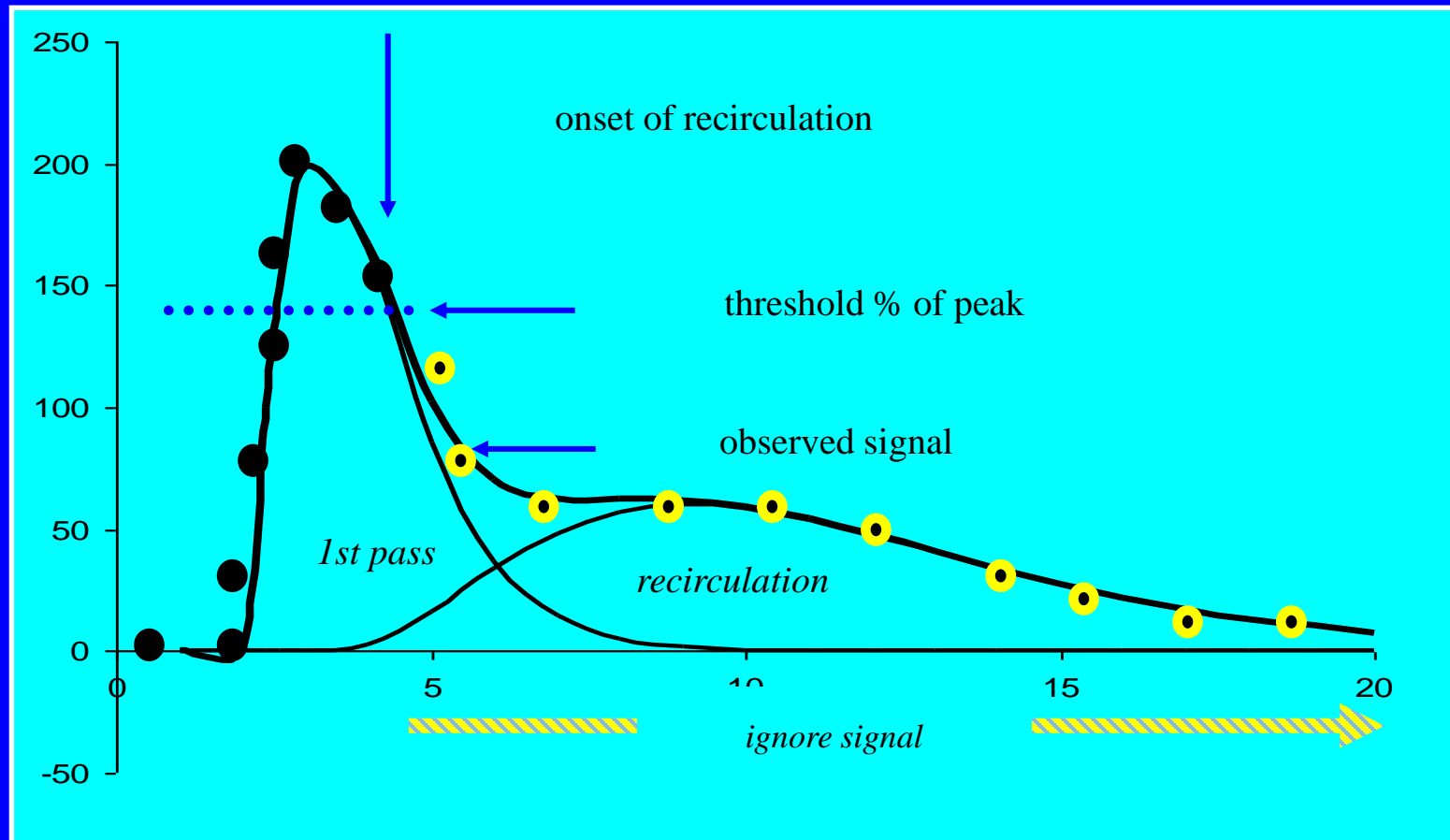


Normalized

χ^2

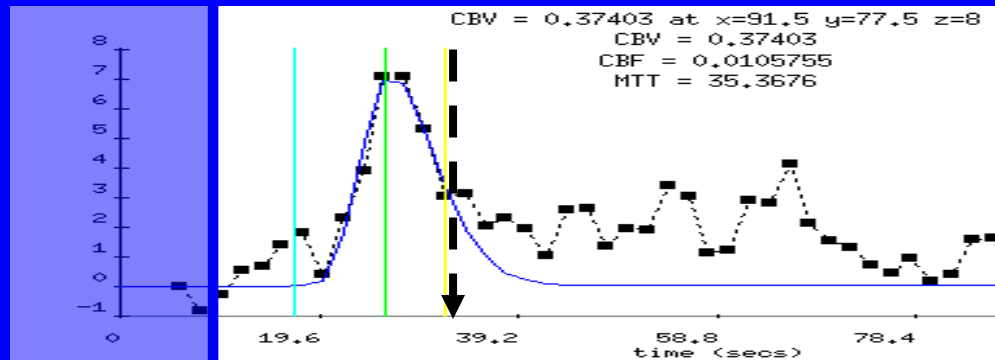
Why a Recirculation Threshold ?

Because volume fraction (relCBV) is based on the total amount of tracer, that drains from an ‘open’ system, we must find a way to identify and integrate the **first-pass response**, independent of recirculation effects.

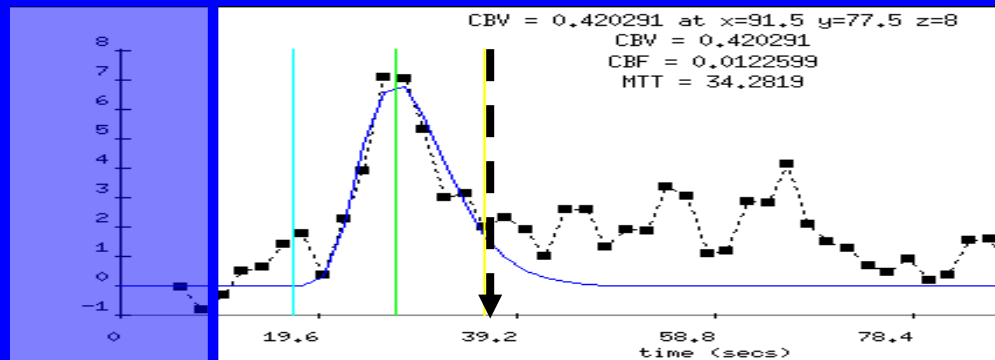


A common approach is to set a threshold relative to peak and ignore all later data that dips below that threshold.

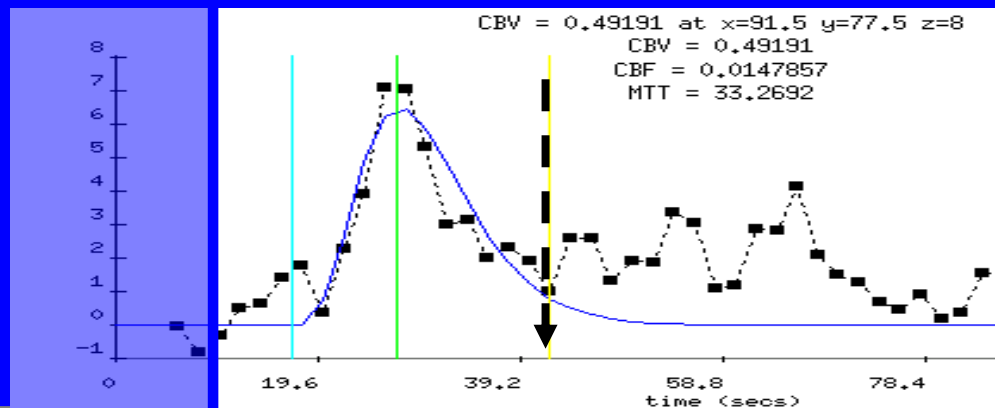
CBV- Effect of Recirculation Threshold



Thresh = 50 %
CBV = 0.37
 $X^2 = 0.008$



Thresh = 30 %
CBV = 0.42
 $X^2 = 0.010$



Thresh = 20 %
CBV = 0.49
 $X^2 = 0.180$

Why an *SVD* threshold? - 1

Singular Value Decomposition is used to solve an approximation to expression (1) which relates the *convolution* of the arterial input function $C_a(t)$ and the Residue function, $R(t)$, to the tissue concentration, $C_t(t)$:

$$C_t(t) = \left[\frac{\rho}{K_h} \right] CBF \cdot \int_0^t C_a(T) R(t-T) dT \quad (1)$$

We approximate equation (1) as follows:

$$b = Ax \quad (2)$$

$$C_t = f \cdot AR \quad (3)$$

where:

$$\begin{bmatrix} C_t(1) \\ \vdots \\ C_t(n) \end{bmatrix} = f \begin{bmatrix} A_1 & \cdots & A_{n1} \\ A_{12} & \ddots & \vdots \\ A_{13} & & \\ \vdots & & \\ A_{14} & \cdots & A_n \end{bmatrix} \begin{bmatrix} R_1 \\ \vdots \\ R_n \end{bmatrix} \quad (4)$$

Why an *SVD* threshold? - 2

According to SVD, we can represent the A matrix in terms of **the diagonal matrix, Σ** , made up of **singular values, σ_i** :

$$C_t = f \cdot Q_2 \Sigma Q_1^T \cdot R \quad (5)$$

We then solve equation (2) by:

$$f \cdot R = Q_1 [\text{diag}(1/\sigma_j)] Q_2^T \quad (6)$$

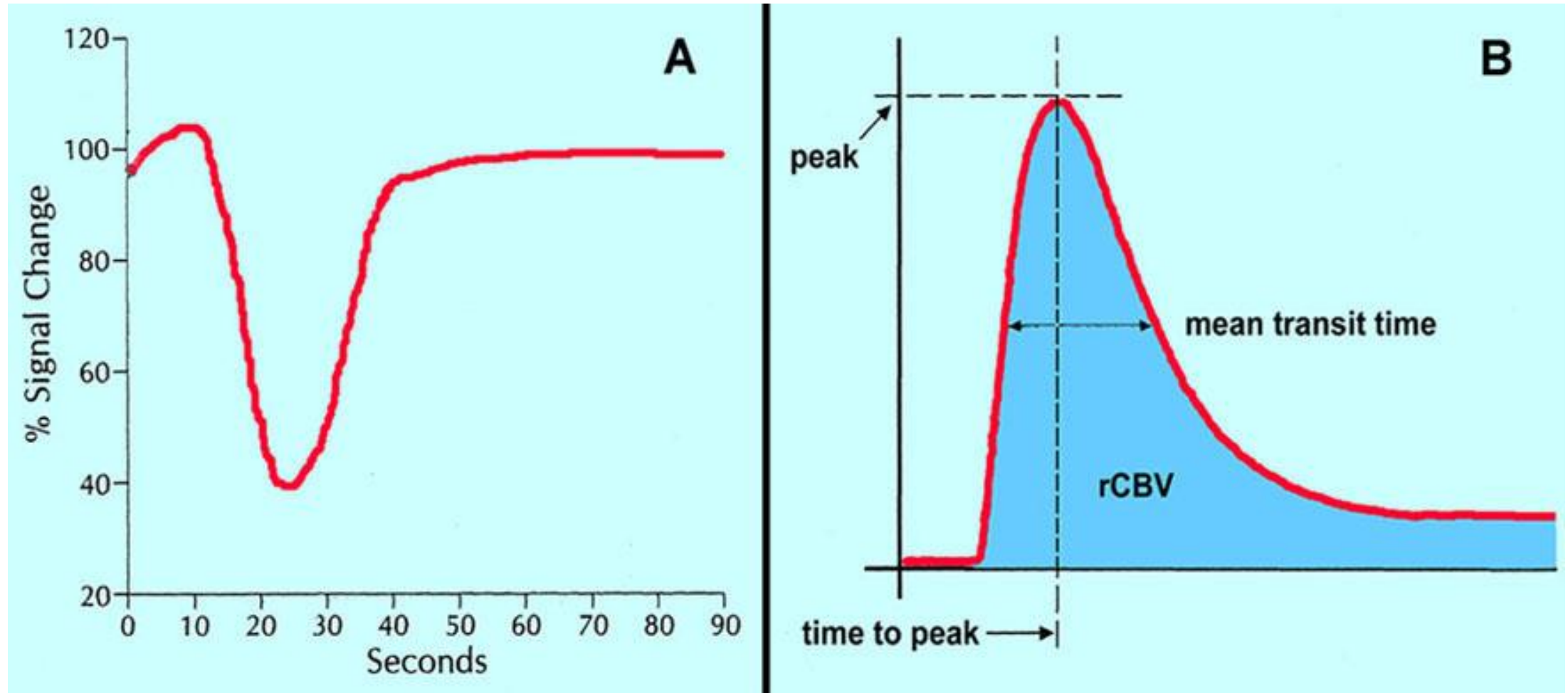
$$= Q_1 \begin{bmatrix} \frac{1}{\sigma_1} & 0 & 0 & 0 \\ 0 & \frac{1}{\sigma_2} & & \vdots \\ 0 & & \ddots & \\ 0 & \dots & & \frac{1}{\sigma_n} \end{bmatrix} Q_2^T \quad (7)$$

But **very small singular values**, σ_i , that may result from roundoff error are zeroed using a specified (threshold) percentage of the maximum singular value.

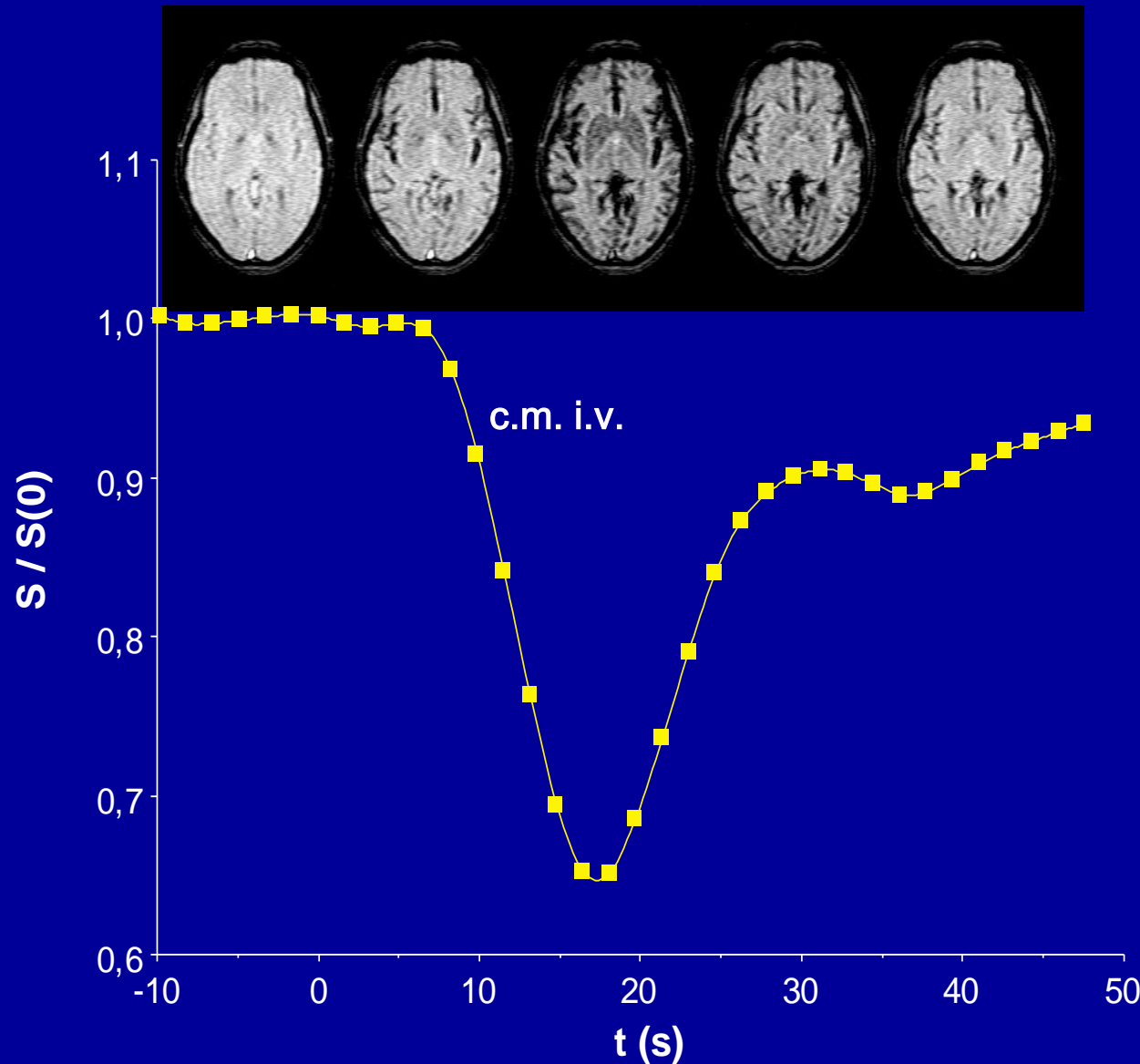
Perfusion Weighted Imaging (DSC)

- T2* susceptibility effects of gadolinium, rather than the T1 shortening effects make gadolinium a suitable agent.
- Susceptibility here refers to the loss of MR signal, most marked on T2* (gradient echo)- and T2 (SE), caused by the magnetic field-distorting effects of paramagnetic substances.
- The ultimate goal of DSC perfusion MRI is to measure the blood flow and volume perfused in organ.
- This flow corresponds to single compartment microcirculatory tissue perfusion rather than the flow of the main vascular axes
- CBF is expressed in milliliters per 100 gram of tissue per minute.

DSC compared to CT perfusion



Perfusion-weighted MRI (DSC-PWI) measurement



Fast, repetitive T2*-weighted Sequences (GE) to follow the capillary passage of c.m.

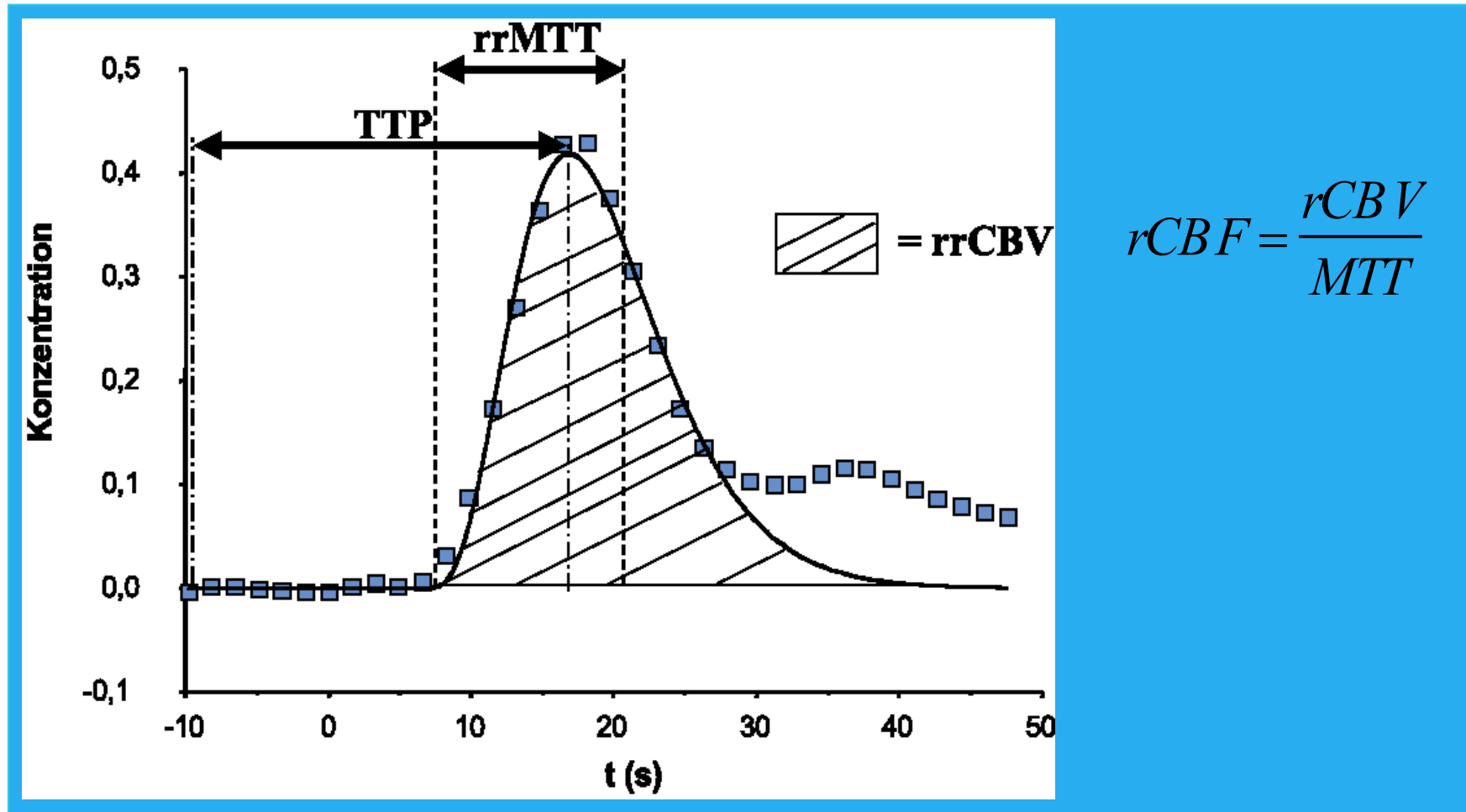
Susceptibility-derived signal decrease

Calculation of RELATIVE hemodynamic parameter maps

(a) Time: TTP, MTT

(b) Perfusion: rCBF, rCBV

Perfusion-weighted MRI (DSC-PWI) measurement



Comparison to contralateral side → regional relative CBF/CBV

In DSC, MR signal intensity can be converted to Gd concentration
(no T2 measurement is required)

$$C_m(t) = -K \cdot \ln \frac{S(t)}{S_0},$$

- $C_m(t)$ is the measured concentration of Gd with respect to time,
- K is a proportionality constant that is inversely proportional to the TE and depends on the MR scanner,
- concentration of Gd-DTPA in a tissue is then given by:

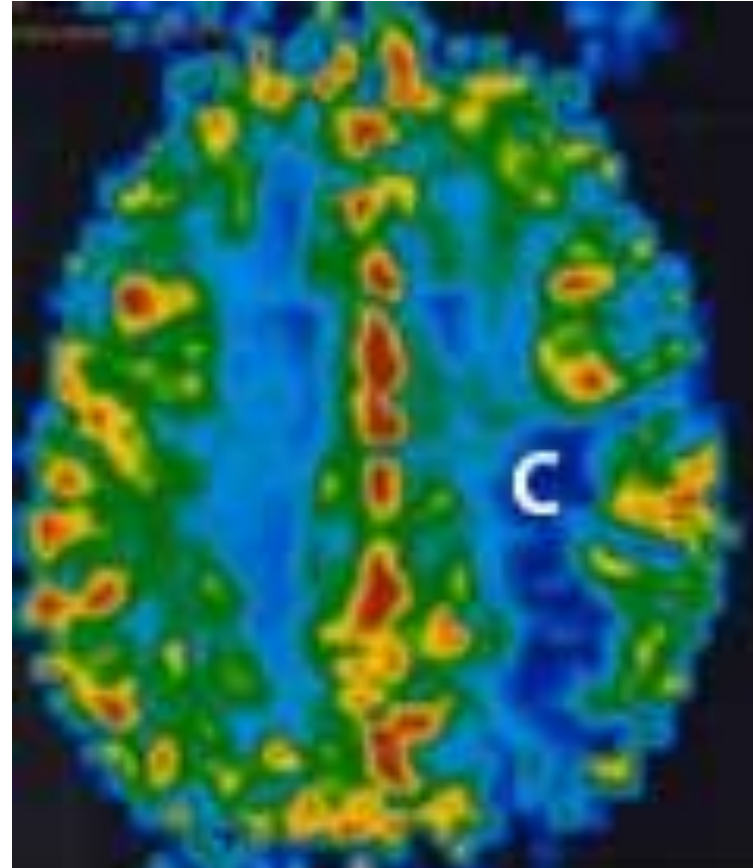
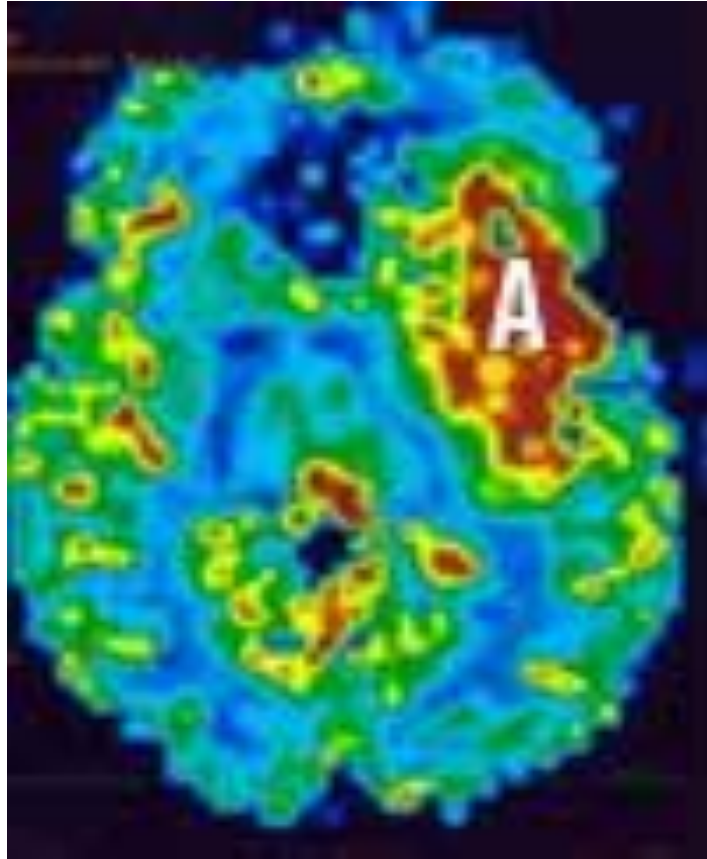
$$C(t) = C_m(t) \otimes^{-1} \text{AIF}(t)$$

Main DSC Perfusion parameters

- **TA**: time of arrival of the contrast agent in the slice after injection
- **TTP** (Time To Peak): time corresponding to the maximum contrast variation
- **MTT** (mean transit time)
- **Peak amplitude**: percentage loss of intensity of the maximal signal

- **Following parameters are extracted by post-processing the signal curves, as described in DCE method:**
- **rCBV** (regional cerebral blood volume): The area below the decreasing signal curve
- **rCBF** (regional cerebral blood flow): The ratio $rCBV/MTT$.
- RCBV and rCBF are relative measurements, giving the calculation of ratios between pathological zone and healthy zone (which serves as a reference).

Perfusion MRI



- Perfusion MRI is a technique for evaluation of microscopic blood flow in cerebral capillaries and venules.
- (Left) Perfusion of a **high grade brain tumor** demonstrates areas of increased capillary blood volume in tumor (red)
- (Right) Loss of perfusion due to Stroke